CHAIR OF MULTISCALE BIOENGINEERING

FACULTY OF TECHNOLOGY

BIELEFELD UNIVERSITY

DISSERTATION

in fulfillment of the requirements for the degree

Doctor of Natural Sciences (Dr. rer. nat.)

Establishing the Weimberg pathway in *Corynebacterium glutamicum* as an alternative route for D-xylose utilization

---

submitted by

Andreas Willi RADEK

born on the 7th of October 1987 in Hamm

Jülich, April 18, 2018

Selbstständigkeitserklärung

Hiermit erkläre ich, die vorliegende Dissertation selbstständig und nur unter Benutzung der angegebenen Quellen angefertigt zu haben. Alle aus der Literatur wörtlich oder sinngemäß entnommenen Zitate und Abbildungen habe ich als solche kenntlich gemacht. Weiterhin erkläre ich, dass diese Arbeit weder vollständig noch teilweise einer anderen Prüfungsbehörde mit dem Ziel vorgelegt wurde, einen akademischen Titel zu erwerben.

Unterschrift:

Ort, Datum:

The practical work of this thesis has been performed at the **Research Center Jülich** in Jülich in the group of Bioprocesses and Bioanalytics of the Institute of Biotechnology from 2014 to 2017 under the supervision of **Dr. Stephan Noack**.

Reviewers:

Main reviewer: Jun. -Prof. Dr. Alexander Grünberger
Professor for Multiscale Bioengineering
Chair of Multiscale Bioengineering,
Bielefeld University

Secondary reviewers: Prof. Dr. Wolfgang Wiechert
Director at IBG-1, Forschungszentrum Jülich and
Professor for Computational Systems Biology,
RWTH Aachen University

Prof. Dr. Karl Friehs
Professor for Fermentation Technology
Chair of Fermentation Engineering,
Bielefeld University

Printed on non-ageing paper ISO 9706

Parts of this thesis have been published in:

- Unthan S*, **Radek A***, Wiechert W, Oldiges M, Noack S, (2015) Bioprocess automation on a Mini Pilot Plant enables fast quantitative microbial phenotyping. *Microbial Cell Factories* 14:32 **equal contribution*
- **Radek A**, Krumbach K, Gätgens J, Wendisch VF, Wiechert W, Bott M, Noack S, Marienhagen J, (2014) Engineering of *Corynebacterium glutamicum* for minimized carbon loss during utilization of D-xylose containing substrates. *Journal of Biotechnology* 192, 156:160
- **Radek A**, Müller MF, Gätgens J, Eggeling L, Krumbach K, Marienhagen J, Noack S, (2016) Formation of xylitol and xylitol-5-phosphate and its impact on growth of D-xylose-utilizing *Corynebacterium glutamicum* strains. *Journal of Biotechnology* 231, 160-166
- **Radek A***, Tenhaef N*, Müller MF, Brüsseler C, Wiechert W, Marienhagen J, Polen T, Noack S, (2017) Miniaturized and automated adaptive laboratory evolution: Evolving *Corynebacterium glutamicum* towards an improved D-xylose utilization. *Bioresource technology *equal contribution*
- Steffen V, Otten J, Engelmann S, **Radek A**, Limberg M, Koenig BW, Noack S, Wiechert W, Pohl M, (2016) A Toolbox of Genetically Encoded FRET-Based Biosensors for Rapid L-Lysine Analysis. *Sensors*, 16(10), 1604.
- Baumgart M, Unthan S, Kloss R, **Radek, A.**, Polen T, Tenhaef N, Müller MF, Küberl A, Siebert D, Brühl N, Marin K, Hans S, Krämer R, Bott M, Kalinowski J, Wiechert W, Seibold G, Frunzke J, Rückert C, Wendisch VF, Noack S, (2017) *Corynebacterium glutamicum* chassis C1*: Building and testing a novel platform host for synthetic biology and industrial biotechnology. *ACS synthetic biology*.
- Brüsseler C, **Radek A**, Tenhaef N, Krumbach K, Noack S, Marienhagen J, (2017) The *myo*-inositol/proton Symporter IolT1 contributes to D-xylose uptake in *Corynebacterium glutamicum*. *Bioresource technology*.
- Tenhaef N, **Radek A**, Gätgens J, Krumbach K, Marienhagen J, Noack S, (2017) D-xylonate production using a non-genetically modified *Corynebacterium glutamicum* strain. (*manuscript in preparation*).

Parts of this thesis have been published as patents:

- **Radek A**, Krumbach K, Marienhagen J, Noack S, Verfahren zur Herstellung von D-Xylonat und coryneformes Bakterium PT1.2754 (2016).

Lecture on excerpts of the work was held at:

- Society for Industrial Microbiology and Biotechnology (SIMB) Annual Meeting 2014, Saint Louis Missouri, USA. Title: *"Microscale assay development for advanced microbial phenotyping in higher throughput"*

Posters were presented at:

- DECHEMA Himmelfahrtstagung 2015, Hamburg. Title: *"Bioprocess Automation for Fast Microbial Strain Selection and Detailed Quantitative Phenotyping"*
- Chalmers PhD Course "Industrial Biotechnology for Lignocellulose Based Processes" 2015, Göteborg, Sweden. Title: *Engineering of Corynebacterium glutamicum as platform for flexible and efficient utilization of D-xylose containing feedstocks*

"Life is like riding a bicycle, to keep your balance you must keep moving."

Albert Einstein

Abstract

Establishing the Weimberg pathway in *Corynebacterium glutamicum* as an alternative route for D-xylose utilization

by Andreas Willi RADEK

In times of scarcity of fossil resources and climate change, the need of renewable resources for the biobased economy becomes increasingly important. Within this thesis a contribution was done to achieve the aim to produce chemicals biobased and not anymore only petrochemical based. To accomplish this, the industrial relevant microorganism *Corynebacterium glutamicum* was engineered to utilize the hemicellulose derived pentose sugar D-xylose via an alternative pathway. This utilization was made feasible via the Weimberg pathway without loss of carbon in terms of products derived from alpha-ketoglutarate. During the first investigation two major by-products, D-xylonate and xylitol, of the new synthetic pathway were found. The latter is known as inhibitor of different microorganisms, which could be also confirmed in this thesis for *C. glutamicum*. The inhibition studies showed different target genes, which are partly responsible for this inhibitory effect (e.g. *xylB*). Interestingly, the reference strain in this thesis, a strain expressing the isomerase pathway (including the *xylB* gene), was already inhibited by low amounts of extracellular xylitol and accumulates the highest amount of intracellular xylitol-5-phosphate.
Within this thesis a high amount of engineered strains had to be screened and charaterized. Therefore, it was the initial aim to develop new robotic workflows and automated enzymatic assays on a robotic platform. The extended Mini Pilot Plant enables now the high-throughput microbial phenotyping with connected analytics in 384-well format. Further, it is now possible to run a complete process with separation of cell-free supernatants for analytics under sterile conditions without human interruption. Another new robotic workflow which was designed within this thesis is the miniaturized and automated repetitive batch cultivation. The developed workflow was used for fully automated adaptive laboratory evolution (ALE) of the engineered *C. glutamicum* strain expressing the Weimberg pathway for D-xylose utilization. The ALE process was successful and the final strain had an 260% increased maximal growth rate of μ_{max} = 0.26 h^{-1}on D-xylose as sole carbon source. The final D-xylose utilizing strain ($WMB2_{evo}$) grows stable during lab-scale bioreactor operation, which demonstrates the high potential of this strain for future projects with biorefinery applications. Additionally, the occurred mutations during the ALE process were analyzed by genome sequencing and revealed about 15 potential key mutations for improved D-xylose assimilation. These found mutations can be used for rational strain engineering within further biorefinery projects. But for now the final D-xylose utilizing strain ($WMB2_{evo}$) is the fastest growing *C. glutamicum* strain on D-xylose as sole carbon source in literature.

Kurzfassung

Etablierung des Weimberg Stoffwechselweges in *Corynebacterium glutamicum* als alternative Route zur D-xylose Verstoffwechselung

In Zeiten des Klimawandels und des zunehmenden Verbrauchs an fossilen Rohstoffen nimmt der Bedarf an nachwachsenden Rohstoffen und deren direkter Verarbeitung, sowie auftretender Abfallströme, für die Bioökonomie stetig zu. Mit der vorliegenden Arbeit wird ein Beitrag dazu geleistet, Chemikalien nicht weiterhin nur petrochemisch sondern auch bio-basiert produzieren zu können. Das in der industriellen Biotechnologie weitverbreitet eingesetzte Bakterium *Corynebacterium glutamicum* wurde dazu so verändert, dass eine effiziente Verstoffwechslung, des aus Hemicellulose gewonnenen Pentose-Zuckers D-Xylose erreicht wurde. Diese Verstoffwechslung ist nun über den sogenannten Weimberg Stoffwechselweg möglich, der im Gegensatz zu anderen Stoffwechselwegen D-Xylose ohne Kohlenstoffverlust zu Produkten abgeleitet von alpha-Ketoglutatrat umsetzt. In den ersten Untersuchungen von diesem neuen synthetischen Stoffwechselweg wurden zwei Nebenprodukte (D-Xylonat und Xylitol) entdeckt. Wobei Xylitol als Wachstumsinhibitor für verschiedene Mikroorganismen bekannt ist, was in dieser Arbeit auch für *C. glutamicum* in verschiedenen Inhibierungsstudien gezeigt werden konnte. Zur generellen Stammcharakterisierung und für die Inhibierungsstudien wurde in dieser Arbeit eine Vielzahl an gentechnisch veränderten Stämmen kultiviert. Daher war es das initiale Ziel zunächst neue Prozesse auf einer Robotik Plattform zu etablieren. So wurden u.a. neue analytische enzymatische Assays etabliert, wie auch komplett automatisierte Prozesse entwickelt. Die nun erweiterte Mini Pilot Plant ermöglicht das Hochdurchsatzscreening zur mikrobiellen Phänotypisierung mit angeschlossener Analytik im 384-well Format. Des Weiteren ist es nun möglich komplette Prozesse mit Zellseparation für angeschlossene Analytik voll automatisiert unter sterilen Bedingungen ablaufen zu lassen.

Ein weiterer entwickelter Prozess ist die miniaturisierte und automatisierte repetitive Satz-Kultivierung. Dieser Prozess kann für Langzeitkultivierungen genutzt werden oder für die adaptive Labor Evolution (ALE). Mit diesem ALE Prozess wurde ein optimierter D-xylose verstoffwechselnder *C. glutamicum* Stamm $WMB2_{evo}$ generiert. Dieser Stamm weist eine um 260 % höhere Wachstumsrate als der Ausgangsstamm auf und ist mit $\mu_{max} = 0.26\ h^{-1}$der derzeit schnellst-wachsende *C. glutamicum* Stamm auf D-Xylose. Zudem ergaben die Untersuchungen der Genom Sequenzierung des adaptierten Stammes ca. 15 Hauptmutationen, welche im Zusammenhang mit der verbesserten D-Xylose Verstoffwechslung stehen könnten. Auf diesen Mutationen aufbauend können wiederum neue D-Xylose verstoffwechselnde Stämme gezielt entwickelt werden. Da jedoch der $WMB2_{evo}$ Stamm äußerst stabil im Labormaßstab wächst, bietet er sich bereits für weitere Bioraffinerie Projekte an.

Danksagung

Zunächst einmal möchte ich mich für die sehr angenehme und motivierende Atmosphäre in der Arbeitsgruppe von Herrn **Prof. Dr. Marco Oldiges** (Bioprozesse und Bioanalytik) und im Speziellen dem Team von Herrn **Dr. Stephan Noack** (Quantitative Microbial Phenotyping) bedanken. Durch die sehr kommunikative und freundliche Arbeitsumgebung, sowie die fruchtbaren Statusseminare, konnte ich meine Arbeit stets weiter ausbauen und verfeinern.

Ein ganz besonderer Dank gilt dabei Herrn **Dr. Stephan Noack**, dem Betreuer meiner Doktorarbeit. Ich hätte mir keinen besseren Supervisor vorstellen können. So hattest du für alle meine Anliegen stets ein offenes Ohr und konntest mir immer sehr konstruktiv und fast väterlich unter die Arme greifen. Dafür von ganzem Herzen meinen Dank Stephan! Ich wünsche dir, dass du deinen Weg weiter so gehen kannst und so bleibst wie du bist!

Des Weiteren möchte ich Herrn **Prof. Dr. Wolfgang Wiechert** dafür danken, dass ich meine Doktorarbeit am Institut für Biotechnologie am IBG-1 des Forschungszentrums Jülich anfertigen durfte und er als mein Doktorvater mir auch stets mit offenen Ohren zur Seite stand und mich, wo immer es ging, unterstützt hat.

So will ich mich auch hiermit bedanken, dass mich meine Vorgesetzten nach meinem schweren Unfall persönlich in meiner langen Reha besucht haben. Dies hat mir enorm viel Kraft gegeben schnell wieder zurück zu meiner Arbeit zu finden.

Mein weiterer Dank gilt auch Herrn **Prof. Dr. Alexander Grünberger**, welcher mir während der Zeit meiner Doktorarbeit am Forschungszentrum Jülich mit diversen Kooperationsprojekten in der Mikrofluidik und vielen intensiven Gesprächen sehr geholfen hat das Ziel am Ende des Tunnels nicht aus den Augen zu verlieren. Ich möchte mich daher auch ganz besonders herzlich bedanken, dass du dich nach deinem Wechsel an die Universität Bielefeld, bereit erklärt hast die Begutachtung meiner Arbeit zu übernehmen. Für deine Zeit in Bielefeld wünsche ich dir alles erdenklich Gute!

Ein Großteil dieser Doktorarbeit wäre jedoch nicht ansatzweise möglich gewesen ohne meine Kooperationspartner, welche die molekularbiologischen Arbeiten übernommen haben. Unter der Leitung von **Dr. Jan Marienhagen** hat mir **Karin Krumbach** quasi wöchentlich neue Stämme generiert, welche ich dann charakterisieren und kultivieren konnte. Diese enorm produktive und extrem freundliche Zusammenarbeit war einzigartig und hat mir enorm viel bedeutet. Daher dafür mein ganz besonderer Dank an euch Beide!

Eine Person muss ich ganz besonders aus unserer Arbeitsgruppe hervorheben und das ist **Jochem Gätgens**. Denn ohne dich lieber Jochem und deine Hingabe am GC-ToF-MS hätten wir nicht so schnell die Nebenprodukte des neuen Stoffwechselweges identifizieren können und die Stämme weiter charakterisieren können. Deine einzigartige Hingabe zur Forschung und die Diskussionen mit dir über die Ergebnisse haben mich sehr inspiriert und motiviert, vielen Dank dafür!

Zudem wäre es mir nicht alleine möglich gewesen eine solche Vielzahl an Ergebnissen zu generieren ohne die Mithilfe meiner Studenten **Arabel Eich** und **Moritz Fabian Müller**. Vielen Dank euch beiden für die hervorragende Unterstützung und euren Elan im Labor. Dir lieber Moritz wünsche ich weiterhin viel Erfolg in der Arbeitsgruppe als Ingenieur und dir Arabel weiterhin viel Erfolg bei deinem Studium. Bleibt einfach beide so wie ihr seid!

Aber auch neben dem Anfertigen der Doktorarbeit hatte ich eine ganz besonders schöne Zeit in Jülich, und dies lag besonders an dem „Nebenprojekt“ des Bierbrauens mit meinen Kollegen und Freunden von **JuBräu**. Eine echt starke Truppe mit der es immer wieder Spaß gemacht hat auch mal komplette Samstage an der Arbeitsstelle zu verbringen. Ihr seid super, danke!

Aus diesem Team ist dann ein nicht minder erfolgreiches und motivierendes „Nebenprojekt“ entstanden, welches mir auch viel Halt in schwierigen Zeiten gegeben hat, nämlich unsere Ausgründung **RheinCraft**. Es bedeutet mir sehr viel Teil dieses Teams zu sein und ich bedanke mich hiermit für all eure Unterstützung und all das was wir bisher erreicht haben. Danke an euch und weiter so!

All die letzten Jahre meines Studiums, die Auslandsaufenthalte in Vancouver und Boston sowie diese Doktorarbeit hätte ich nicht so gut überstanden, hätte ich nicht eine so geniale **Familie** und einen solch tollen **Freundeskreis** um mich gehabt. Meine **Eltern** und meine **Schwestern** geben mir den Halt, den ich gebraucht habe um auch schwierige und aussichtslose Phasen durchzustehen. Deshalb hiermit an euch alle meinen ganzen Dank dafür dass ihr immer für mich da seid!

Den wichtigsten Anteil an dem Gelingen dieser Doktorarbeit und meinem gesamten Weg zurück nach einer langen Auszeit, sowie der ganz besondere Halt in meinem Leben gilt meiner einzigartigen **Frau Constanze**. Ohne dich mein Schatz wäre mir diese Arbeit so nicht möglich gewesen. In Liebe, vielen Dank für alles!

Contents

Abstract **vii**

Danksagung **ix**

Contents **xi**

List of Figures **xii**

List of Tables **xiii**

List of Abbreviations **xiv**

1 Introduction and Background **1**
1.1 Biobased economy 1
1.2 Lignocellulosic biomass 2
1.3 *Corynebacterium glutamicum* as microbial workhorse 5
1.4 Accelerated microbial phenotyping via miniaturization and lab automation 7
1.5 Adaptive laboratory evolution for strain development 9

2 Aims of this work **11**

3 Results and Discussion **13**
3.1 Bioprocess automation on a Mini Pilot Plant enables fast quantitative microbial phenotyping 13
3.1.1 Short introduction to this manuscript 13
3.1.2 Manuscript I 15
3.1.3 Main achievements of this manuscript 27
3.2 Engineering of *Corynebacterium glutamicum* for minimized carbon loss during utilization of D-xylose containing substrates 28
3.2.1 Short introduction to this manuscript 28
3.2.2 Manuscript II 30
3.2.3 Supplementary material 36
3.2.4 Main achievements of this manuscript 46
3.3 Formation of xylitol and xylitol-5-phosphate and its impact on growth of D-xylose-utilizing *Corynebacterium glutamicum* strains 47
3.3.1 Short introduction to this manuscript 47

3.3.2 Manuscript III 48
3.3.3 Supplementary material 56
3.3.4 Main achievements of this manuscript 61
3.4 Miniaturized and automated adaptive laboratory evolution: Evolving *Corynebacterium glutamicum* towards an improved D-xylose utilization 62
3.4.1 Short introduction to this manuscript 62
3.4.2 Manuscript IV 63
3.4.3 Supplementary material 73
3.4.4 Main achievements of this manuscript 76

4 Conclusions and Outlook **77**

Bibliography **82**

List of Figures

1.1 Composition of terrestrical biomass 2
1.2 Structure of lignocellulosic biomass 3
1.3 Electron micrograph of wild-type *Corynebacterium glutamicum* 5
1.4 Relation between bioprocess scales 7

3.1 Mini Pilot Plant 14
3.2 Weimberg pathway expression plasmid 29
3.3 Selected chromatograms from untargeted metabolome screening . . . 40
3.4 Selected chromatograms showing the depletion of D-glucose after 20 h of cultivation. 41
3.5 Selected chromatograms showing the depletion of D-xylose after 30 h of cultivation. 42
3.6 Selected chromatograms showing the by-product formation of D-xylonate. 43
3.7 Selected chromatograms showing the accumulation of xylitol. 44
3.8 Automated estimation of specific growth rates from online backscatter data 74

List of Tables

3.1 Oligonucleotides used in manuscript II 38
3.2 Strains and plasmids used in manuscript II. 39
3.3 Oligonucleotides used in manuscript III 57
3.4 Differential expression of proteins in C. glutamicum WT P during growth on D-xylose containing media. 59

List of Abbreviations

ALE	**A**daptive **L**aboratory **E**volution
BDO	**1**,4-**B**utane**di**o**l**
CAS	**C**RISPR-**as**sociated
CRISPR	**C**lustered **R**egularly **I**nterspaced **S**hort **P**alindromic **R**epeats
DO	**D**issolved **o**xygen
FACS	**F**luorescence-**a**ctivated **c**ell **s**orting
GC-ToF	**G**as **c**hromatography coupled **t**ime-**o**f-**f**light mass spectrometry
GRLP	**G**enome **r**educed **L**-lysine **p**roducer strain
HPLC	**H**igh **p**erformance**l**iquid **c**hromatography
IPTG	**I**so**p**ropyl-β-D-**t**hio**g**alactopyranosid
ISO	**Iso**merase strain
MPP	**M**ini**P**ilot **P**lant
MTP	**M**icro**T**iter **P**late
NAD(P)H	**N**icotinamide**a**denine **d**inucleotide **p**hosphate reduced
OTR	**O**xygen**T**ransfer **R**ate
PEP	**P**hosho**e**nol**p**yruvate
PHK	**P**hosho**h**o**k**etolase
PPP	**P**entose**p**hosphate **p**athway
RI	**R**efractive **i**ndex
rpm	**R**evolutions **p**er **m**inute
TCA	**T**ri**c**arboxylic **a**cid
WMB	**W**ei**mb**erg strain

Für meine großartigen Eltern ***Maria und Willi,***
meine wundervolle und liebenswerte Frau ***Constanze***
und unsere bezaubernde Tochter ***Madita!***

Chapter 1

Introduction and Background

1.1 Biobased economy

In view of rare fossil resources, climate change and the growing world population, it has become urgent to develop sustainable strategies that enable efficient use of the natural resources on planet earth. Many products we use every day are based on petroleum, which represents the most important source of raw materials and energy for the chemical industry. But the usage of fossil resources such as petroleum, coal and gas represent an appreciable burden on our climate and our environment. Therefore, the biobased economy can provide an essential contribution to the solution of these problems and has been raised attention since several years (Langeveld et al. 2010).

Biobased economy offers the opportunity to achieve economic growth in harmony with the protection of nature and environment. The field of biobased economy also describes a sustainable market which can be predicted for technologies that produce chemicals, materials and pharmaceuticals from plant-based feedstocks (Sanders et al. 2007).

To make the efficient use of renewable resources possible, the biobased economy has to cover all industrial and economic sectors. This means to use these resources for producing products and providing services using innovative biological and technological knowledge and processes. Areas for the application of these new knowledge and new processes can be found in agriculture, forestry, energy sector, fisheries and aquaculture, chemistry and pharmacy, the food industry, industrial biotechnology, cosmetics, paper and textile industries as well as environmental protection (McLaren 2005). In particular in the field of industrial biotechnology the replacement of petrochemical processes by usage of microorganisms to produce highly added-value products is a major aim.

1.2 Lignocellulosic biomass

The predominantly components of terrestrical biomass are cellulose, hemicellulose, lignin, lipids, proteins, sugars and starch, whereby over 90 % of this biomass is lignocellulose (Figure 1.1). Cellulose is the main part of lignocellulosic material, and is comprised of a crystalline structure of D-glucose molecules, which are linked to one another primarily by glycosidic bonds. Hemicellulose, the second most abundant constituent (up to 40 %), is not a chemically well-defined compound but rather a family of polysaccharides, composed of different C5- and C6-monosaccharide units (mainly D-xylose and further, e.g., D-glucose, D-galactose, D-mannose, D-arabinose) (Figure 1.2). It links cellulose fibres into microfibrils and cross-links with lignin, creating a complex network of bonds that provide structural strength (Scheller and Ulvskov 2010). Lastly lignin, a three-dimensional polymer of phenylpropanoid units, can be described as the cellular glue, providing the plant tissue and the individual fibres with compressive strength and the cell wall with stiffness. Furthermore, it provides resistance to insects and pathogens (Rubin 2008).

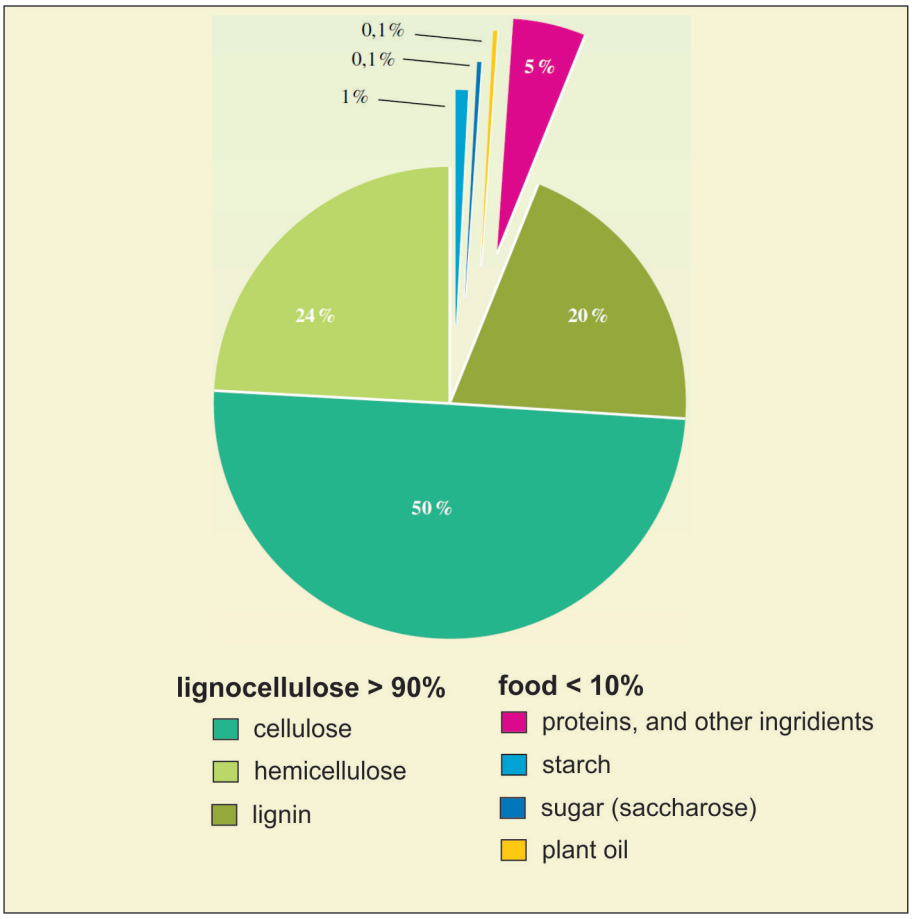

FIGURE 1.1: Composition of terrestrical biomass. Modified according to: (Acatech 2012).

Recently, lignocellulosic biomass was recognized as a potential feedstock for the industrial biobased economy to replace finite hydrocarbons. This is because of less expenses for waste streams of lignocellulosic biomass like corn stover, sugarcane bagasse or wooden material compared to the usage of refined sugars, like D-glucose (from starch hydrolysates) or D-fructose and sucrose (from molasses) for fermentation. Therefore, there is no conflict with agriculture in view of land use. Hence in recent years, much research was started in this new field of industrial biotechnology to use this new feedstocks based on plant biomass.

The composition of plant biomass is very well known since decades. In particular its complex structure is very recalcitrant for bio-degradation and therefore it is not possible to use it directly as feedstock for industrial biotechnology processes.

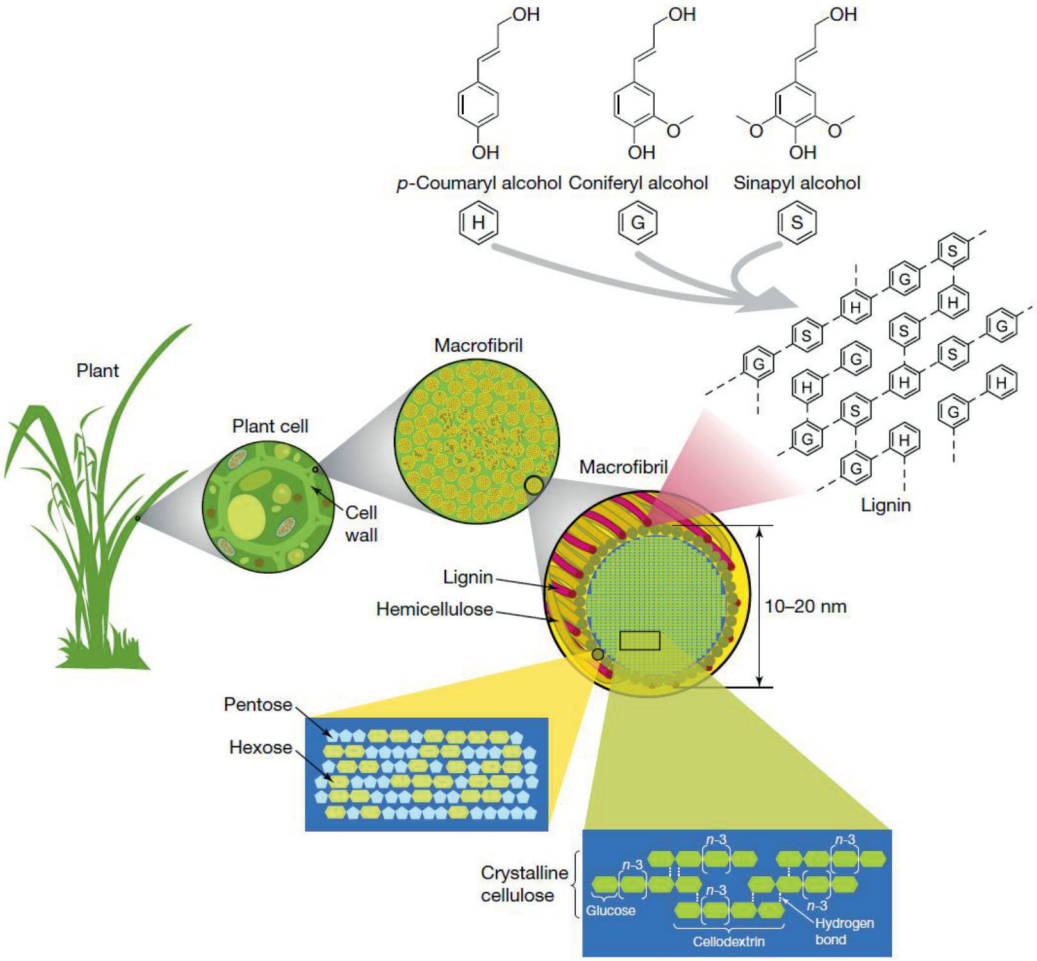

FIGURE 1.2: Structure of lignocellulosic biomass. Source: (Rubin 2008)

Consequently, before the usage as biotechnological feedstock, it must firstly be pretreated, either via chemical (e.g. acidic or alkaline hydrolysis), physical (e.g. steam

pretreatment, hot water extraction, wet oxidation) (Galbe and Zacchi 2012) or enzymatic methods (e.g. cellulases) (Alvira et al. 2010). Some of these pretreatments produce inhibitors like furfural and 5-hydroxymethylfurfural, which decrease the overall yield of the putative fermentation process, because of inhibition of the cell growth (Almeida et al. 2007). Since all of the listed processes have benefits and challenges, usually a cascade of combined processes is used to generate suitable feedstock streams with preferably low amounts of inhibitors.

Furthermore, the choice of the lignocellulosic raw material has a great impact on the final feedstock stream quality. For example, switchgrasses are rich in D-xylose, due to their cell wall composition of mainly glucuronoarabinoxylan and xyloglucans (Scheller and Ulvskov 2010), whereas softwood like pine is rich in glucomannan and lignin (Olsson 2004).

1.3 *Corynebacterium glutamicum* as microbial workhorse

The discovery of the Gram-positive soil bacterium *Corynebacterium glutamicum* 60 years ago in Japan (Kinoshita et al. 1957) was a milestone for industrial biotechnology. The aim of Kinoshita and his colleagues was to find a microbial strain which was able to produce the important flavor enhancer L-glutamate. They named this microorganism *Micrococcus glutamicus* because of its coccal appearance at first view. After further taxonomical studies the bacterium was renamed to *Corynebacterium glutamicum* because of its rod-shape phenotype (Abe et al. 1967; Eggeling and Bott 2005) (Figure 1.3).

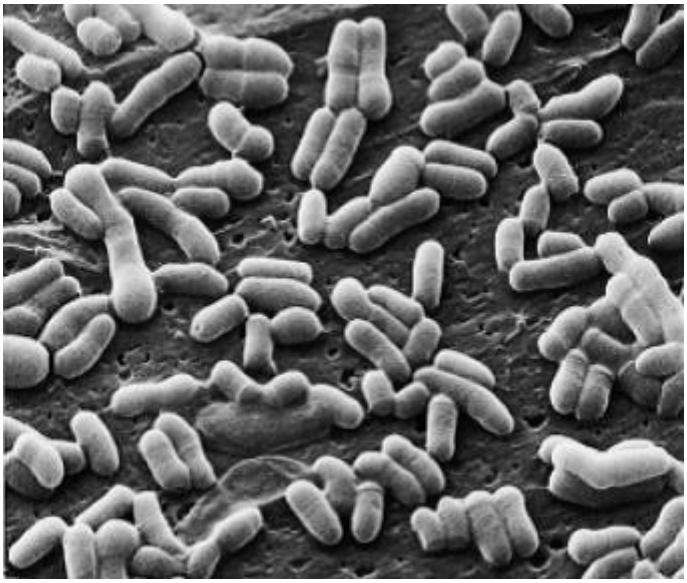

FIGURE 1.3: Electron micrograph of wild-type *Corynebacterium glutamicum*. Source: (Sahm et al. 2000)

Besides the commercial production of amino acids, like L-glutamate (2 million tons per year) and L-lysine (1.5 million tons per year), *C. glutamicum* is engineered towards the production of biobased chemicals and materials like 1,5-diaminopentane (cadaverine) and 1,4-diaminobutane (putrescine), which serve as important monomers for biobased polyamides (Kind and Wittmann 2011).

Important for metabolic engineering of this industrial workhorse was the availability of the complete genome sequence (3,283 kb) of the wild-type strain *C. glutamicum* ATCC 13032 (Kalinowski et al. 2003). Since then this organism was intensely studied as a model system and as a host for industrial process development using powerful metabolic engineering methods. Especially the latest achievements in systems biotechnology (Sahm et al. 2000; Wendisch 2007) including mechanistic pathway modeling (Wiechert and Noack 2011) further increased the product portfolio of *C.*

glutamicum as well as the fundamental knowledge on cellular metabolism. More recently, *C. glutamicum* was engineered towards a novel chassis organism for industrial biotechnology containing a minimized genome (Unthan et al. 2015). Furthermore, new synthetic biology methods like CRISPR/Cas for fast targeted metabolic engineering were developed and successfully applied to this microorganism (Cleto et al. 2016; Peng et al. 2017).

With respect to its substrate spectrum *C. glutamicum* has been genetically modified to use starch, cellobiose, D-galactose and L-arabinose as additional carbon and energy sources (Barrett et al. 2004; Kotrba et al. 2003; Seibold et al. 2006). Unfortunately, the key building block of hemicellulose, the pentose sugar D-xylose, cannot be directly utilized by *C. glutamicum* (Meiswinkel et al. 2013). Consequently, there is a strong motivation for engineering this host for D-xylose utilization by introduction of suitable heterologous genes and functional expression thereof (Aristidou and Penttilä 2000; Kawaguchi et al. 2006). The frequently integrated pathway for D-xylose utilization in *C. glutamicum* is the so called isomerase pathway, consisting of the two enzymes XLI (xylose isomerase) and XLK (xylulose kinase) (Kawaguchi et al. 2006; Meiswinkel et al. 2013; Sasaki et al. 2009). For the production of alpha-ketoglutarate-derived products such as L-glutamate, and L-proline, this pathway, however, has the drawback that a significant fraction of the carbon from D-xylose is lost in the form of CO_2, lowering the overall product yield. Here, the so called Weimberg pathway first discovered in *Pseudomonas fragi* and later also in *Haloferax volcanii* and *Caulobacter crescentus* (Johnsen et al. 2009; Stephens et al. 2007; Weimberg 1961) represents a promising alternative for an efficient D-xylose assimilation. By this route, D-xylose is directly oxidized to alpha-ketoglutarate in five sequential steps, that can be operated orthogonal to the central metabolism.

1.4 Accelerated microbial phenotyping via miniaturization and lab automation

Novel techniques in molecular biology for fast and reliable strain engineering as well as multifactorial bioprocess optimization demand for rapid microbial phenotyping approaches. The classical way of strain phenotyping is based on cultivation experiments in baffled shake flasks (V = 50 - 500 mL) or lab-scale bioreactors (V = 1 - 5 L), which is related to substantial manual work and material input (Figure 1.4). Therefore there is a high demand of miniaturization and lab automation in the field of industrial biotechnology, to increase reproducibility, throughput as well as to reduce human effort and material costs (Scott C. 2010; Sonnleitner 1997).

In the red (pharmaceutical) biotechnology such technologies are already well established since years and used for small molecule screenings and drug-target-interaction studies (Smith 2002). In the field of white (industrial) biotechnology a similar development is slowly progressing and one simple reason is that bioprocess development is much more complex than substance or interaction screening.

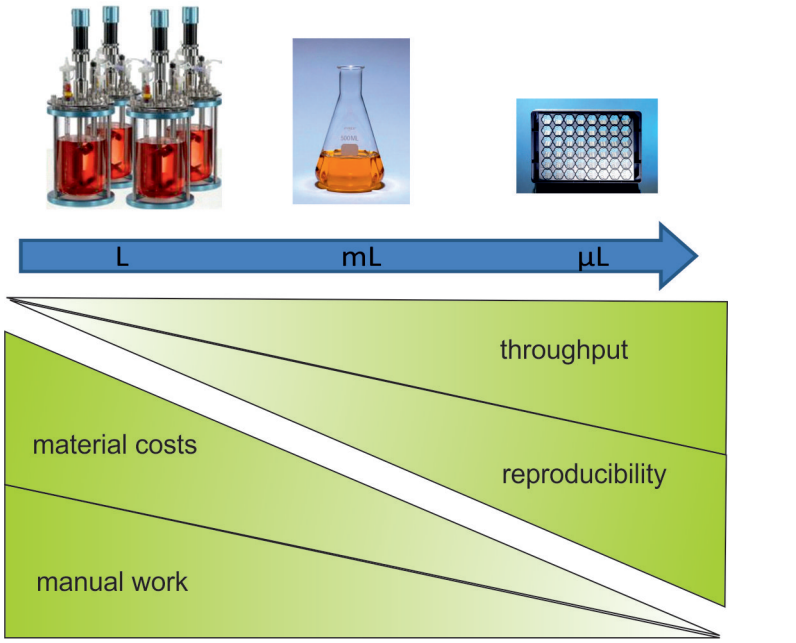

FIGURE 1.4: Relation between bioprocess scales, process insight and experimental throughput.

To get more information out of the screening approaches, miniaturized cultivation devices (V = 0.5 - 3 mL) should be integrated into liquid handling platforms to allow complete automation of the bioprocess development. However, until now only a few examples exist in this developing field (Hemmerich and Kensy 2013; Huber et al. 2009; Knepper et al. 2014; Rohe et al. 2012). Nevertheless, the overall benefits of

any liquid handling platform are faster sample processing and higher reproducibility of results, which is because of the independent pipetting actions from the accuracy of the manual operators (Sonnleitner 1997).

In recent years different types of microscale cultivation devices were developed, which vary from miniaturized stirred tank reactors (e.g. ambr, Satorius) via shaken bubble columns (e.g. Micro-24, Pall) to MTP-based systems (e.g. BioLector, m2p-labs). Due to the application in this work, the focus will be on the MTP-based BioLector system in the following.

The BioLector is designed for cultivation experiments in 48-well baffled microtiter plates (FlowerPlates, m2p-labs), with a maximal working volume of 1 mL (Funke et al. 2009). The baffled well geometry enables a higher turbulence in the culture during shaking and the resulting oxygen transfer rate (OTR) with a maximal k_La of 600 h^{-1} (Funke et al. 2009),which is clearly higher than in standard round 96-well plates with 150 - 160 h^{-1} (Hermann et al. 2003). Additionally, the temperature as well as the humidity is controlled to prevent evaporation. Moreover, the BioLector integrates online monitoring of biomass via light scattering (backscatter) (Samorski et al. 2005), dissolved oxygen (DO) and pH via immobilized fluorophores on the well bottom (John et al. 2003), as well as products through fluorescence detection with specific integrated LED filters (Kensy et al. 2009). All these signals can be measured while shaking the microtiter plate without interrupting the cultivation.

1.5 Adaptive laboratory evolution for strain development

Over the past decades different strategies have been developed for strain engineering within the field of microbial biotechnology. On the one hand, targeted engineering is conducted with the help of different genetic tools, e.g. plasmid-based gene expression, Gibson Assembly and nowadays the CRISPR/Cas technology. In many cases several rounds of strain modification and phenotyping are necessary to finally obtain a robust and sufficiently productive mutant. Hence, targeted strain engineering can be very time consuming. On the other hand, there is a natural mechanism which can be used for untargeted strain development, which relies on the ability of microorganisms to adapt quickly to changing environmental conditions. Already a decade ago the adaptive laboratory evolution (ALE) was developed as a valuable method in metabolic engineering for strain development and optimization (Maaheimo H et al. 2001). During microbial ALE, a microorganism is cultivated under clearly defined conditions for prolonged periods of time, in the range of weeks to years, which allows the selection of improved phenotypes. Thus in contrast to rational strain engineering strategies by selected targeted mutations, the undirected evolution of microorganisms has still benefits. The main benefit is that the microorganisms can adapt, during ALE, via the occurence of broad mutations. These mutations can occur in many different genes or regulatory regions in parallel. Moreover, due to new technologies, including massive next-generation DNA sequencing (Liu et al. 2012), phenotype-genotype correlations can be easily obtained.

Especially for industrial biotechnology different ALE strategies have become widely available, for example to improve product yields (Fong et al. 2005), or to activate latent pathways of non-native substrates, shown for 1,2-propanediol utilization in *E. coli* (Lee and Palsson 2010). Moreover, it was recently shown that developing of high-copy numbers of plasmids in *C. glutamicum* by applying ALE is possible (Choi et al. 2017).

In most ALE processes the key selection criterion is an increased growth rate, since cells with a higher growth rate inherently prevail during cultivation. Nowadays ALE is mainly used to utilize nonnative substrates or to produce nonnative products by increasing the robustness of the engineered strains against the desired substrates or products. (Atsumi et al. 2010; Fischer et al. 2010). Besides, ALE was successfully applied to enhance the growth performance of microbial strains (Cheng et al. 2014; Li et al. 2015), as well as, to increase the productivity by using stress conditions (Reyes et al. 2014; Yu et al. 2013). Furthermore, ALE strategies were developed to increase productivity, e.g., by selection using a biosensor and FACS (Mahr et al. 2015) or by enhancing tolerance against the target product (Mundhada et al. 2017). Moreover, ALE was already successfully applied to adapt biotechnologically relevant microorganisms to lignocellulosic material (Qin et al. 2016; Wang et al. 2014), to improve

biodegradation capabilities (Lasik et al. 2010) and to improve the robustness against lignocellulose derived inhibitors (Wang et al. 2017).

Routinely, ALE experiments are performed in shaking flasks or in lab-scale bioreactors either in continuous cultivation or repetitive batch mode (Dragosits and Mattanovich 2013; Portnoy et al. 2011). Due to long experimentation times and many manual handling steps these approaches are challenging and prone to errors. Although first microfluidic systems have already been developed (Sjostrom et al. 2014), no system is currently available that enables to run ALE experiments under process conditions similar to lab-scale bioreactors and in a fully automated manner without any user intervention.

Chapter 2

Aims of this work

D-xylose as alternative substrate for *C. glutamicum*

Lignocellulosic biomass is the most abundant biomass on earth. It arises especially as waste streams from agriculture products like corn, sugarcane, rice or palm oil. Thus it would be great to use this biomass also as feedstock for industrial biotechnology applications in a future biobased economy.

As D-xylose is the main building block for the hemicellulose xylan, it is one of the most abundant sugars derived from lignocellulosic biomass. Unfortunately, the industrially relevant microbial workhorse *C. glutamicum* is not able to utilize this pentose naturally.

Therefore it is the major aim of this thesis to engineer a *C. glutamicum* strain which can efficiently utilize D-xylose. It is the major goal to establish a new pathway for D-xylose utilization into *C. glutamicum*, which has no carbon loss on the route to alpha-ketoglutarate. The Weimberg pathway, found in different bacteria and archaea, meets this requirement and it has also the potential to express this pathway growth decoupled for production of interesting products derived from alpha-ketoglutarate (like 1,4-butanediol or succinate). The Weimberg pathway from *Caulobacter crescentus*, a Gram-negative fresh water bacterium, should be functionally integrated into *C. glutamicum*. For comparison and evaluation of the engineered strain the already established, so called, isomerase pathway for D-xylose utilization will be used. Especially the growth phenotype of both strain backgrounds will be compared, but also the analysis of the by-product spectrum is of main interest.

Robotic workflows and new automated bioprocesses

Classically strain phenotyping is performed in baffled shake flasks or bioreactors, which means high material costs and human effort. With MTP-based microscale devices it becomes possible to screen a high number of strains in parallel under various environmental conditions.

In this thesis new enzymatic assays and robotic workflows will be integrated into a Mini Pilot Plant to enable the characterization of the substrate uptake or product formation in more detail. Finally, this should replace expensive and time consuming HPLC and LC-MS measurements. Furthermore, a fully automated harvest procedure should be established, which samples up to 48 wells from BioLector cultivations in response to individually defined trigger conditions. The samples will be clarified by centrifugation and finally frozen for subsequent analysis. This should accelerate the strain engineering and characterization process and also lays the basis for further process development on the robotic platform.

Automated and miniaturized ALE process

D-xylose is not a natural carbon source for *C. glutamicum*, thus it could be worthwhile to adapt this organism additionally, after successful metabolic engineering, via adaptive laboratory evolution (ALE) to this new carbon source. The classical cultivation devices for ALE approaches are baffled shake flasks or bioreactors. Hence, it is one aim of this thesis to miniaturize and automate the ALE process into the microliter scale on the Mini Pilot Plant. At first an automated repetitive batch cultivation must be established as a new robotic workflow on the Mini Pilot Plant. Within such a process the cells can always be transferred into the next cultivation, e.g., when they are in the middle of the exponential growth phase. The final aim of the automated and miniaturized ALE process development is to get an optimized strain, which efficiently utilizes D-xylose and shows a stable high specific growth rate on this new substrate. Further, it is the aim to transfer the results from the microliter scale into laboratory scale to show the applicability of the hopefully optimized strain, harboring an alternative route for an efficient D-xylose utilization, for future biorefinery projects.

Chapter 3

Results and Discussion

3.1 Bioprocess automation on a Mini Pilot Plant enables fast quantitative microbial phenotyping

3.1.1 Short introduction to this manuscript

The Mini Pilot Plant (MPP) technology was initially established by Rohe et al. 2012 for automated preparation of cultivation media and the optimization of heterologous protein expression at microtiter plate scale . The MPP is based on a liquid handling robotic station (JANUS workstation, Perkin Elmer), consisting of a deck accessible by robotic manipulators for the displacement of labware as well as a pipetting arm for liquid manipulation (see Figure 3.1). The liquid pipetting is driven by a sterile system liquid with 8 washable Teflon-coated steel needles for persistent application. The narrow tip diameter allows pipetting in 384-well plates and conductance measurements enable liquid detection during aspiration or dispension steps. For decontamination, the complete hydraulic system as well as the steel needles can be flushed with 70 % ethanol. On the pipetting deck, devices are integrated for sample mixing up to 3000 rpm, sample cooling down to -10 °C as well as heating up to 95 °C. For downstream sample processing a deep well plate centrifuge (IXION, Sias) is connected to the robotic station and for executing of different kinetic assays a MTP plate reader (EnSpire, Perkin Elmer) is integrated. All connected devices can be reached by the robotic manipulator for establishing completely automated processes, which are part of the following manuscripts. Additionally, the microscale fermentation system BioLector (m2p-labs, Baesweiler, Germany) is embedded in the MPP, which enables strain phenotyping at higher throughput. For sterile media preparation as well as independent sampling and dosing during a running process, the complete working station is housed into a laminar airflow.

So far, no robotic workflow has been presented, by which supernatants from biomass in samples from microtiter plate cultivations are automatically separated. Such an at-line clarification would enable the direct analysis of supernatants by applying, e.g., sensitive enzyme assays for substrate and product quantification at microscale.

Therefore, the major aims of this manuscript were the development of a fully automated cell separation procedure as well as different at-line enzymatic assays, which resulted in a reduction of costs and human effort in comparison to HPLC or mass spectrometry measurements. The newly developed methods were applied to screen a library of genome-reduced mutant strains regarding their growth phenotypes (Unthan et al. 2015), as well as to characterize some newly constructed *C. glutamicum* strains in more detail (see chapter 3.2).

FIGURE 3.1: Setup of the Mini Pilot Plant used in this work.

3.1.2 Manuscript I

Bioprocess automation on a Mini Pilot Plant enables fast quantitative microbial phenotyping

Published as:

Unthan S*, Radek A*, Wiechert W, Oldiges M, Noack S, Bioprocess automation on a Mini Pilot Plant enables fast quantitative microbial phenotyping. ***Microbial Cell Factories*** **(2015) 14:32 **equal contribution***

Unthan et al. Microbial Cell Factories (2015) 14:32
DOI 10.1186/s12934-015-0216-6

MICROBIAL CELL FACTORIES

TECHNICAL NOTES Open Access

Bioprocess automation on a Mini Pilot Plant enables fast quantitative microbial phenotyping

Simon Unthan†, Andreas Radek†, Wolfgang Wiechert, Marco Oldiges and Stephan Noack*

Abstract

Background: The throughput of cultivation experiments in bioprocess development has drastically increased in recent years due to the availability of sophisticated microliter scale cultivation devices. However, as these devices still require time-consuming manual work, the bottleneck was merely shifted to media preparation, inoculation and finally the analyses of cultivation samples. A first step towards solving these issues was undertaken in our former study by embedding a BioLector in a robotic workstation. This workstation already allowed for the optimization of heterologous protein production processes, but remained limited when aiming for the characterization of small molecule producer strains. In this work, we extended our workstation to a versatile Mini Pilot Plant (MPP) by integrating further robotic workflows and microtiter plate assays that now enable a fast and accurate phenotyping of a broad range of microbial production hosts.

Results: A fully automated harvest procedure was established, which repeatedly samples up to 48 wells from BioLector cultivations in response to individually defined trigger conditions. The samples are automatically clarified by centrifugation and finally frozen for subsequent analyses. Sensitive metabolite assays in 384-well plate scale were integrated on the MPP for the direct determination of substrate uptake (specifically D-glucose and D-xylose) and product formation (specifically amino acids). In a first application, we characterized a set of *Corynebacterium glutamicum* L-lysine producer strains and could rapidly identify a unique strain showing increased L-lysine titers, which was subsequently confirmed in lab-scale bioreactor experiments. In a second study, we analyzed the substrate uptake kinetics of a previously constructed D-xylose-converting *C. glutamicum* strain during cultivation on mixed carbon sources in a fully automated experiment.

Conclusions: The presented MPP is designed to face the challenges typically encountered during early-stage bioprocess development. Especially the bottleneck of sample analyses from fast and parallelized microtiter plate cultivations can be solved using cutting-edge robotic automation. As robotic workstations become increasingly attractive for biotechnological research, we expect our setup to become a template for future bioprocess development.

Keywords: Mini Pilot Plant, Bioprocess automation, Microtiter plate assay, Scale-up, Scale-down, High-throughput, Screening, Microbial phenotyping, D-xylose, Ninhydrin, L-lysine, *C. glutamicum*

Background

Time is the most limiting factor in the initial establishment of new bioprocesses and currently forces process developers to draw conclusions from few experiments with little process insight. Such early decisions are typical for the screening of strain libraries for an improved production strain or during the first coarse-grained characterization of a set of top producer candidates. Clearly, any misinterpretation of the resulting limited data sets can strongly impair the further process development. To solve this dilemma new technological approaches are needed that enable the fast and quantitative assessment of multiple strains under well-defined cultivation conditions.

To this end, sophisticated microliter scale cultivation devices were established, which overcome some limitations considering process insight by online monitoring of biomass, pH and dissolved oxygen as well as the direct determination of oxygen transfer rates [1,2]. However, all these devices still depend on manual work to

* Correspondence: s.noack@fz-juelich.de
†Equal contributors
Institute of Bio- and Geosciences, IBG-1: Biotechnology, Systems Biotechnology, Forschungszentrum Jülich, 52425 Jülich, Germany

prepare, sample and finally analyze cultivation experiments and, thus, cannot fully remove the bottleneck of today's bioprocess development [3].

To overcome these limitations, we already embedded a microtiter plate cultivation device (BioLector) in a robotic liquid handling platform and could show its benefits for the preparation of cultivation media and the optimization of heterologous protein expression [4]. However, no robotic workflow has been presented yet that automatically separates supernatants from biomass in samples of microtiter plate cultivations. Such an at-line clarification would enable the direct analysis of supernatants applying, e.g., sensitive enzyme assays for metabolite quantification. Moreover, it would minimize the reaction of periplasmic or membrane-bound enzymes with extracellular metabolites as well as leakage of intracellular metabolites from cells to the supernatant during sample storage [5]. Current microliter scale cultivations are also not well suited for determining substrate uptake or metabolite production kinetics of an organism as the removal of an adequate sample volume for offline-analytics critically influences the cultivation conditions. For instance, the volume reduction due to sampling immediately changes the oxygen transfer rates in the particular well of a microtiter plate even in cases with less than 10% volume loss [6]. Fortunately, microtiter plate cultivations in a BioLector system offer high well-to-well reproducibility [1] and hence identically inoculated cultures can be started in parallel wells of which one is harvested at a time.

In this work, we extended our robotic approaches to automate complete workflows for the quantitative phenotyping of small molecule producer strains. The resulting Mini Pilot Plant (MPP) now covers a broad range of procedures to automatically harvest, clarify and analyze BioLector cultivation wells after reaching individual triggers. To enable fast analyses of those clarified samples, photometrical assays were developed to instantly quantify substrate and product metabolites in 384-well plate scale. The established fully automated methods were finally applied to address two basic challenges in bioprocess development, namely to identify top producers from a strain library and to investigate the substrate uptake of a novel engineered strain during mixed carbon source cultivation.

Results and discussion

Improved triggered sampling of cell-free cultivation supernatants

For the screening of protein expression strains, Rohe et al. showed that by transferring cultures to 4°C after their individual turn to stationary phase the amount of produced enzymes could be assessed with higher reproducibility compared to overnight cultivations harvested together at the same timepoint [4]. In this work we further improved the handling of triggered samples on our MPP by introducing additional steps for a rapid centrifugation and freezing to −4°C to generate suitable cell-free samples for subsequent metabolite analyses (Figure 1A).

Our new workflow starts with the harvest of 500 µl from each well of a BioLector cultivation, provided that the individually defined biomass- or time-dependent triggers are reached. Samples are then directly pipetted into a 96 deep-well plate (DWP). After less than 3 minutes interruption, the BioLector closes its lid and continues the cultivation. The time required for the initial sampling depends on the number of wells harvested in parallel, which can vary between 1 and 48 for each cycle. Due to the variable sample number, a second DWP as tare plate for centrifugation is subsequently filled with an equal volume of water and in the same pattern as the sample plate. After following a centrifugation step at 4500 rpm, the resulting cell-free supernatants are transferred to a third DWP at −4°C, the tare DWP is emptied and the MPP is ready for the next sampling event (cf. Figure 1A). The newly introduced rapid cell separation by centrifugation and subsequent freezing of cell-free supernatants diminishes the extent of metabolite leakage, protects heat labile metabolites and prevents the reaction of extracellular enzymes with metabolites during sample storage. One cycle of the developed harvest procedure is finished after 12 to 17.5 minutes for 1 to 48 samples, respectively, and runs fully automated on our MPP without any manual effort.

The established workflow combines the quantitative analysis of a comprehensive set of 48 cultivation experiments wherein different strains under well-defined environmental conditions can be compared with respect to growth and production properties. For example, it can be used to compare the product titers of: (*i*) one production strain cultivated in 48 different media compositions; or (*ii*) a library of 48 different strains cultivated in the same medium; or (*iii*) any reasonable set of 48 combinations thereof (Figure 1B). Furthermore, this workflow can provide insight into the metabolite uptake and production kinetics of an organism when multiple wells of a plate are inoculated with an identical culture and repetitively harvested one after another according to a time-dependent trigger profile (Figure 1C).

Development and validation of metabolite quantification in microtiter plate scale

To enable the phenotyping of a wide range of amino acid producer strains on our MPP, we developed fast and robust photometric assays for the quantification of amino acids as well as D-glucose and D-xylose in the culture supernatants originating from triggered sampling.

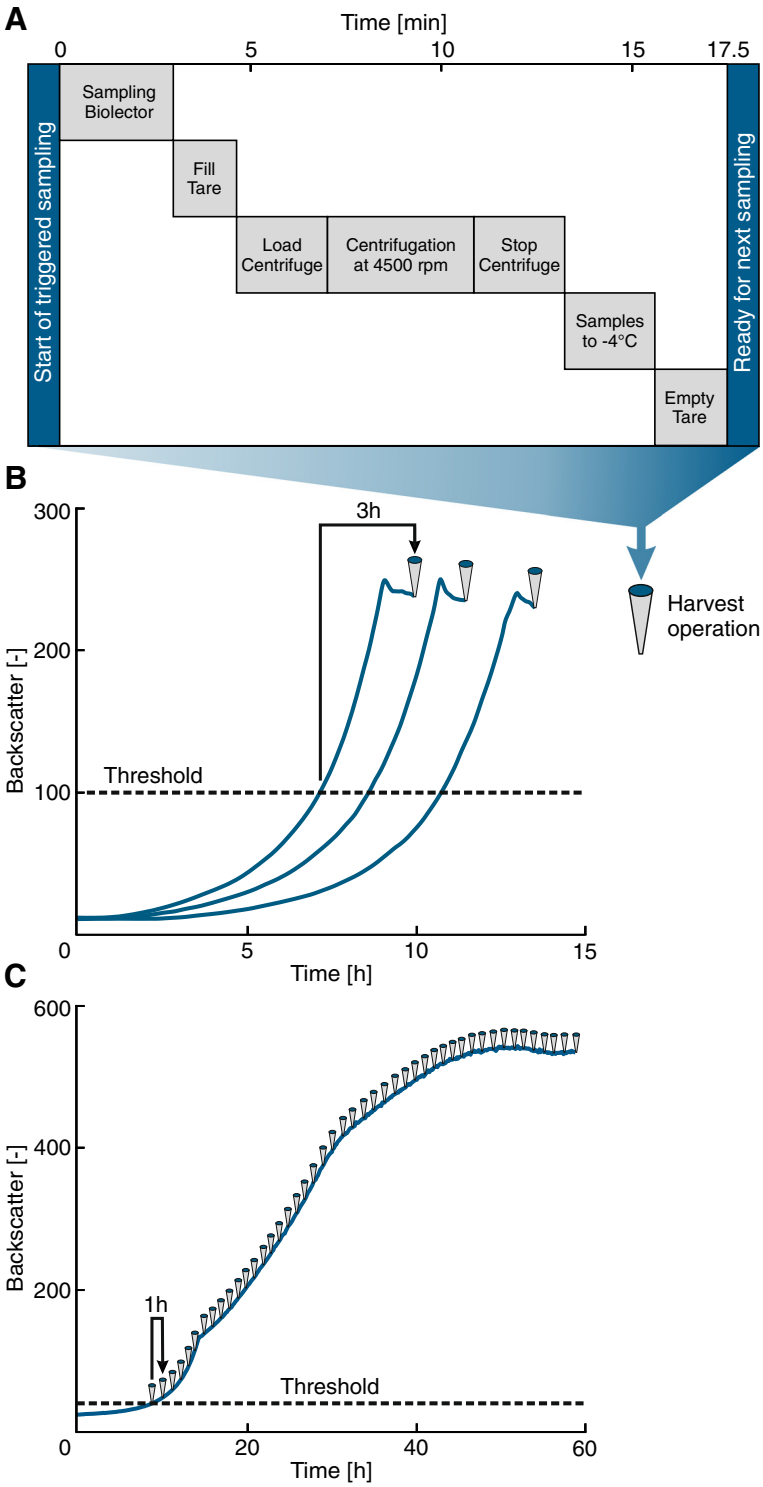

Figure 1 Fully automated workflow to harvest cell-free cultivation samples from microtiter plate cultivations on the MPP. A: Steps of the automated harvest operation to generate a variable number (1 - 48) of cell-free supernatants in parallel from BioLector cultivations. **B**: Triggered process to sample supernatants after turn to stationary phase to compare different producer strains considering final product titers. **C**: Time-dependent harvest profile of identically inoculated parallel cultivations to assess metabolite formation or uptake kinetics.

For the determination of amino acid concentrations the well-known Ninhydrin assay [7] was transferred to microtiter plate scale. In short, Ninhydrin reacts with an amino acid to a Schiff base before decarboxylation, dehydration and addition of a second Ninhydrin molecule leads to the formation of the Ruhemann's purple (Figure 2A). During the transfer of the established Ninhydrin protocols to microtiter plate scale we tested and optimized the influence of pH, temperature, additives, reagent volumes and reaction times (data not shown).

In the resulting method, 48 culture supernatants are filled in a 384-well plate in triplicates both undiluted as well as in one dilution step. Moreover, specific standards for the amino acid of interest are prepared by the liquid handling station from a stock solution in 9 replicates per standard on the same 384-well plate. The reaction is subsequently initiated by the addition of the Ninhydrin solution, incubated at room temperature and stopped after 4 minutes by the addition of water (see Methods section for more details). Finally, the plate is automatically transferred to the photometer integrated on the MPP and the formation of the Ruhemann's purple is quantified at 570 nm.

Noteworthy, when measuring a culture supernatant, the formed Ruhemann's purple results from the reaction

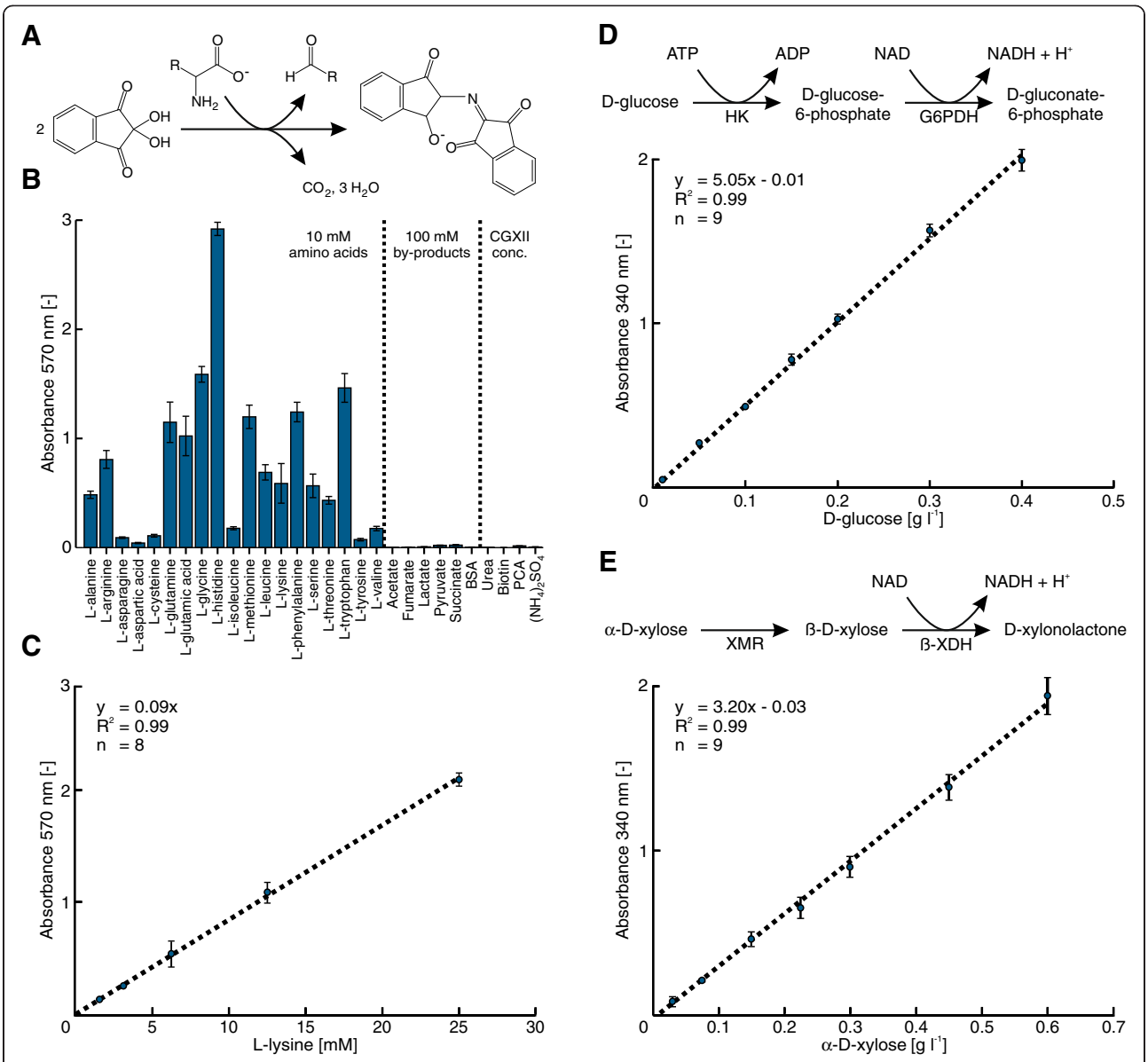

Figure 2 Development and validation of metabolite quantification in microtiter plate scale on the MPP. A-C: Fast photometric quantification of amino acids was realized by the application of the developed Ninhydrin assay in 384-well microtiter plates. The assay was tested with regard to the measurable metabolite spectrum as well as its selectivity against relevant by-products and media components of the model host *C. glutamicum*. **D-E**: Enzymatic assays to quantify D-glucose or D-xylose in culture supernatants were automated in 384-well microtiter plates.

of Ninhydrin with all amino acids present in the sample and cannot be directly accounted to a single amino acid species. Moreover, it was reported that the yield of the Ninhydrin reaction is not identical among different amino acids, because the residual groups can influence conversion rates and equilibria of the reaction intermediates [7]. In order to check the sensitivity and selectivity of the developed microtiter plate approach, we first measured 19 different amino acids, each at a concentration of 10 mM. By comparing the resulting signal intensities we indeed observed great differences in the Ruhemann's purple formation (Figure 2B). We then tested the influence of selected media components and cultivation by-products that typically play a role during the cultivation of the model amino acid producer *Corynebacterium glutamicum*. As a result, only free alpha amino groups reacted with Ninhydrin, while none of the tested media components or by-products resulted in a detectable absorption. Finally, we checked the linear dynamic range of the assay, exemplarily for the amino acid L-lysine (Figure 2C). The resulting concentration range of 1.56 to 25 mM directly covers most of the L-lysine titers typically reached by *C. glutamicum* producer strains under lab-scale screening conditions [8-10]. Therefore, large series of error-prone dilution steps can be skipped, what further improves the speed and accuracy of the microtiter plate assay.

In another approach, we established the quantification of D-glucose and the emerging carbon source D-xylose by implementing two-step enzymatic assays on the MPP (Figure 2D and E). D-glucose is first phosphorylated via Hexokinase (HK) and then oxidized by Glucose-6-phosphate dehydrogenase (G6PDH) under formation of NADH. D-xylose is first interconverted from the α-anomeric to the ß-anomeric form by D-xylose mutarotase (XMR) and then oxidized by ß-xylose dehydrogenase (ß-XDH) under NADH formation. Prior to the D-xylose assay, D-glucose was removed from the samples with HK, since a slight side activity of the ß-XDH had been reported elsewhere [11].

Both enzymatic assays were fully automated for routine application and run without any manual work, except for the preparation of specific mastermix solutions (see Methods section). For each assay 48 cultivation samples were pipetted from a DWP to a 384-well plate in triplicates of two different pre-dilution steps. Standard samples for each run were prepared by the liquid handling station from a stock solution of D-glucose or D-xylose and pipetted in 9 replicates per standard on 384-well plates. For D-xylose quantification, the aforementioned D-glucose removal was achieved by first mixing the samples with HK and ATP surplus. After 2 minutes incubation the blank at 340 nm was measured and later subtracted from the final absorbance. Subsequently, both assays were started by addition of a mastermix and incubated for 30 minutes. Finally, the plates were automatically transferred to the photometer on the MPP and measured at 340 nm. The dynamic linear ranges for the developed microtiter plate assays were 0.05 to 0.4 g l^{-1} for D-glucose and 0.025 to 0.6 g l^{-1} for D-xylose (cf. Figure 2D and E).

Characterization of L-lysine producers on the MPP

In a first MPP application, we screened a mutant library of *C. glutamicum* L-lysine producer strains for altered growth and production performances. The strain library consisted of 17 different genome-reduced L-lysine producers (GRLP) which were recently constructed by the targeted deletion of non-essential gene clusters from the model L-lysine producer DM1933 [12]. L-lysine production is generally coupled to primary metabolism [13], thus, highest product titers are expected after turn to stationary phase in a batch culture.

DM1933 and all 17 GRLP were cultivated multiple times ($n \geq 4$) in CGXII medium with 40 g l^{-1} D-glucose on the MPP. The developed harvest procedure was used to automatically generate and freeze cell-free supernatants from all cultures, one hour after turn to stationary phase (cf. Figure 1B). Subsequently, the DWP with all frozen samples was thawn to measure the total amino acid titers by following the automated procedure described above. As a result, GRLP45 showed the lowest maximum growth rate ($\mu_{max} = 0.16 \pm 0.04$ h^{-1}) which was only half the rate of the reference strain DM1933 ($\mu_{max} = 0.32 \pm 0.01$ h^{-1}) (Figure 3A). In contrast, the highest amino acid titers were measured in the supernatants of GRLP45 ($c_{AA,max} = 59.1 \pm 1.3$ mM) while the reference strain DM1933 produced only two thirds of GRLP45 ($c_{AA,max} = 39.2 \pm 6.1$ mM).

In further experiments we tested whether the screening results obtained on our MPP can be transferred to lab-scale bioreactors. Therefore, GRLP45 and DM1933 were cultivated in 1 l bioreactors on CGXII medium with 10 g l^{-1} D-glucose (Figure 3B). Samples were taken manually every hour and subsequently measured with the developed Ninhydrin assay for total amino acid concentration as well as with an established LC-MS/MS protocol for L-lysine concentration. As a result, the significantly slower growth of GRLP45 ($\mu_{max} = 0.19 \pm 0.01$ h^{-1}) compared to DM1933 ($\mu_{max} = 0.27 \pm 0.01$ h^{-1}) was reproduced in bioreactor scale. Moreover, the Ninhydrin assay indicated once more a higher total amino acid production by GRLP45 compared to DM1933, which was confirmed to be an increased L-lysine titer by the LC-MS/MS measurements. Noteworthy, the highest amino acid and L-lysine concentrations were observed one hour after turn to stationary phase in all bioreactor cultivations, basically supporting the set-up of the harvest procedure for this particular product on the MPP.

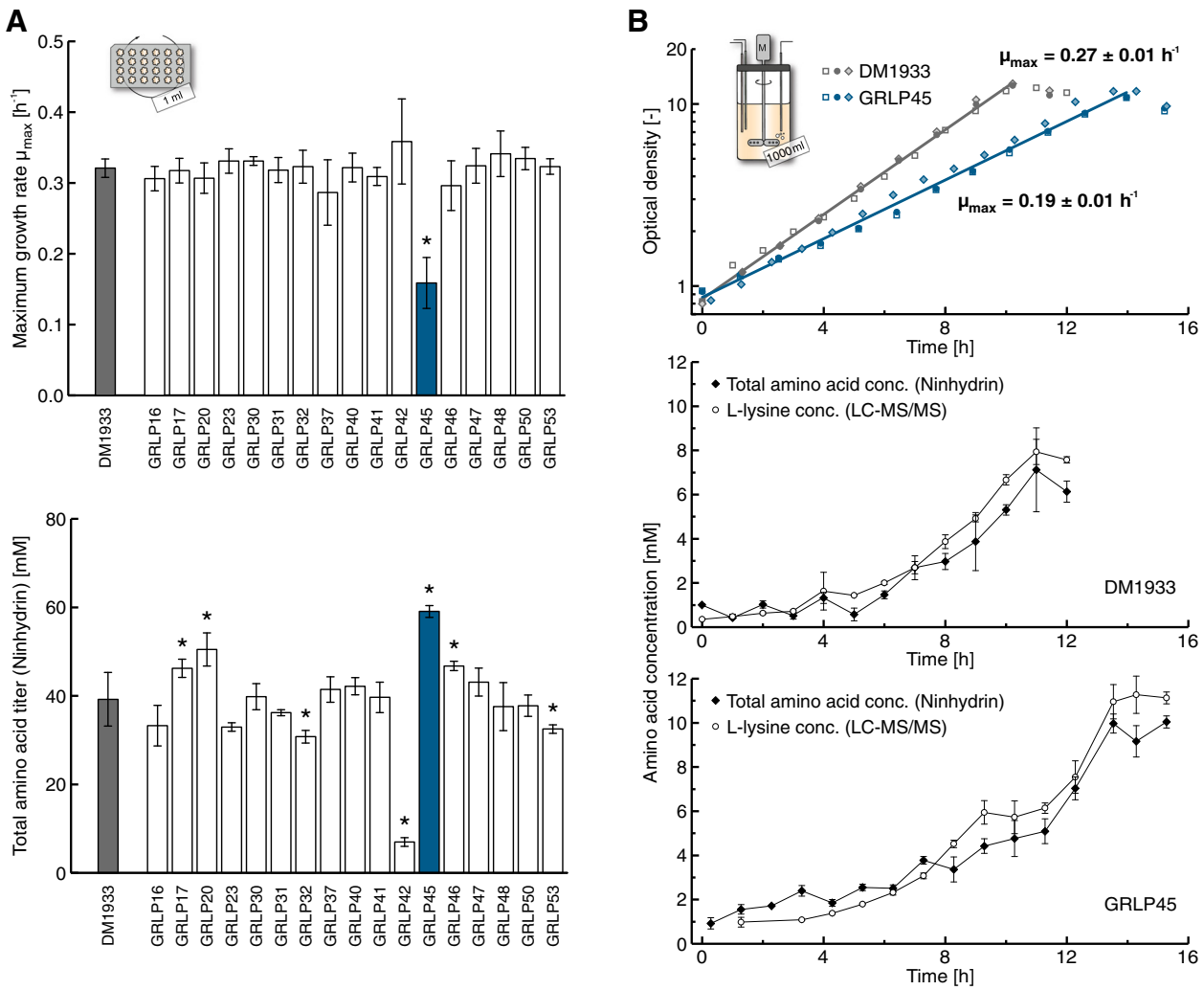

Figure 3 Screening of a strain library on the MPP and scale-up of the best performer in lab-scale bioreactors. A: Determination of maximum growth rate and total amino acid titer of a set of genome reduced L-lysine producers (GRLP) using the developed harvest procedure in combination with the Ninhydrin assay ($n \geq 4$ biological replicates, cf. Figure 1B and 2C). Strains with significant changes in either parameter compared to the model L-lysine producer DM1933 were determined by one-way ANOVA ($p < 0.01$) and marked with an asterisk. GRLP45 showed highly elevated amino acid titers in BioLector cultivations while displaying a decreased maximum growth rate. **B**: Both observations for GRLP45 obtained on the MPP were confirmed in 1 l lab-scale bioreactor experiments ($n = 3$ biological replicates). Amino acids and L-lysine were quantified in one cultivation run of GRLP45 and DM1933, respectively, using the automated Ninhydrin assay as well as an established LC-MS/MS protocol ($n = 3$ technical replicates).

Fast assessment of substrate uptake kinetics on the MPP

In another proof of principle study we determined substrate uptake kinetics of the newly constructed strain *C. glutamicum xylXABCD*$_{Cc}$. This strain contains a pEKEx3-plasmid with five genes for D-xylose assimilation via the Weimberg pathway to enable the growth of *C. glutamicum* on D-xylose with minimized carbon loss [14]. In general, the phenotypic characterization of such a newly constructed strain would typically start with a shaking flask or bioreactor experiment followed by a successive sampling to determine the specific uptake rates for the new carbon substrate. However, with the developed methods at hand we now can address this question in a fully automated manner on our MPP.

46 wells of one 48-well FlowerPlate were filled with an identically inoculated culture of *C. glutamicum xylXABCD*$_{Cc}$ on CGXII medium with 10 g l^{-1} D-glucose and 30 g l^{-1} D-xylose. Two wells were only filled with CGXII medium and carried as sterile controls. At the start of the cultivation the first well was instantly harvested and the cell-free supernatant was frozen as first sample. The remaining wells were harvested one by one following a time-dependent pattern after the backscatter had surpassed a threshold value (cf. Figure 1C).

After the cultivation was finished, all frozen cell-free supernatants were thawed to quantify the remaining D-glucose and D-xylose concentrations by following the automated procedures described above. In addition, both substrates were quantified via HPLC measurement to validate the results with an established method.

The phenotype of all parallel cultivated cultures was highly comparable (Figure 4) and, until the first harvest at $t = 13$ h, the well-to-well variability (coefficient of variation) between all 46 cultures was estimated as 3.9% and 4.4% for the backscatter and dissolved oxygen measurements, respectively. The averaged dissolved oxygen (DO) signal indicated a short interruption of oxygen consumption after 20 hours, before the DO dropped again until 26 hours. This dynamic pattern was accompanied by a drop in the maximum growth rate of the culture from $\mu_{max,I} = 0.28 \pm 0.01\ h^{-1}$ to $\mu_{max,II} = 0.08 \pm 0.01\ h^{-1}$. Both observations already pointed to a bi-phasic growth behavior which could subsequently be confirmed by the substrate analytics established on the MPP. As shown in Figure 4, within a first growth phase mainly D-glucose was utilized as carbon source while the pronounced catabolization of D-xylose first started after D-glucose becomes limiting.

All D-glucose concentrations determined with the microtiter plate assay are in good agreement with the measurements obtained by the established HPLC protocol. However, in case of D-xylose the concentration data only matched for the first samples. Noteworthy, the complete consumption of D-xylose was observed after 31 hours by the microtiter plate assay, which is also in accordance with the rising DO signal and a second bend in the backscatter curve. At this time the HPLC measurements indicated a higher remaining D-xylose concentration (5.2 mM) and these deviations were most likely caused by the limited selectivity of the applied HPLC method. Indeed subsequent GC-ToF-MS measurements of all supernatants confirmed the presence of significant amounts of D-xylonate as a by-product from D-xylose assimilation via the Weimberg pathway [14], and both compounds can actually not be separated by HPLC [15]. This exemplary result shows that the developed microtiter plate assays are not only faster, but can also lead to better separation results as compared to standard HPLC approaches, providing that the specificity of the applied enzyme for its substrate is high enough.

Conclusions

In a previous work we showed how automated sampling with liquid handling robotics can improve the reproducibility of cultivation experiments in microtiter plates [4]. In this work we report the further improvement of our robotic Mini Pilot Plant (MPP) by introducing rapid clarification of supernatant samples and quantification of metabolites in microtiter plate scale. We show the application of completely autonomous workflows to generate cell-free supernatants from microtiter plate cultivations within minutes.

To quantify metabolites in samples at elevated throughput we developed biochemical and enzymatic assays on our MPP. The well-established Ninhydrin reaction for amino acid quantification was transferred from manual and time-consuming milliliter-scale protocols to a fast and parallelized 384-well microtiter plate scale application. Recently, the Ninhydrin assay was successfully applied

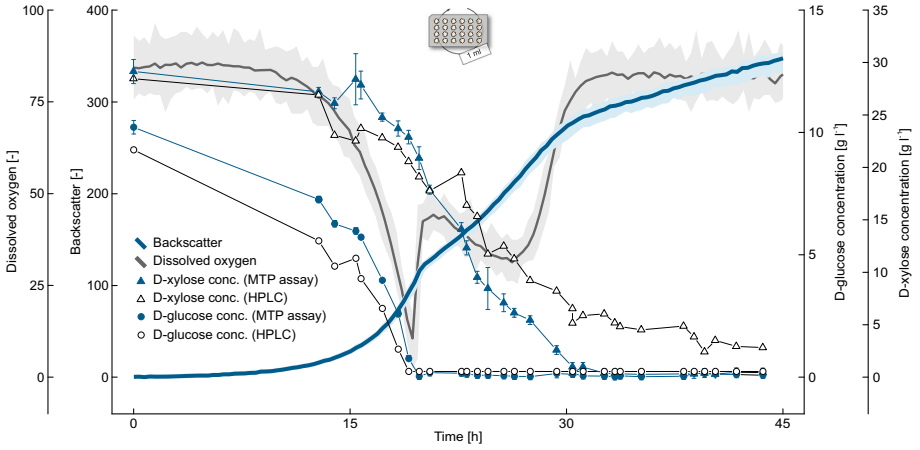

Figure 4 Substrate uptake characteristics of *C. glutamicum xylXABCD*$_{Cc}$ during growth on CGXII medium with D-glucose and D-xylose. The cultivation was performed in 46 identically inoculated wells of a FlowerPlate, of which each well was harvested automatically following a time-dependent pattern (cf. Figure 1C). Supernatant samples were automatically clarified via centrifugation, stored at −4°C and subsequently analyzed for D-glucose and D-xylose concentrations ($n = 3$ technical replicates). The results of both enzymatic substrate quantification methods were confirmed with established HPLC protocols. Mean values for backscatter and dissolved oxygen were estimated from unsampled replicate cultures ($n \geq 3$). Confidence intervals (shaded areas) were spanned from the minimum and maximum value at each measurement point.

to screen 311 bacterial isolates for those growing on 1-aminocyclopropane-1-carboxylate as sole carbon source [16]. However, in this study all cultures were harvested and clarified manually and the Ninhydrin assay was carried out in open 96-well plates in a boiling water bath by following single pipetting steps. In contrast, our Ninhydrin assay is operated in 384-well plates and omits heating and sealing steps, which greatly minimizes the assay duration and simplifies the automation. By the usage of DMSO we observed reduced precipitation of the Ruhemann's purple as also reported elsewhere [17]. With this increased color stability we observed a linear detection range of 1 to 25 mM for the particular amino acid L-lysine. As product titers produced by *C. glutamicum* are typically found in this range, the assay provides the benefit to estimate the total amino acid concentration in undiluted cultivation samples within minutes. In a MPP screening with our improved Ninhydrin assay, we found the *C. glutamicum* strain GRLP45 to produce higher L-lysine titers as compared to DM1933, which was subsequently confirmed in lab-scale bioreactor experiments. The reason for the increased product formation of GRLP45, harboring deletions in the gene cluster Δ2990-3006 [12], is currently under investigation.

In further work, we focused on the substrate side and transferred enzymatic assays for D-glucose and D-xylose to 384-well plate scale to establish their quantification on the MPP. All dilutions of standards and samples were executed by the liquid handling station to achieve fast and highly reproducible results. In summary, 48 cultivation samples are automatically processed and measured in triplicates of two different dilutions within less than 30 minutes. The throughput of our method is less than one minute per sample measured in replicates and, hence, competitive to other quantitative methods based on HPLC or MS technologies. Moreover, the costs per sample for chemicals and consumables are low and robotic workstations can work with low demand on maintenance. To apply our assays, we quantified D-glucose and D-xylose in cell-free supernatants derived from a time-dependent sampling of batch cultures with the newly constructed strain *C. glutamicum xylXABCD*$_{Cc}$ [14]. From the completely automated workflow of cultivation, harvest and substrate quantification, we could deduce that *xylXABCD*$_{Cc}$ grows in two phases on D-xylose/D-glucose substrate mixtures and switches to D-xylose consumption when D-glucose has been depleted. The fast assessment of such phenotypes at microtiter plate scale omits the more time-demanding bioreactor cultivations for this task. Consequently, it builds a solid basis for subsequent *in-depth* phenotyping experiments including quantitative omics measurements requiring at least milliliter scale operations.

Recently, Knepper et al. reported on robotic workflows for intermittent measurement of OD, pH and metabolites from cultures in 96-well plates in seven cycles at fixed times during 48 h cultivations [18]. Their successive sampling from plates incubated without humidity control led to a total volume reduction of 47% per well over 48 hours. For product analysis, cultures were harvested and clarified manually after cultivation and at-line enzymatic substrate analytics were performed without biomass separation resulting in incorrect measurement values for D-glucose concentration. In contrast, our BioLector-based system shows lower evaporation (<10% per well over 48 hours) and, most importantly, we avoid repeated sampling from identical wells to minimize disturbance of the culture, i.e. by altering oxygen transfer due to changing culture volumes [6]. Moreover, the established workflow allows to initiate sampling events in response to individually measured online biomass values and the fully automated substrate and product assays run with cell-free samples in 384-well plates with an accordingly higher number of technical replicates.

In summary, the presented MPP allows a quick assessment of questions typically encountered during early-stage bioprocess development, i.e. during a strain screening or the first quantitative phenotyping of a few selected strains. The bottleneck of sample analytics from parallel microliter scale cultivations must be tackled nowadays and could be solved by applying easily adaptable microtiter plate assays in combination with robotic automation.

Methods

If not stated otherwise, all chemicals or consumables for liquid handling used in this study were purchased from SIGMA Aldrich, Carl Roth or Greiner Bio-One, respectively.

Growth medium

Cultivations were performed on defined CGXII medium which contained per liter of distilled water: 20 g $(NH_4)_2SO_4$, 1 g K_2HPO_4, 1 g KH_2PO_4, 13.25 mg $CaCl_2$*$2H_2O$, 0.25 g $MgSO_4$*$7H_2O$, 1 mg $FeSO_4$*$7H_2O$, 1 mg $MnSO_4$*H_2O, 0.02 mg $NiCl_2$*$6H_2O$, 0.313 mg $CuSO_4$*$5H_2O$, 1 mg $ZnSO_4$*$7H_2O$, 0.2 mg biotin and 30 mg protocatechuic acid [19]. The primary carbon and energy source was D-glucose with 10 or 40 g l^{-1} or a mixture of 10 g l^{-1} D-glucose with 30 g l^{-1} D-xylose. The medium for cultivation in bioreactors or microtiter plates was supplemented with 3% (v v^{-1}) AF204 antifoam agent or 5 g l^{-1} urea and 42 g l^{-1} MOPS buffer, respectively. For medium preparation some substances were added sterile after autoclaving (D-glucose/D-xylose, PCA, biotin, trace elements and AF204) and 4 M HCl/4 M NaOH was used to adjust the pH to 7.0 in bioreactors.

Strain storage and cultivation

Cryo cultures of all strains were prepared from exponentially growing cultures on CGXII medium in shaking flask. Cells were harvested at OD_{600} = 10, washed once with 0.9% (w v^{-1}) NaCl and stored at −80°C in a solution containing 20% (v v^{-1}) glycerol and 0.9% (w v^{-1}) NaCl.

Bioreactor cultivations were carried out in 1.5 l reactors (DASGIP AG, Jülich, Germany) in batch mode at 30°C and 1 vvm air flow. Aerobic process conditions were controlled via stirrer speed (200 – 1200 rpm) to maintain 30% dissolved oxygen (DO) concentration. The pH of the culture was regulated to pH 7.0 with 4 M HCl and 4 M NaOH. Online measurements were taken for pH (405-DPAS-SC-K80/225, Mettler Toledo) and DO (Visiferm DO 225, Hamilton). Cultures were inoculated per liter with 0.5 ml cryo culture aliquots and sampling as well as monitoring of growth was started when cultures had reached an OD > 0.5 on the next day. Samples for biomass determination were taken every hour and measured photometrically at λ = 600 nm (OD_{600}).

Microtiter plate cultivations were carried out in 48-well FlowerPlates (m2p-labs GmbH, Baesweiler, Germany) with DO and pH optodes in a BioLector (m2p-labs GmbH) at 1000 rpm, 95% humidity, 30°C and backscatter gain 20. Cultures were started at OD_{600} = 0.1 by inoculation of 990 μl medium with 10 μl cryo culture per well. Maximum growth rates were calculated directly from backscatter values as described elsewhere [12].

Robotic workflow of automated harvest

Robotic workflows were developed on a JANUS Automated Workstation (PerkinElmer, Waltham MA, USA) equipped with a pipetting arm (Varispan) with 8 steel needles and a gripper arm for transport of plates. The track of both arms was extended by 400 mm in order to reach a BioLector (m2p-labs, Baesweiler, Germany), the MTP centrifuge IXION (Sias, Hombrechtikon, Switzerland) and the MTP photometer EnSpire (PerkinElmer, Waltham MA, USA) outside of the regular liquid handling deck. Cooling of samples down to −10°C was performed on a DWP cooling rack (MeCour, Groveland MA, USA) connected to the cryostat Unichiller (Huber, Offenburg, Germany). Further details about the setup and evaluation of the robotic workstation were described elsewhere [4].

Cultivations for automated harvesting were performed with 22 minute measurement cycles in the BioLector and monitored by the RoboLector agent software (m2p-labs, Baesweiler, Germany). This software pauses as well as opens the BioLector and writes a CSV-based handshake file, provided that trigger conditions (here: timer after biomass threshold) had been reached. This handshake file indicates positions of those wells of the FlowerPlate that have reached their individual trigger condition and was then immediately used by the liquid handling platform to transfer 500 μl of those wells from the BioLector to a DWP. Subsequently, the handshake file was first copied by automated execution of a batch script, before the original file was deleted by the WinPrep software (Version 4.6, PerkinElmer). This deletion process triggers the RoboLector agent software to close the BioLector lid and to continue the cultivation. The copied handshake file was then used by the liquid handling platform to fill a second DWP with water as tare. Both DWPs were transferred to the IXION centrifuge and rotated at 4500 rpm for 5 minutes. The obtained cell-free supernatants were aspirated completely at a fixed height (4 mm above well bottom) and transferred to a third DWP at −4°C, closed with an aluminum sealing foil. Finally, the tare plate was also emptied at the same height to equal its weight for the following centrifugation steps. The developed protocol takes 12 to 17.5 minutes depending on the number of wells harvested at a time and runs without manual intervention or replacement of consumables (DWPs). The resulting cell-free supernatants were stored in the −4°C DWP in the same layout as in the BioLector experiment in order to avoid cross contamination.

MTP Ninhydrin assay

As Ninhydrin solution for the MTP assay 2 g Ninhydrin were solved in 75 ml DMSO and 25 ml 4 M sodium acetate buffer (pH 6.0 adjusted with 25% acetic acid). The mastermix was prepared fresh for each experiment and stored in dark until use. A 100 mM L-lysine-HCl stock solution was prepared in CGXII medium for standard dilution series.

The robotic workflow of the Ninhydrin assay was started with three independent 1:2 dilution series of the L-lysine stock solution using CGXII medium down to 1.56 mM in a DWP. 30 μl of each dilution series was pipetted in triplicates in a 384-well plate, resulting in a total number of 9 wells for each standard concentration. 48 cell-free supernatants were pipetted from a DWP to the 384-well plate in triplicates of 45 μl. Subsequently, 15 μl of these undiluted samples were aspirated from the 384-well plate and dispensed in other wells of the same plate and mixed with 15 μl medium to derive 1:2 dilutions of each cultivation sample in triplicates. The reaction was finally started with addition of 30 μl Ninhydrin solution to each well, incubated at room temperature and stopped after exactly 4 minutes by the addition of 40 μl distilled water. The plate was immediately transferred to the photometer on the MPP by the gripper arm and read for absorbance at λ = 570 nm. During subsequent analysis, raw data were first blanked by wells with sole medium as sample, before the standard curve (1.56 – 25 mM) was used to quantify total amino acids in the cell-free supernatants.

MTP assay for D-glucose and D-xylose quantification

Enzymatic reactions were used to quantify D-glucose and D-xylose in cell-free supernatants on the MPP. For the D-glucose assay a mastermix was freshly prepared by mixing: 47.4 ml TRIS-maleat buffer (100 mM, pH 6.8), 2.2 ml $MgSO_4$ solution (100 mM), 1 ml NAD^+ stock (50 mg ml^{-1}), 1 ml ATP stock (34 mg ml^{-1}) and 236 μl Hexokinase/Glucose-6-phospate dehydrogenase mix (Roche Diagnostics, Mannheim, Germany). The automated workflow on the MPP started with the preparation of three independent dilution series of standards in the range of 0.4 to 0.01 g l^{-1} from a 1 g l^{-1} D-glucose stock. Afterwards, 20 μl of each standard solution was pipetted in triplicates in a 384-well plate, resulting in 9 wells for each D-glucose standard concentration. All 48 cell-free supernatants were diluted in two different steps (typically 1:10 and 1:40) by successive aspiration of water and sample, followed by common dispense in a DWP. 20 μl of these 96 diluted samples were subsequently pipetted in a 384-well plate in triplicates. Then, 80 μl mastermix was added to each well before the plate was incubated for 45 minutes at room temperature to allow for a complete reaction. Finally, the plate was automatically transferred to the photometer and measured for absorbance at λ = 340 nm. During analysis, raw data were first normalized by wells with water as sample, before the standard curve (0.01 – 0.4 g l^{-1}) was used to quantify D-glucose in the cell-free supernatants.

For the D-xylose assay two mastermixes were prepared, the first (M1) by mixing: 47.4 ml TRIS-maleat buffer (100 mM, pH 6.8), 2.2 ml $MgSO_4$ solution (100 mM), 1 ml NAD^+ stock (50 mg ml^{-1}), 1 ml ATP stock (34 mg ml^{-1}) and 236 μl Hexokinase (Megazyme, Wickow Ireland). For the second mastermix (M2) 5.09 ml distilled water was mixed with 410 μl β-xylose-Dehydrogenase/D-xylose mutarotase mix (Megazyme, Wickow Ireland). The automated workflow started with the preparation of standards in three independent dilution series ranging from 0.6 to 0.01 g l^{-1} from a 1.5 g l^{-1} D-xylose stock. Afterwards, 10 μl of each standard solution was pipetted in a 384-well plate in triplicates, resulting in 9 wells for each D-xylose standard concentration. For the D-xylose assay all 48 samples were diluted 1:10 and 1:100 to cover the whole expected range of D-xylose concentrations and 10 μl of these diluted samples were pipetted in a 384-well plate in triplicates. Then, 80 μl of the M1 was added to each well to allow a complete removal of D-glucose in order to exclude unspecific reactions of the D-xylose mutarotase. After 2 minutes incubation at 37°C the absorbance at λ = 340 nm was measured before 10 μl of the M2 was added to all wells. Afterwards, the plate was again incubated at 37°C for 30 minutes until the final absorbance at λ = 340 nm was measured. During data analysis, the difference between absorbance after first reaction and second reaction was calculated in order to blank the final values with the background absorbance after the enzymatic removal of D-glucose.

LC-MS/MS and HPLC measurements

For LC-MS/MS analysis, cell-free supernatants were first pre-diluted with distilled water to the linear range (0.025 μM – 25 μM) of the LC-MS/MS protocol. To eliminate artefacts from the running buffer and the used internal standard the last 1:2 dilution step was performed with 100% MeOH to gain a final 50% MeOH concentration in the sample. Targeted quantification of L-lysine in supernatant samples was conducted by isotope dilution mass spectrometry as described by Paczia et al. [20].

D-glucose and D-xylose were quantified by HPLC with a 300 × 8 mm organic acid column (CS Chromatographie, Langerwehe, Germany) at 40°C using isocratic elution with 0.1 M H_2SO_4 at a flow rate of 0.5 ml min^{-1}. Carbohydrates were detected via refraction index (Agilent, Santa Clara, CA, USA) and concentrations were determined by calibration with external standards.

Competing interests

The authors declare that they have no competing interests.

Authors' contributions

SU designed new workflows and assays on the robotic platform, performed the characterization of GRLPs in microtiter plates and lab-scale bioreactors, analyzed the data and wrote the manuscript. AR designed new workflows and assays on the robotic platform, performed the characterization of GRLPs and *xylXABCD*$_{Cc}$ in microtiter plates and lab-scale bioreactors, and analyzed the data. WW helped to finalize the manuscript. MO designed and supervised the construction of the robotic platform and helped to finalize the manuscript. SN supervised the characterization of GRLPs and *xylXABCD*$_{Cc}$ and wrote the manuscript. All authors read and approved the final manuscript.

Acknowledgements

The authors wish to thank Meike Baumgart, Christian Rückert and Marius Herbst for providing the GRLPs strains and Jan Marienhagen for providing the *xylXABCD*$_{Cc}$ strain. This work was partly funded by the Bundesministerium für Bildung und Forschung (BMBF, grant. no. 0316017B) and the European Commission's Seventh Framework Programme (FP7/2007-2013) under the grant agreement STREPSYNTH (project no 613877).

Received: 13 November 2014 Accepted: 23 February 2015
Published online: 11 March 2015

References

1. Kensy F, Zang E, Faulhammer C, Tan RK, Büchs J. Validation of a high-throughput fermentation system based on online monitoring of biomass and fluorescence in continuously shaken microtiter plates. Microb Cell Fact. 2009;8:31.
2. Weuster-Botz D. Parallel reactor systems for bioprocess development. Adv Biochem Eng Biotechnol. 2005;92:125–43.
3. Long Q, Liu X, Yang Y, Li L, Harvey L, McNeil B, et al. The development and application of high throughput cultivation technology in bioprocess development. J Biotechnol. 2014;192(Pt B):323–38.
4. Rohe P, Venkanna D, Kleine B, Freudl R, Oldiges M. An automated workflow for enhancing microbial bioprocess optimization on a novel microbioreactor platform. Microb Cell Fact. 2012;11:144.
5. Noack S, Wiechert W. Quantitative metabolomics: a phantom? Trends Biotechnol. 2014;32:238–44.

6. Käss F, Prasad A, Tillack J, Moch M, Giese H, Buchs J, et al. Rapid assessment of oxygen transfer impact for *Corynebacterium glutamicum*. Bioprocess Biosyst Eng. 2014;37:2567–77.
7. Friedman M. Applications of the ninhydrin reaction for analysis of amino acids, peptides, and proteins to agricultural and biomedical sciences. J Agric Food Chem. 2004;52:385–406.
8. van Ooyen J, Noack S, Bott M, Reth A, Eggeling L. Improved L-lysine production with *Corynebacterium glutamicum* and systemic insight into citrate synthase flux and activity. Biotechnol Bioeng. 2012;109:2070–81.
9. Kind S, Becker J, Wittmann C. Increased lysine production by flux coupling of the tricarboxylic acid cycle and the lysine biosynthetic pathway–metabolic engineering of the availability of succinyl-CoA in *Corynebacterium glutamicum*. Metab Eng. 2013;15:184–95.
10. Buchholz J, Schwentner A, Brunnenkan B, Gabris C, Grimm S, Gerstmeir R. Platform Engineering of *Corynebacterium glutamicum* with Reduced Pyruvate Dehydrogenase Complex Activity for Improved Production of L-Lysine, L-Valine, and 2-Ketoisovalerate. Appl Environ Microbiol. 2013;79:5566–75.
11. Yamanaka K, Gino M, Kaneda R. Specific NAD-D-Xylose Dehydrogenase from Arthrobacter-Sp. Agric Biol Chem. 1977;41:1493–9.
12. Unthan S, Baumgart M, Radek A, Herbst M, Siebert D, Bruhl N, et al. Chassis organism from *Corynebacterium glutamicum* - a top-down approach to identify and delete irrelevant gene clusters. Biotechnol J. 2015;10:290–301.
13. Eggeling L, Bott M. Handbook of Corynebacterium glutamicum. CRC Press tailor and Francis Group; 2005
14. Radek A, Krumbach K, Gätgens J, Wendisch V, Wiechert W, Bott M, et al. Engineering of *Corynebacterium glutamicum* for minimized carbon loss during utilization of D-xylose containing substrates. Biotechnol J. 2014;192(Pt A):156–60.
15. Nygard Y, Toivari MH, Penttila M, Ruohonen L, Wiebe MG. Bioconversion of D-xylose to D-xylonate with *Kluyveromyces lactis*. Metab Eng. 2011;13:383–91.
16. Li Z, Chang S, Lin L, Li Y, An Q. A colorimetric assay of 1-aminocyclopropane-1-carboxylate (ACC) based on ninhydrin reaction for rapid screening of bacteria containing ACC deaminase. Lett Appl Microbiol. 2011;53:178–85.
17. Friedman M. Solvent effects in the absorption spectra of the Ninhydrin chromophore. Microchem J. 1971;16:204–9.
18. Knepper A, Heiser M, Glauche F, Neubauer P. Robotic Platform for Parallelized Cultivation and Monitoring of Microbial Growth Parameters in Microwell Plates. J Lab Autom. 2014;19:593–601.
19. Unthan S, Grünberger A, van Ooyen J, Gätgens J, Heinrich J, Paczia N, et al. Beyond growth rate 0.6: What drives *Corynebacterium glutamicum* to higher growth rates in defined medium. Biotechnol Bioeng. 2014;111:359–71.
20. Paczia N, Nilgen A, Lehmann T, Gätgens J, Wiechert W, Noack S. Extensive exometabolome analysis reveals extended overflow metabolism in various microorganisms. Microb Cell Fact. 2012;11:122.

3.1.3 Main achievements of this manuscript

• Triggered sampling of cell-free cultivation supernatants enables a more detailed analysis of microtiter plate experiments.

• Fast and robust photometric assays (for D-glucose, D-xylose and total amino acids) were developed and validated for quantification at 384-well plate scale.

• A mutant library of genome-reduced L-lysine producer strains (GRLP) were screened for differences in growth rates and L-lysine titers.

• One potentially interesting strain (GRLP45) could be identified that showed the lowest maximum growth rate ($\mu_{\text{max}} = 0.16 \pm 0.04\ h^{-1}$), but a significant higher amino acid titer ($cAA_{\text{max}} = 59.1 \pm 1.3\ mM$) compared to the reference producer strain DM1933. Moreover, the screening results from the GRLP45 strain were successfully transferred to laboratory scale.

• A tri-phasic growth behavior of the newly constructed strain *C. glutamicum xylX-ABCD*$_{\text{Cc}}$ during growth on mixture of D-xylose and D-glucose could be confirmed by the additional substrate analytics established on the Mini Pilot Plant.

• The extended Mini Pilot Plant lays the foundation for a variety of novel automated workflows for strain phenotyping and optimization (e.g. repetitive batch cultivations, see chapter 3.4)

3.2 Engineering of *Corynebacterium glutamicum* for minimized carbon loss during utilization of D-xylose containing substrates

3.2.1 Short introduction to this manuscript

C. glutamicum is naturally unable to metabolize D-xylose, thus, metabolic engineering is required to overcome this limitation. At the beginning of this work one pathway for D-xylose assimilation was already introduced and tested in *C. glutamicum*, the so called isomerase pathway (ISO). Here, D-xylose is converted in two steps into the pentose phosphate pathway intermediate xylulose-5-phosphate. The resulting ISO strain (Meiswinkel et al. 2013) showed a maximal specific growth rate of μ_{max} = 0.199 h^{-1}.

Within this work an alternative route for D-xylose utilization, the so called Weimberg pathway (Weimberg 1961), was integrated into wild-type *C. glutamicum* ATCC 13032. Within this five-step pathway D-xylose is oxidized to the TCA-cycle intermediate alpha-ketoglutarate.
In general, different approaches do exist to integrate artificial pathways into microorganisms (e.g. genome integration via Gibson assembly or CRISPR/Cas). Moreover, the classical way of engineering is the expression of the desired genes from a synthetic pathway on a shuttle plasmid, which is transferred into the target cells, e.g., by electroporation. This was also performed within the following manuscript, where the genes from *Caulobacter crescentus* were inserted in the origin sequence into the pEKEx3 plasmid (see Figure 3.2), which was then transferred into *C. glutamicum*.

The strain characterization presented in the following manuscript was performed on the previously extended Mini Pilot Plant. Single cultivation wells from the BioLector were harvested for detailed at-line supernatant analysis, for substrate consumption as well as by-product formation analysis. For substrate analysis the prior established microtiter enzymatic assays for D-glucose and D-xylose (cf. chapter 3.1) were used. Putative by-product formation was investigated by untargeted GC-ToF-MS analyses.

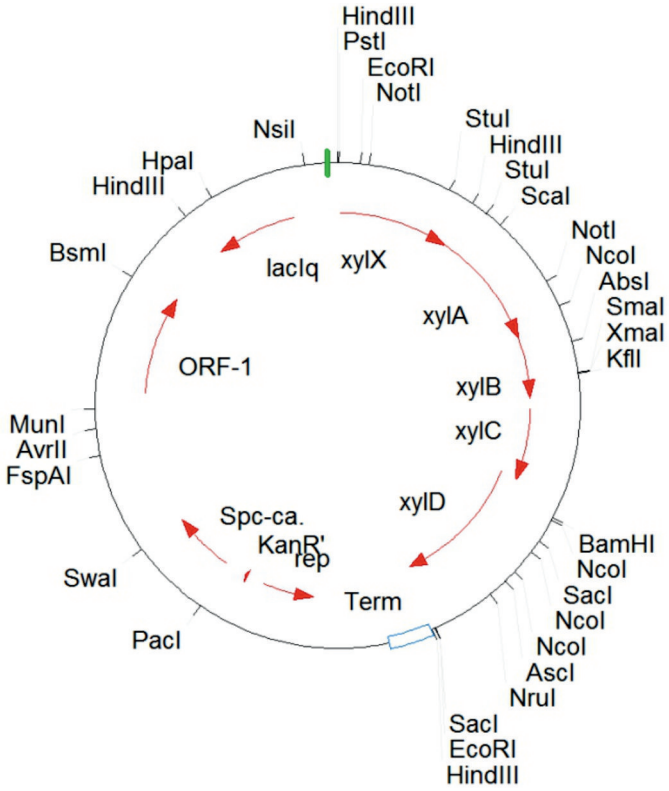

FIGURE 3.2: pEKEx3-xylXABCD$_{Cc}$ plasmid for Weimberg pathway expression.

3.2.2 Manuscript II

Engineering of *Corynebacterium glutamicum* for minimized carbon loss during utilization of D-xylose containing substrates

Published as:

Radek A, Krumbach K, Gätgens J, Wendisch VF, Wiechert W, Bott M, Noack S, Marienhagen J, Engineering of *Corynebacterium glutamicum* for minimized carbon loss during utilization of D-xylose containing substrates. *Journal of Biotechnology* 192 (2014) 156:160

Journal of Biotechnology 192 (2014) 156–160

Contents lists available at ScienceDirect

Journal of Biotechnology

journal homepage: www.elsevier.com/locate/jbiotec

Short communication

Engineering of *Corynebacterium glutamicum* for minimized carbon loss during utilization of D-xylose containing substrates

Andreas Radek[a], Karin Krumbach[a], Jochem Gätgens[a], Volker F. Wendisch[b], Wolfgang Wiechert[a], Michael Bott[a], Stephan Noack[a,*], Jan Marienhagen[a,*]

[a] *Institute of Bio- and Geosciences, IBG-1: Biotechnology, Forschungszentrum Jülich GmbH, Jülich D-52425, Germany*
[b] *Chair of Genetics of Prokaryotes, Faculty of Biology & CeBiTec, Bielefeld University, Bielefeld D-33615, Germany*

ARTICLE INFO

Article history:
Received 19 August 2014
Received in revised form
24 September 2014
Accepted 30 September 2014
Available online 7 October 2014

Keywords:
Corynebacterium glutamicum
Metabolic engineering
D-Xylose
Weimberg pathway
α-Ketoglutarate

ABSTRACT

Biomass-derived D-xylose represents an economically interesting substrate for the sustainable microbial production of value-added compounds. The industrially important platform organism *Corynebacterium glutamicum* has already been engineered to grow on this pentose as sole carbon and energy source. However, all currently described *C. glutamicum* strains utilize D-xylose via the commonly known isomerase pathway that leads to a significant carbon loss in the form of CO_2, in particular, when aiming for the synthesis of α-ketoglutarate and its derivatives (e.g. L-glutamate). Driven by the motivation to engineer a more carbon-efficient *C. glutamicum* strain, we functionally integrated the Weimberg pathway from *Caulobacter crescentus* in *C. glutamicum*. This five-step pathway, encoded by the *xylXABCD*-operon, enabled a recombinant *C. glutamicum* strain to utilize D-xylose in D-xylose/D-glucose mixtures. Interestingly, this strain exhibited a tri-phasic growth behavior and transiently accumulated D-xylonate during D-xylose utilization in the second growth phase. However, this intermediate of the implemented oxidative pathway was re-consumed in the third growth phase leading to more biomass formation. Furthermore, *C. glutamicum* pEKEx3-*xylXABCD*$_{Cc}$ was also able to grow on D-xylose as sole carbon and energy source with a maximum growth rate of $\mu_{max} = 0.07 \pm 0.01\ h^{-1}$. These results render *C. glutamicum* pEKEx3-*xylXABCD*$_{Cc}$ a promising starting point for the engineering of efficient production strains, exhibiting only minimal carbon loss on D-xylose containing substrates.

Introduction

The pentose D-xylose is a key building block of most hemicelluloses and thus a main constituent of lignocellulosic biomass (5–20%) available for biotechnological production processes (Aristidou and Penttila, 2000). For the microbial production of amino acids, organic acids or alcohols with *Corynebacterium glutamicum*, the hexoses D-glucose (from starch hydrolysates), D-fructose and sucrose (from molasses) are traditionally used (Blombach and Seibold, 2010). Naturally, the substrate spectrum of *C. glutamicum* also includes the disaccharide maltose or the pentose ribose, and this bacterium has been genetically modified to use starch, cellobiose, D-galactose and L-arabinose as carbon and energy source (Schneider et al., 2011; Kotrba et al., 2003; Barrett et al., 2004; Seibold et al., 2006).

Similarly, *C. glutamicum* has been also engineered for growth on D-xylose (Kawaguchi et al., 2006; Meiswinkel et al., 2013; Kang et al., 2014). In this case, heterologous expression of a xylose isomerase XLI (encoded by *xylA*) from *Escherichia coli* is sufficient to convert D-xylose to D-xylulose, which is then phosphorylated by an endogenous xylulokinase XLK (encoded by *xylB*) to yield xylulose-5-phosphate as intermediate of the pentose phosphate pathway (Fig. 1, left). It could be also shown that an overexpression of xylose isomerases from other sources in combination with the endogenous xylulokinase resulted in a doubled growth rate on D-xylose and allowed the microbial synthesis of amino acids such as L-lysine, L-glutamate and L-ornithine as well as the diamine putrescine from this carbon source (Meiswinkel et al., 2013). However, for the latter three products, which are all derived from the TCA-cycle intermediate α-ketoglutarate, the introduction of this isomerase pathway for D-xylose assimilation in *C. glutamicum*

* Corresponding authors at: Forschungszentrum Jülich GmbH, Institut für Bio- und Geowissenschaften IBG-1: Biotechnologie, Leo-Brandt-Strasse, 52425 Jülich, NRW, Germany. Tel.: +49 2461 61 2843/+49 2461 61 6044; fax: +49 2461 61 2710.
E-mail addresses: s.noack@fz-juelich.de (S. Noack), j.marienhagen@fz-juelich.de (J. Marienhagen).

http://dx.doi.org/10.1016/j.jbiotec.2014.09.026
0168-1656/

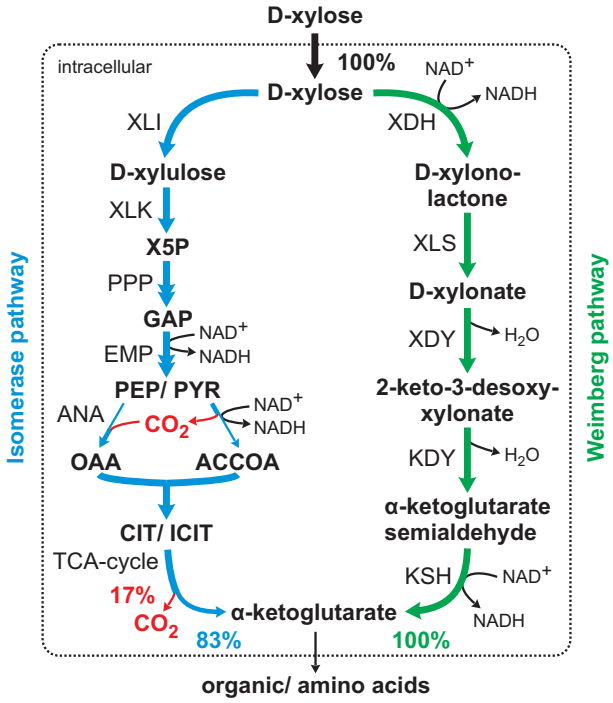

Fig. 1. Two alternative metabolic routes from D-xylose to α-ketoglutarate in *C. glutamicum*. Whereas the isomerase pathway leads to a significant carbon loss in the TCA-cycle (left), does the newly established Weimberg pathway allow for a complete carbon conversion (right).

has the drawback that a significant fraction of the D-xylose-derived carbon is lost in the form of CO_2 during product synthesis, lowering the overall product yield (cf. Fig. 1, left).

The Weimberg pathway, first discovered in *Pseudomonas fragi* and later also in *Haloferax volcanii* and *Caulobacter crescentus* (Weimberg, 1961; Johnsen et al., 2009; Stephens et al., 2007), represents a promising alternative for D-xylose assimilation. In this five-step oxidative pathway the pentose D-xylose is exclusively oxidized to the C_5-compound α-ketoglutarate without carbon loss (cf. Fig. 1, right). The functional implementation of the Weimberg pathway enabled *Pseudomonas putida* to grow on D-xylose as sole carbon source with a maximum growth rate of $\mu_{max} = 0.21\ h^{-1}$ (Meijnen et al., 2009). The Weimberg pathway has not been introduced to *C. glutamicum* before. However, it offers the advantage of a direct conversion of D-xylose to α-ketoglutarate, which is a precursor of the above mentioned products and also an interesting product itself (Barrett and Yousaf, 2008; Otto et al., 2011; Stottmeister et al., 2005). In this study we functionally integrated the Weimberg pathway from *C. crescentus* into *C. glutamicum* and compared this pathway to the already established isomerase pathway in the same organism. Furthermore, we provide a detailed analysis of biomass formation and substrate utilization during growth on D-xylose and mixed substrates and identified the accumulation of the pathway intermediate D-xylonate as a bottleneck during D-xylose assimilation.

Materials and methods

Construction of strains and plasmids

Routine methods such as PCR, DNA restriction or DNA ligation were carried out according to standard protocols (Sambrook and Russell, 2001). The oligonucleotides used for cloning, colony-PCRs and DNA sequencing were obtained from EurofinsMWGOperon (Ebersberg, Germany) and are listed in the Supplementary Table S1. Bacterial strains and plasmids used or constructed in the course of this work are listed in the Supplementary Table S2. All details regarding strain and plasmid construction can be found in the Supporting Information.

Cultivations

The defined medium CGXII (Keilhauer et al., 1993) supplemented with indicated D-glucose and D-xylose concentrations was used for all cultivations. The pH of the medium was adjusted with 4 M NaOH to 7.0. Supplements such as biotin, protocatechuate, trace elements, IPTG, spectinomycin, D-xylose, and D-glucose were added after autoclaving.

All cultivations were carried out in 48-well FlowerPlates (m2p-labs GmbH, Baesweiler, Germany) incubated in a BioLector (m2p-labs GmbH) embedded in a liquid handling station (JANUS™ working station, Perkin Elmer, Waltham MA, USA) for automated sampling and sample processing. Cultures were inoculated with 50 μl cell suspension either from cryo-stocks or fresh seed culture into 1 ml fresh medium. The cultivation settings were always kept at 1000 rpm, 95% humidity and 30 °C. Depending on the experiment the online signals for biomass (backscatter; gain 20), dissolved oxygen (pO_2; gain 35) and pH (gain 35) were measured in intervals of 9 (unsampled process) or 22 min (triggered sampling process), respectively. The FlowerPlates were covered with a gas permeable sealing foil (m2p-labs GmbH) to prevent contaminations and to allow a uniform gas exchange. Medium preparation and inoculation were performed manually under a sterile bench. For the estimation of substrate-specific biomass yields ($Y_{X/S}$) the corresponding backscatter (BS) measurements were recalculated to cell dry weight (CDW) data using the calibration model $CDW\ [g\,l^{-1}] = 0.048 \times BS\ g\,l^{-1} - 0.78\ g\,l^{-1}$ (Rohe et al., 2012).

GC–ToF–MS analysis

Untargeted metabolome screening in culture supernatants was performed via an Agilent 6890N gas chromatograph coupled to a Waters Micromass GCT Premier high resolution time of flight mass spectrometer. For details regarding sample preparation, MS operation and peak identification the reader is referred to Paczia et al. (2012).

Determination of D-glucose and D-xylose in culture supernatants

For substrate analytics two enzymatic assays were transferred into an automated 384-well microtiter plate format using the JANUS™ working station and an integrated plate reader (EnSpire™ Multimode Plate Reader, Perkin Elmer, Waltham MA, USA). D-glucose was measured with a standard protocol (Peterson and Young, 1968) and D-xylose with an enzymatic D-xylose assay kit (Megazyme, Wickow, Ireland). In both cases the NADH increase at 340 nm was monitored.

Results & discussion

Expression of the Weimberg pathway from C. crescentus for D-xylose assimilation in C. glutamicum

C. crescentus metabolizes D-xylose through the five-step Weimberg pathway yielding α-ketoglutarate (Fig. 1, right). All five enzymes of this catabolic route are encoded in the *xylXABCD* operon in the genome of this bacterium (Stephens et al., 2007). The D-xylose catabolism is initiated by the oxidation of D-xylose to D-xylonolactone, catalyzed by a xylose dehydrogenase (XDH, encoded by *xylB*). Subsequently, a xylonolactonase (XLS, encoded by *xylC*)

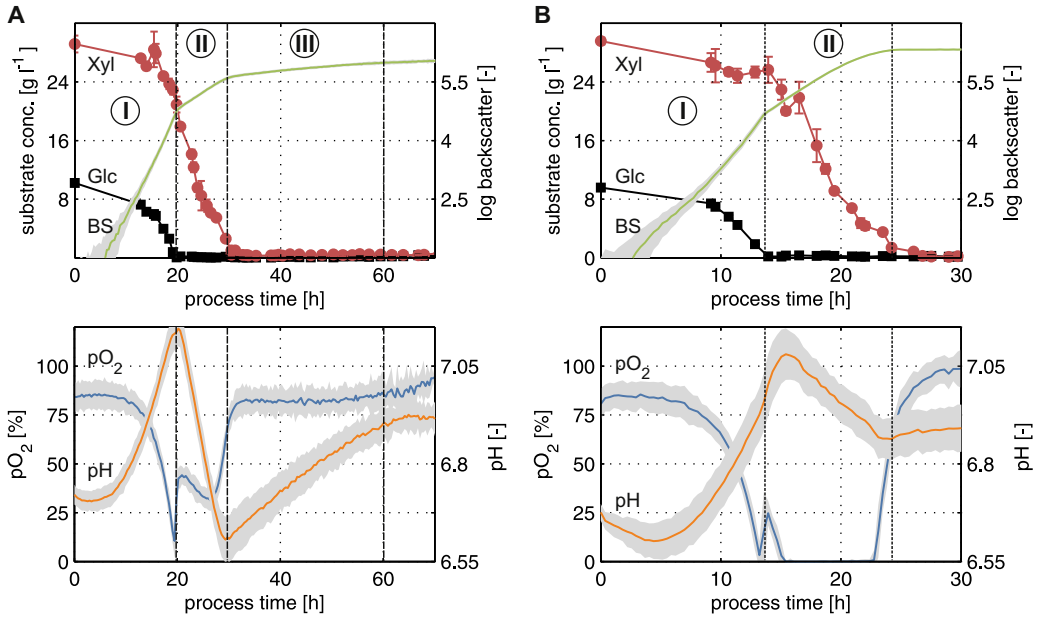

Fig. 2. Growth of *C. glutamicum* pEKEx3-*xylXABCD*$_{Cc}$ (A) and *C. glutamicum* pEKEx3-*xylA*$_{Xc}$-*xylB*$_{Cg}$ (B) on CGXII medium with a mixture of 30 g l^{-1} D-xylose (Xyl) and 10 g l^{-1} D-glucose (Glc) as carbon and energy source. Cultivations were performed in a single FlowerPlate™, in each case with online measurements of backscatter (BS), dissolved oxygen (pO$_2$) and pH. Mean values and confidence intervals (shaded in grey) were estimated from unsampled replicate cultures. Single wells were harvested for supernatant analyses including substrate consumption via enzymatic assays and by-product formation via untargeted GC–ToF–MS.

opens the lactone ring to form D-xylonate, which is dehydrated twice in two successive reactions by a xylonate dehydratase (XDY, encoded by *xylD*) and a 2-keto-3-desoxyxylonate dehydratase (KDY, encoded by *xylX*). The resulting α-ketoglutarate semialdehyde is finally oxidized to the TCA intermediate α-ketoglutarate by the α-ketoglutarate semialdehyde dehydrogenase (KSH, encoded by *xylA*).

With the aim to implement this catabolic pathway for D-xylose into *C. glutamicum*, the *xylXABCD*$_{Cc}$ operon was first PCR-amplified from genomic DNA of *C. crescentus*. Subsequently, this operon was cloned in the expression vector pEKEx3 (Hoffelder et al., 2010) under the transcriptional control of the promoter P*tac* and the resulting vector pEKEx3-*xylXABCD*$_{Cc}$ was introduced to *C. glutamicum* ATCC 13032. Successful expression of the heterologous genes could be confirmed by SDS-PAGE analysis (data not shown).

C. glutamicum pEKEx3-xylXABCD$_{Cc}$ *can utilize* D*-xylose in* D*-xylose/*D*-glucose mixtures via the Weimberg pathway*

The newly constructed strain *C. glutamicum* pEKEx3-*xylXABCD*$_{Cc}$ was able to grow on a mixture of 30 g l^{-1} D-xylose and 10 g l^{-1} D-glucose and consumed both carbon sources completely within 30 h of cultivation (Fig. 2A). During cultivation, three different growth phases were observed. Within the first growth phase, both sugars were consumed in parallel resulting in a maximum specific growth rate of $\mu_{max,I} = 0.28 \pm 0.005\ h^{-1}$. This growth rate is lower compared to the observed growth rate when cultivating this strain solely on 10 g l^{-1} D-glucose as sole carbon and energy source ($\mu_{max} = 0.35 \pm 0.004\ h^{-1}$, Fig. 3), indicating a potential growth inhibiting effect of D-xylose or an intermediate of the Weimberg pathway. Noteworthy, when cultivating the empty vector control strain *C. glutamicum* pEKEx3 on sole glucose, the resulting growth rate ($\mu_{max} = 0.35 \pm 0.011\ h^{-1}$) is equal to *C. glutamicum* pEKEx3-*xylXABCD*$_{Cc}$, but also significantly lower compared to the *C. glutamicum* wild-type growing under the same conditions ($\mu_{max} = 0.42 \pm 0.03\ h^{-1}$, Grünberger et al., 2013). This effect might be due to the metabolic burden of the plasmid or growth in selective media.

After 20 h of cultivation D-glucose was fully depleted. Although the same amount of D-xylose was taken up by the cells in this period, the biomass yield of $Y_{X/S} = 15\ g_{CDW}\ C\ mol_{Glc}^{-1}$ roughly corresponds to that of pure D-glucose cultures ($Y_{X/S} = 18\ g_{CDW}\ C\ mol_{Glc}^{-1}$, (Rohe et al., 2012) and cf. Fig. 3), thus showing that D-xylose does not directly contribute to biomass formation during the first growth phase. In the second growth phase D-xylose served as the main carbon and energy source, resulting in a growth rate of $\mu_{max,II} = 0.08 \pm 0.011\ h^{-1}$. Interestingly, after 30 h, when both sugars were depleted, biomass formation still continued at a very low rate of $\mu_{max,III} = 0.02 \pm 0.002\ h^{-1}$, indicating utilization of previously formed by-products.

The observed tri-phasic growth is also supported by online measurements of dissolved oxygen (pO$_2$) and external pH during cultivation (cf. Fig. 2A). When D-glucose became limiting the pO$_2$ sharply increased from 5% to 40% and then decreased again. However, in this second growth phase the pO$_2$ only decreased to 30% due to lower growth and concomitant oxygen consumption. Subsequently, when D-xylose became limiting the pO$_2$, showed again a stepwise increase to 75% and maintained at that level until the end of the third growth phase. In contrast, the pH dropped from 7.1 to 6.6 and increased to 6.9 after depletion of D-xylose. This underlines the formation of at least one organic acid as by-product, which was then re-consumed during the third growth phase.

In comparison to *C. glutamicum* pEKEx3-*xylXABCD*$_{Cc}$, the reference strain *C. glutamicum* pEKEx3-*xylA*$_{Xc}$-*xylB*$_{Cg}$ showed a bi-phasic growth with faster consumption of both substrates (carbon depletion after 23 h) and higher growth rates of $\mu_{max,I} = 0.33 \pm 0.005\ h^{-1}$ and $\mu_{max,II} = 0.19 \pm 0.003\ h^{-1}$, respectively (Fig. 2B). The growth rate of *C. glutamicum* pEKEx3-*xylA*$_{Xc}$-*xylB*$_{Cg}$ on D-xylose matches well with the previously reported values (Meiswinkel et al., 2013). Due to the fast growth on the second substrate it can be assumed that the cells were close to oxygen limitation, which in turn might have resulted in the formation of small amounts of organic acids and would explain the observed decrease in the external pH (cf. Fig. 2B). In contrast to *C. glutamicum* pEKEx3-*xylXABCD*$_{Cc}$, these putative by-products were not re-consumed by the reference strain as no additional biomass formation (accompanied by a pH increase)

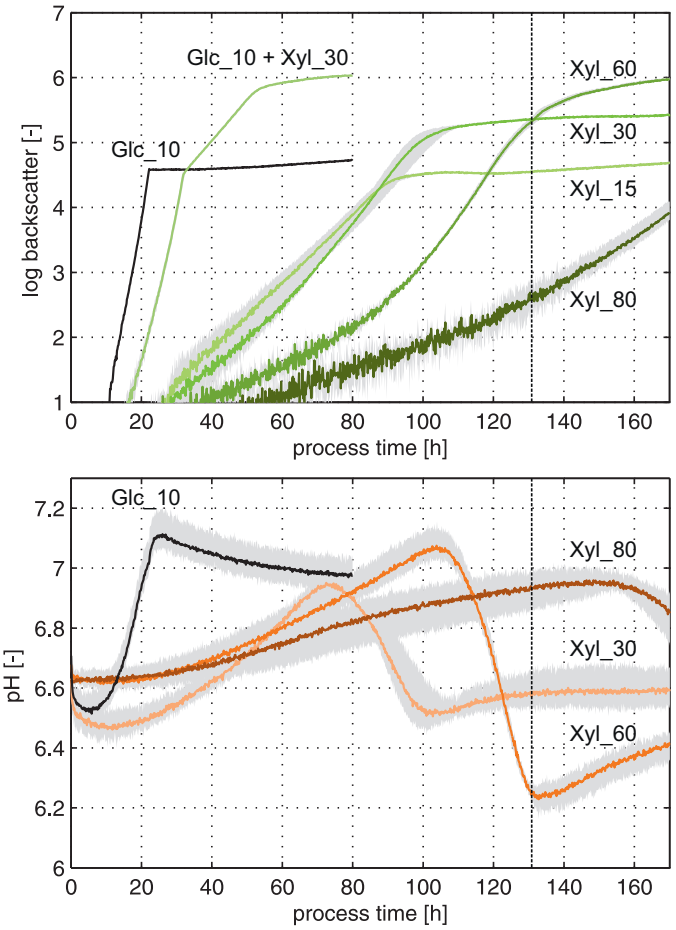

Fig. 3. Growth of *C. glutamicum* pEKEx3-*xylXABCD*$_{Cc}$ on CGXII medium with either 15, 30, 60 or 80 g l^{-1} of D-xylose (Xyl) as sole carbon and energy source. For comparison additional cultures on 10 g l^{-1} D-glucose (Glc) as well as a mixture of 10 g l^{-1} D-glucose and 30 g l^{-1} D-xylose were performed in parallel. All cultivations were carried out in a single FlowerPlate™ with online measurements of backscatter, dissolved oxygen and pH. Mean values were estimated from triplicate cultures. Confidence intervals (shaded in grey) were spanned from the minimum and maximum value at each measurement point. The vertical dashed line indicates the end of the exponential growth phase in the culture with 60 g l^{-1} D-xylose. For the sake of clarity only the pH values of selected cultivations are shown in the lower part.

was observable after D-xylose depletion. Therefore the formation of lactate, a typical by-product of *C. glutamicum* under anaerobic conditions (Käß et al., 2014) is very unlikely.

D-*Xylonate as major by-product during* D-*xylose assimilation in C. glutamicum pEKEx3-xylXABCD*$_{Cc}$

Recent studies showed that *Pseudomonas* species, harboring the Weimberg pathway, accumulate D-xylonate as by-product and reconsume it after depletion of other carbon sources (Meijnen et al., 2009; Köhler et al., 2014). Therefore, we analyzed the supernatant samples from the cultures of *C. glutamiucm* pEKEx3-*xylXABCD*$_{Cc}$, cultivated in the D-xylose/D-glucose mixture (cf. Fig. 2A) in more detail by applying untargeted GC-ToF-MS analysis (Supplementary Figs. S1–S5). This analysis confirmed the complete consumption of D-xylose after 30 h and, indeed, showed an accumulation of D-xylonate already after 12 h of cultivation. The extracellular concentration of D-xylonate steadily increased over time and decreased again with the onset of D-xylose limitation. This strongly indicates that the conversion of D-xylonate to 2-keto-3-desoxy-xylonate by xylonate dehydratase (XDY) is currently a rate-limiting step for efficient D-xylose assimilation via the introduced Weimberg pathway.

Interestingly, we also detected an accumulation of xylitol in the supernatant of *C. glutamicum* pEKEx3-*xylXABCD*$_{Cc}$ over the whole cultivation period (cf. Supplementary Fig. S5). Xylitol as a by-product of D-xylose conversion was also described by Sasaki et al., who recently reported an engineered *C. glutamicum* strain with increased xylitol accumulation from D-xylose under oxygen-deprived conditions (Sasaki et al., 2010). Noteworthy, xylitol is known as a toxic compound inhibiting cell growth of different bacteria such as *E. coli* (Reiner, 1977), *Streptococcus mutans* (Trahan, 1995), *Lactobacillus casei* (London and Hausman, 1982), and *C. glutamicum* (Sasaki et al., 2010). Therefore it is likely that the observed lower growth rates of *C. glutamicum* pEKEx3-*xylXABCD*$_{Cc}$ in comparison to the empty vector strain are due to xylitol inhibition.

The Weimberg pathway enables C. glutamicum to grow on D-*xylose as sole carbon and energy source*

In defined CGXII medium with D-xylose as the sole carbon and energy source, *C. glutamicum* pEKEx3-*xylXABCD*$_{Cc}$ was able to grow with $\mu_{max} = 0.07 \pm 0.01$ h^{-1}, which is comparable to the second growth phase on the D-xylose/D-glucose mixture (Fig. 3).

However, in comparison to growth on D-glucose alone, a long lag-phase was observed before exponential growth started. This effect was already observable in D-xylose/D-glucose mixtures, but is much more pronounced for pure D-xylose media, especially at elevated D-xylose concentrations of 60 g l^{-1} and 80 g l^{-1} (Fig. 3). The corresponding patterns of the external pH signal, namely the drop of pH, are quite comparable to the experiments on mixed substrates when D-xylose was metabolized (cmp. Fig. 2A and Fig. 3). Moreover, for the culture containing 60 g l^{-1} D-xylose, biomass formation slowly continued when the external pH started to increase again (Fig. 3, vertical dashed line). Hence, it can be assumed that in the presence of higher D-xylose concentrations more D-xylonate is produced, which is subsequently re-consumed by the cells. From these observations it can be speculated that a limited downstream assimilation of D-xylose leading to the accumulation of D-xylonate, an inhibition by a toxic by-product such as xylitol, or a combination thereof, are main drivers for the observed growth delay.

Conclusions

In this study we could demonstrate, that the heterologous expression of the Weimberg pathway of *C. crescentus* for the conversion of D-glucose to α-ketoglutarate enables *C. glutamicum* ATCC 13032 to utilize D-xylose either in combination with glucose, or as sole carbon and energy source.

We identified the transient extracellular accumulation of D-xylonate and xylitol during cultivation of the recombinant *C. glutamicum* strain on D-xylose containing media. A balanced, heterologous expression of the individual pathway genes, which could be also codon-optimized for *C. glutamicum*, might minimize D-xylonate as major by-product and help to improve the overall performance of the pathway. The formation of xylitol as potentially inhibiting substance should be investigated in more detail in the future to ensure efficient biomass formation when utilizing D-xylose via the Weimberg pathway.

Furthermore, D-xylose uptake might represent an additional bottleneck. The mechanism of D-xylose uptake in *C. glutamicum* is still unknown, but a potential limitation could be circumvented by expressing known pentose uptake systems from other organisms, such as the arabinose transporter AraE from *C. glutamicum* ATCC 31831 (Sasaki et al., 2009). Functional expression of this transporter already enhanced D-xylose uptake of *C. glutamicum* R three-fold.

Overall, the functional implementation of the Weimberg pathway in *C. glutamicum* represents the first step toward the bio-based

production of α-ketoglutarate or α-ketoglutarate-derived compounds (e.g. L-glutamate) from biomass-derived D-xylose with minimized loss of carbon as CO_2.

Appendix A. Supplementary data

Supplementary data associated with this article can be found, in the online version, at http://dx.doi.org/10.1016/j.jbiotec.2014.09.026.

References

Aristidou, A., Penttila, M., 2000. Metabolic engineering applications to renewable resource utilization. Curr. Opin. Biotechnol. 11, 187–198.

Barrett, D.G., Yousaf, M.N., 2008. Poly(triol α-ketoglutarate) as biodegradable chemoselective, and mechanically tunable elastomers. Macromolecules 41, 6347–6352.

Barrett, E., Stanton, C., Zelder, O., Fitzgerald, G., Ross, R.P., 2004. Heterologous expression of lactose- and galactose-utilizing pathways from lactic acid bacteria in *Corynebacterium glutamicum* for production of lysine in whey. Appl. Environ. Microbiol. 70, 2861–2866.

Blombach, B., Seibold, G.M., 2010. Carbohydrate metabolism in *Corynebacterium glutamicum* and applications for the metabolic engineering of L-lysine production strains. Appl. Microbiol. Biotechnol. 86, 1313–1322.

Grünberger, A., van Ooyen, J., Paczia, N., Rohe, P., et al., 2013. Beyond growth rate 0.6: *Corynebacterium glutamicum* cultivated in highly diluted environments. Biotechnol. Bioeng. 110, 220–228.

Hoffelder, M., Raasch, K., van Ooyen, J., Eggeling, L., 2010. The E2 domain of OdhA of *Corynebacterium glutamicum* has succinyltransferase activity dependent on lipoyl residues of the acetyltransferase AceF. J. Bacteriol. 192, 5203–5211.

Johnsen, U., Dambeck, M., Zaiss, H., Fuhrer, T., et al., 2009. D-Xylose degradation pathway in the halophilic archaeon *Haloferax volcanii*. J. Biol. Chem. 284, 27290–27303.

Kang, M.K., Lee, J., Um, Y., Lee, T.S., et al., 2014. Synthetic biology platform of CoryneBrick vectors for gene expression in *Corynebacterium glutamicum* and its application to xylose utilization. Appl. Microbiol. Biotechnol. 98, 5991–6002.

Käß, F., Junne, S., Neubauer, P., Wiechert, W., Oldiges, M., 2014. Process inhomogeneity leads to rapid side product turnover in cultivation of *Corynebacterium glutamicum*. Microb. Cell Fact. 13, 6.

Kawaguchi, H., Vertes, A.A., Okino, S., Inui, M., Yukawa, H., 2006. Engineering of a xylose metabolic pathway in *Corynebacterium glutamicum*. Appl. Environ. Microbiol. 72, 3418–3428.

Keilhauer, C., Eggeling, L., Sahm, H., 1993. Isoleucine synthesis in *Corynebacterium glutamicum*: molecular analysis of the *ilvB-ilvN-ilvC* operon. J. Bacteriol. 175, 5595–5603.

Köhler, K.A., Blank, L.M., Frick, O., Schmid, A., 2014. D-Xylose assimilation via the Weimberg pathway by solvent-tolerant *Pseudomonas taiwanensis* VLB120. Environ. Microbiol., http://dx.doi.org/10.1111/1462-2920.12537.

Kotrba, P., Inui, M., Yukawa, H., 2003. A single V317A or V317M substitution in Enzyme II of a newly identified beta-glucoside phosphotransferase and utilization system of *Corynebacterium glutamicum* R extends its specificity towards cellobiose. Microbiology 149, 1569–1580.

London, J., Hausman, S., 1982. Xylitol-mediated transient inhibition of ribitol utilization by *Lactobacillus casei*. J. Bacteriol. 150, 657–661.

Meijnen, J.P., de Winde, J.H., Ruijssenaars, H.J., 2009. Establishment of oxidative D-xylose metabolism in *Pseudomonas putida* S12. Appl. Environ. Microbiol. 75, 2784–2791.

Meiswinkel, T.M., Gopinath, V., Lindner, S.N., Nampoothiri, K.M., Wendisch, V.F., 2013. Accelerated pentose utilization by *Corynebacterium glutamicum* for accelerated production of lysine, glutamate, ornithine and putrescine. Microb. Biotechnol. 6, 131–140.

Otto, C., Yovkova, V., Barth, G., 2011. Overproduction and secretion of alpha-ketoglutaric acid by microorganisms. Appl. Microbiol. Biotechnol. 92, 689–695.

Paczia, N., Nielgen, A., Lehmann, T., Gätgens, J., et al., 2012. Extensive exometabolome analysis reveals extended overflow metabolism in various microorganisms. Microb. Cell Fact., 11.

Peterson, J.I., Young, D.S., 1968. Evaluation of the hexokinase-glucose-6-phosphate dehydrogenase method of determination of glucose in urine. Anal. Biochem. 23, 301–316.

Reiner, A.M., 1977. Xylitol and D-arabitol toxicities due to derepressed fructose, galactitol, and sorbitol phosphotransferases of *Escherichia coli*. J. Bacteriol. 132, 166–173.

Rohe, P., Venkanna, D., Kleine, B., Freudl, R., Oldiges, M., 2012. An automated workflow for enhancing microbial bioprocess optimization on a novel microbioreactor platform. Microb. Cell Fact. 11, 144.

Sambrook, J., Russell, D., 2001. Molecular Cloning. A Laboratory Manual. Cold Spring Harbor Laboratory Press, Cold Spring Harbor, NY.

Sasaki, M., Jojima, T., Kawaguchi, H., Inui, M., Yukawa, H., 2009. Engineering of pentose transport in *Corynebacterium glutamicum* to improve simultaneous utilization of mixed sugars. Appl. Microbiol. Biotechnol. 85, 105–115.

Sasaki, M., Jojima, T., Inui, M., Yukawa, H., 2010. Xylitol production by recombinant *Corynebacterium glutamicum* under oxygen deprivation. Appl. Microbiol. Biotechnol. 86, 1057–1066.

Schneider, J., Niermann, K., Wendisch, V.F., 2011. Production of the amino acids L-glutamate, L-lysine, L-ornithine and L-arginine from arabinose by recombinant *Corynebacterium glutamicum*. J. Biotechnol. 154, 191–198.

Seibold, G., Auchter, M., Berens, S., Kalinowski, J., Eikmanns, B.J., 2006. Utilization of soluble starch by a recombinant *Corynebacterium glutamicum* strain: growth and lysine production. J. Biotechnol. 124, 381–391.

Stephens, C., Christen, B., Fuchs, T., Sundaram, V., et al., 2007. Genetic analysis of a novel pathway for D-xylose metabolism in *Caulobacter crescentus*. J. Bacteriol. 189, 2181–2185.

Stottmeister, U., Aurich, A., Wilde, H., Andersch, J., et al., 2005. White biotechnology for green chemistry: fermentative 2-oxocarboxylic acids as novel building blocks for subsequent chemical syntheses. J. Ind. Microbiol. Biotechnol. 32, 651–664.

Trahan, L., 1995. Xylitol: a review of its action on mutans streptococci and dental plaque—its clinical significance. Int. Dent. J. 45, 77–92.

Weimberg, R., 1961. Pentose oxidation by *Pseudomonas fragi*. J. Biol. Chem. 236, 629–635.

3.2.3 Supplementary material

Construction of strains and plasmids & untargeted metabolome screening of culture supernatants

Supporting Information for Radek* et al., *2014

Engineering of *Corynebacterium glutamicum* for minimized carbon loss during utilization of D-xylose containing substrates

Andreas Radek[1], Karin Krumbach[1], Jochem Gätgens[1], Volker F. Wendisch[2], Wolfgang Wiechert[1], Michael Bott[1], Stephan Noack[1]*, Jan Marienhagen[1]*

Construction of strains and plasmids

The enzymes for recombinant DNA work were obtained from Fermentas (St. Leon-Rot, Germany) and Merck Millipore (Billerica, Massachusetts, USA). Chromosomal DNA of *Caulobacter crescentus* ATCC 15252 (synonymous with *Caulobacter vibrioides*) [1], which served as template DNA for the amplification of the *xylXABCD*$_{Cc}$-operon was purchased from the DSMZ (DSMZ-4727; Deutsche Stammsammlung für Mikroorganismen und Zellkulturen GmbH, Braunschweig, Germany). The *xylXABCD*$_{Cc}$-operon (6,317 bp) was PCR-amplified using the oligonucleotides xylXABCD_for and xylXABCD_rev (Table S1). Application of these oligonucleotides replaced the original GTG-START-codon of the first gene (*xylX*) by an ATG and the original TGA-STOP-codon of the last gene (*xylD*) by a TAA-TAA double STOP-codon during PCR-amplification to improve expression in *C. glutamicum*. The obtained 6.3 kb PCR-fragment was restricted by *Pst*I and *Eco*RV and cloned into the *Sma*I/*Pst*I-restricted expression vector pEKEx3. *Escherichia coli* DH5α was transformed with this plasmid using the RbCl-method [2]. Successful cloning was verified by restriction analysis of the resulting plasmid pEKEx3-*xylXABCD*$_{Cc}$, colony-PCRs and DNA sequencing using oligonucleotides specific for the plasmid and the *xylXABCD*$_{Cc}$ operon (Table S1). Subsequently, *C. glutamicum* ATCC 13032 was transformed with pEKEx3-*xylXABCD*$_{Cc}$ yielding *C. glutamicum* pEKEx3-*xylXABCD*$_{Cc}$ [3].

TABLE 3.1: Oligonucleotides used in manuscript II

Oligonucleotide	Sequence (5' → 3') and properties[a]
Amplification of the xyl-operon from the genome of *C. vibroides*	
pXYLXABCD_for	CCGCCTGCAGAAGGAGATATAGATATGGGCGTGAGTGAATTCCTGCCG GAAG (*Pst*I)
pXYLXABCD_rev	GGCGGATATCTTATTAGTGGTTGTGGCGGGGCAGCTTG (*Eco*RV)
Colony PCR-primer/Sequencing primer (vector pEKEx3)	
pEKEx3_for	CGGCGTTTCACTTCTGAGTTCGGC
pEKEx3_for2	CATTCGATGGTGTCAACGTAAATG
pEKEx3_rev	GATATGACCATGATTACGCCAAGC
Sequencing primer (operon *xylXABCD$_{Cc}$*)	
pXYLXA-D_400	TTCAGGCATTGCAGGTCGAC
pXYLXA-D_491	ATGCCTGAAGGCCGCCGGCGTGAC
pXYLXA-D_532	TTGAGCGGGTCATCGAGGAG
pXYLXA-D_793	CAATGACAGCCACTGGAACAAC
pXYLXA-D_979	AACAGGCGGAAGAACGGACC
pXYLXA-D_1145	CGGCTTTGCTTTGTTCCTGGG
pXYLXA-D_1470	TTTGCGCCGACATCATAACG
pXYLXA-D_1736	ACGGCCAGAACCTGGAAAGCAC
pXYLXA-D_1942	TGATGTCGGCCAGCACGTTG
pXYLXA-D_2350	TCCGAAGACCAGATGGAGAC
pXYLXA-D_2379	CTATATCGACATCGCTGCGTCC
pXYLXA-D_2821	TGTCCTCAGCCATCTATCC
pXYLXA-D_2850	CCTTCAGGCTGGGATAGATG
pXYLXA-D_3532	TCTGCACCGGCCACGAATAC
pXYLXA-D_3811	CCCGCCACCGGCGAGCGCTTCAG
pXYLXA-D_4034	ATGGTGCCGAACCACAGACG
pXYLXA-D_4145	ACGGCAAGACCTTCTACCAC
pXYLXA-D_4586	CGCGATTGGTTCGATAACCC
pXYLXA-D_5169	GTGCCCATGGTGTTGCAGTG
pXYLXA-D_5310	TCAAACCGCTCGACATCCTG
pXYLXA-D_5760	AGTTCCGCAAGCGCTACCTG

[a]Recognition sites for the indicated restriction enzymes are underlined.

TABLE 3.2: Strains and plasmids used in manuscript II.

Strain or plasmid	Relevant characteristics	Source or reference
E. coli		
DH5α	F^- φ80dlacΔ(*lacZ*)M15 Δ (*lacZYA-argF*) U169 *endA*1 *recA*1 *hsdR*17 (r_K^-, m_K^+) *deoR thi*-1 *phoA supE*44 λ^- *gyrA*96 *relA*1	Invitrogen (Karlsruhe, Germany)
C. glutamicum		
ATCC 13032	Biotin-auxotrophic wild-type strain	[4]
Plasmids		
pEKEx3	$Spec^R$; *C. glutamicum*/ *E. coli* shuttle vector for regulated gene expression; (P_{tac}, $lacI^Q$, pBL1 $oriV_{Cg}$, pUC18 $oriV_{Ec}$)	[5]
pEKEx3-$xylA_{Xc}$-$xylB_{Cg}$	$Spec^R$; pEKEx3 derivative for the regulated expression of $xylA_{Xc}$ of *X. campestris* and $xylB_{Cg}$ of *C. glutamicum*	[6]
pEKEx3-$xylXABCD_{Cc}$	$Spec^R$; pEKEx3 derivative for the regulated expression of $xylXABCD_{Cc}$ of *C. crescentus*	This work

FIGURE 3.3: Selected chromatograms from untargeted metabolome screening

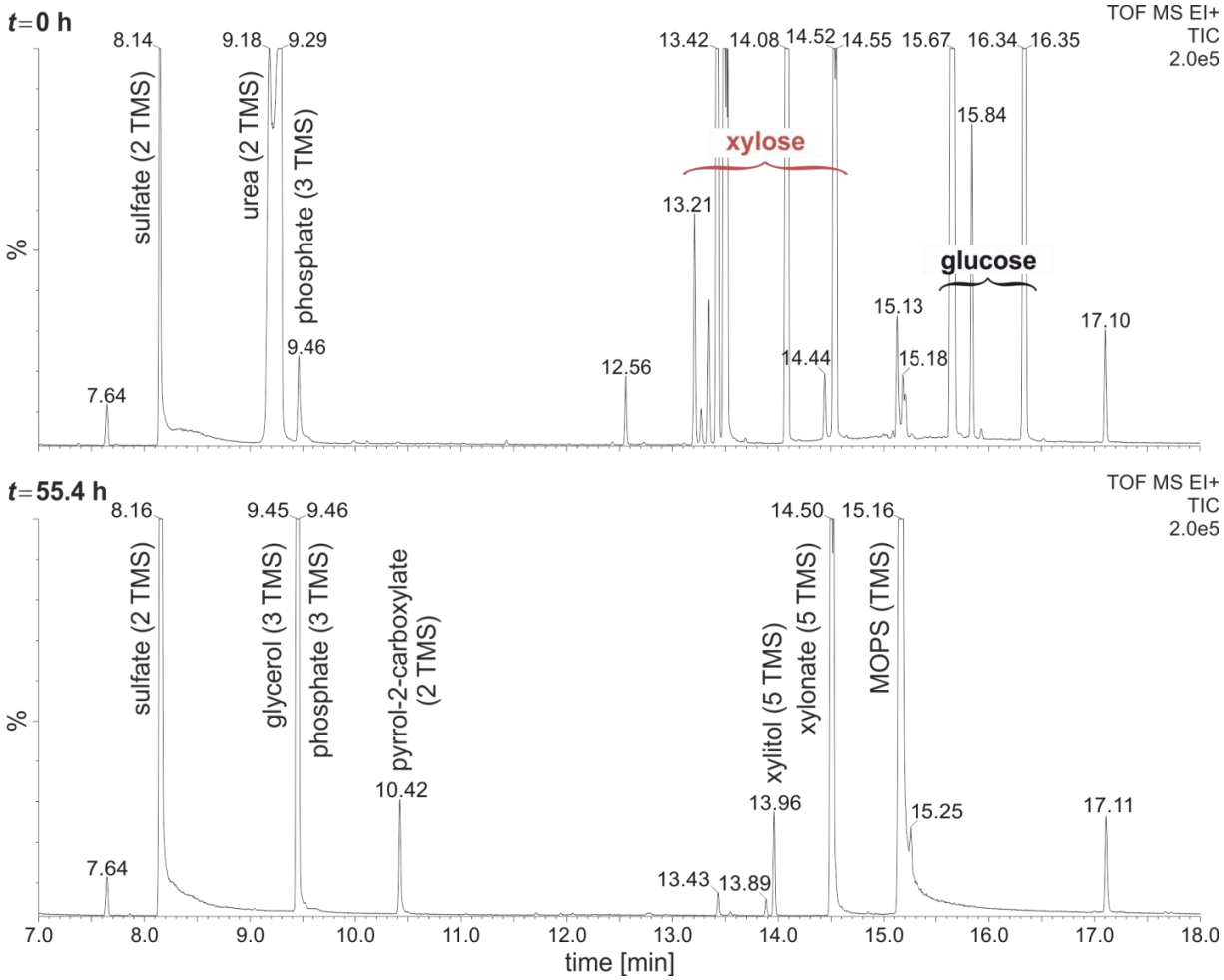

Selected chromatograms from untargeted metabolome screening of culture supernatant samples from batch cultivation of *C. glutamicum* pEKEx3-*xylXABCD*$_{Cc}$, in CGXII medium with a mixture of 10 g l^{-1} D-glucose and 30 g l^{-1} D-xylose as carbon and energy source.

FIGURE 3.4: Selected chromatograms showing the depletion of D-glucose after 20 h of cultivation.

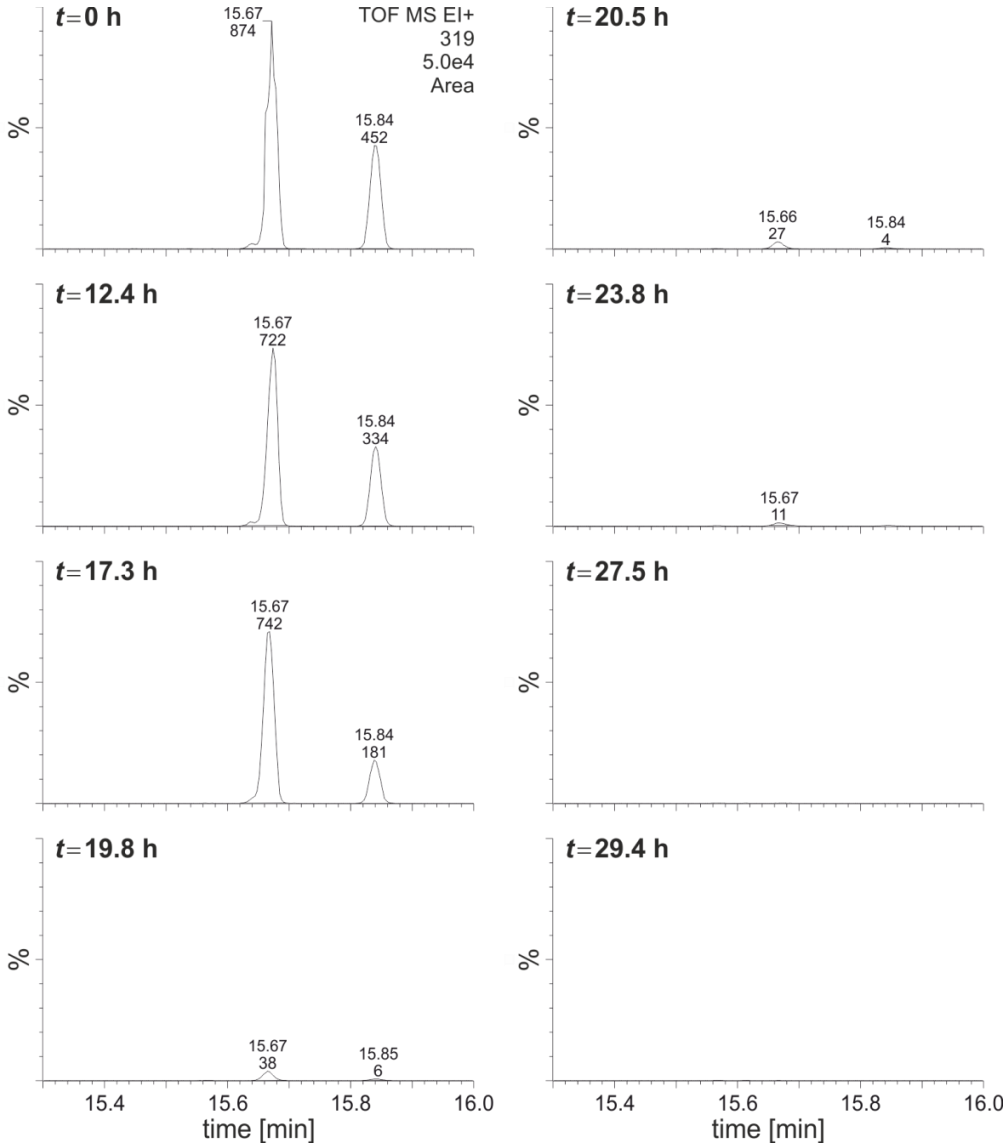

Depletion of D-glucose after 20 h of cultivation.

FIGURE 3.5: Selected chromatograms showing the depletion of D-xylose after 30 h of cultivation.

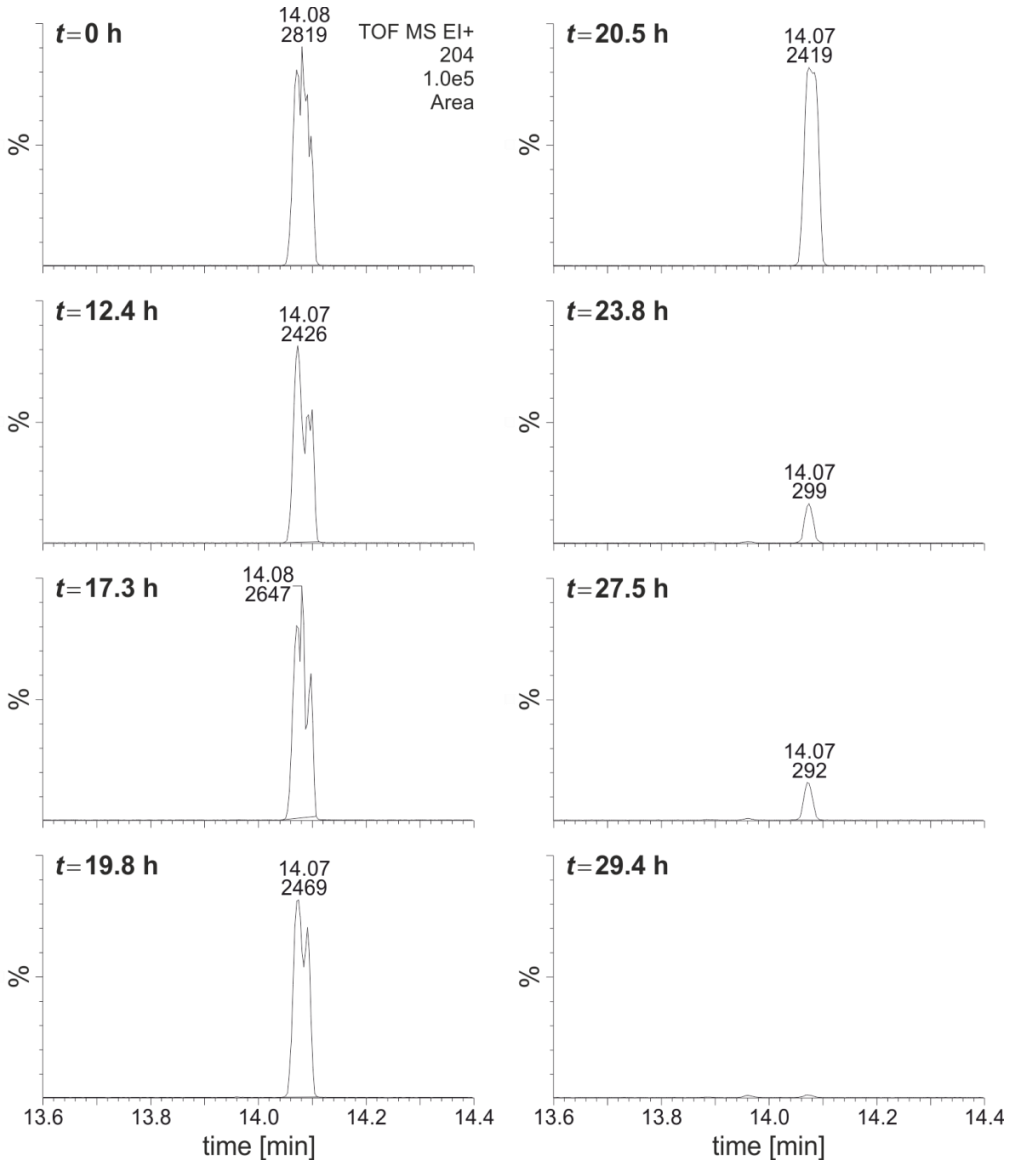

Depletion of D-xylose after 30 h of cultivation.

FIGURE 3.6: Selected chromatograms showing the by-product formation of D-xylonate.

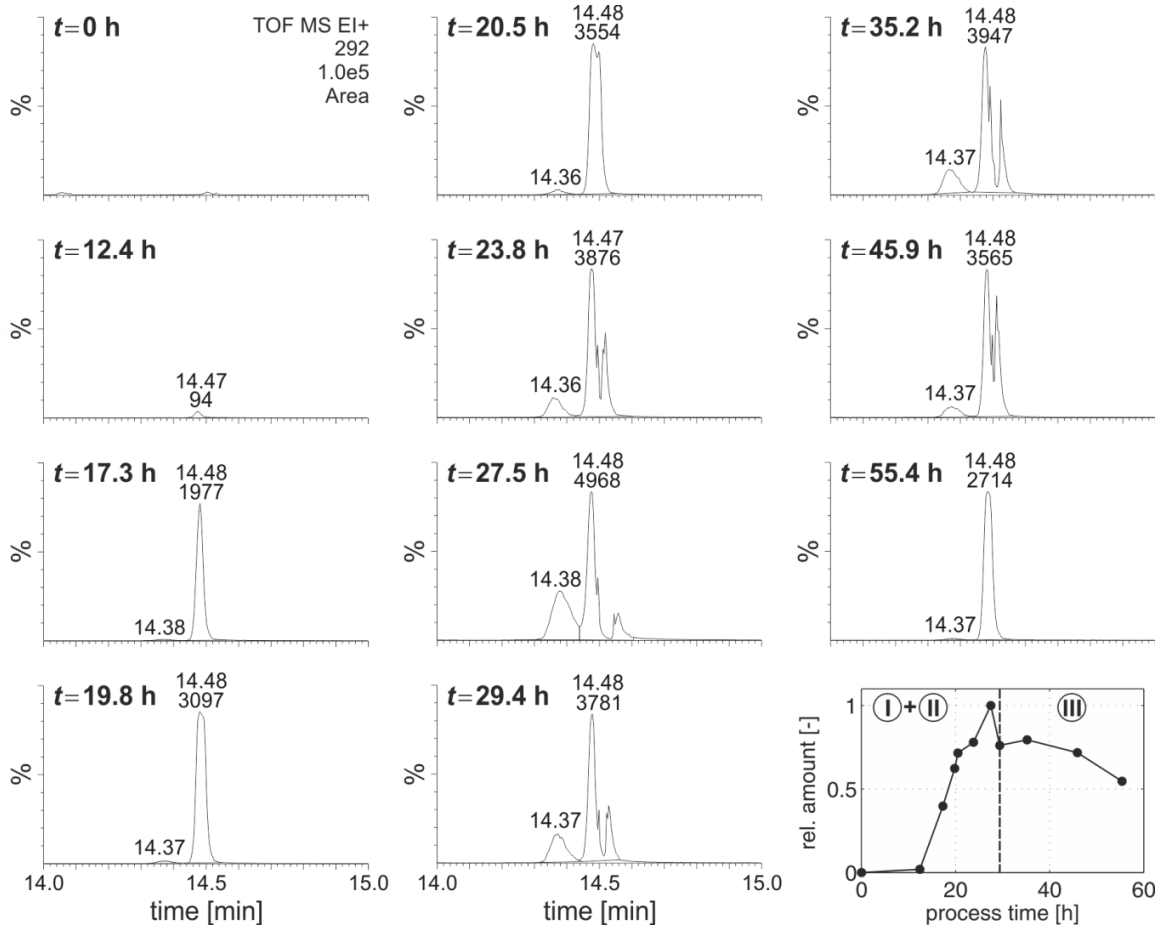

Selected chromatograms showing the by-product formation of D-xylonate within the first two growth phases and its re-consumption in the third growth phase.

FIGURE 3.7: Selected chromatograms showing the accumulation of xylitol.

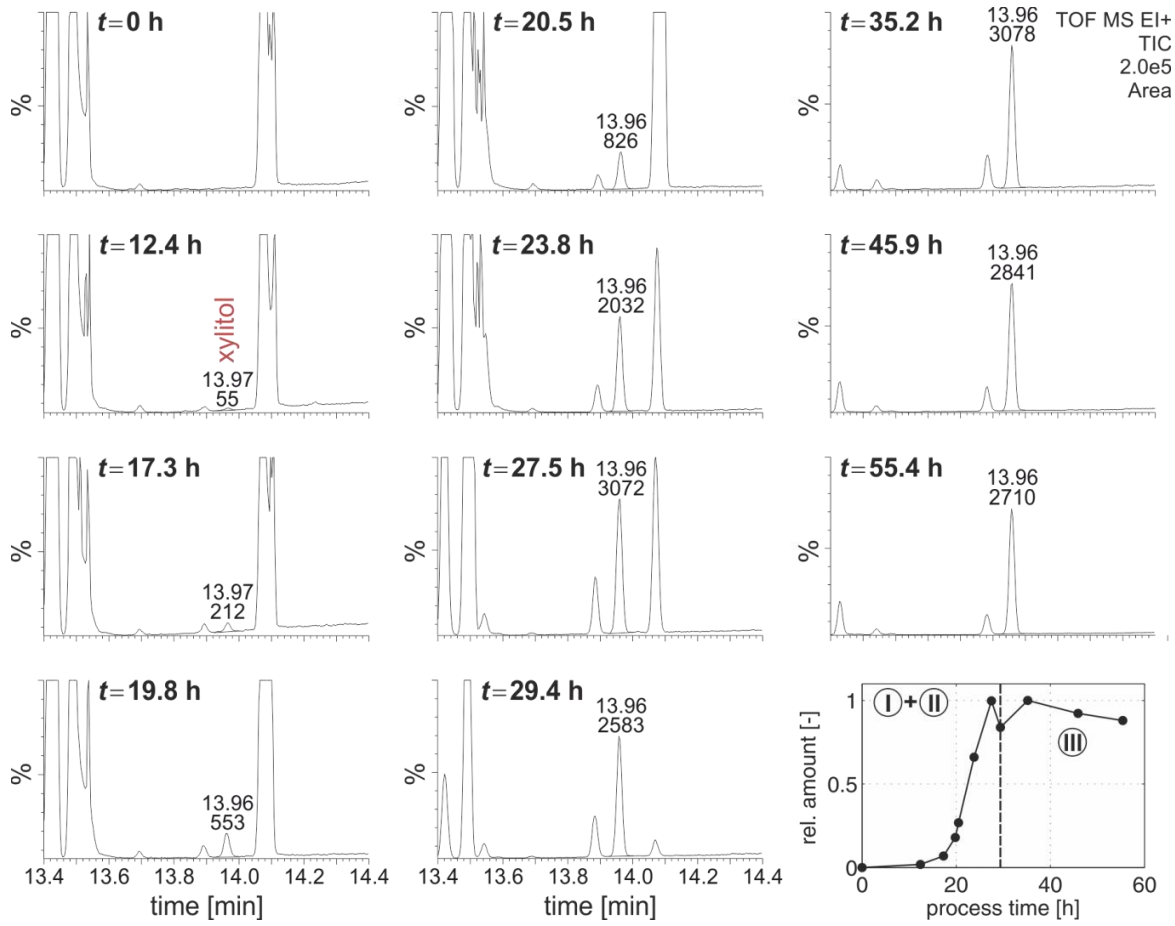

Selected chromatograms showing the accumulation of xylitol in the supernatant over the whole cultivation period.

References

[1] Abraham, W. R., Strompl, C., Meyer, H., Lindholst, S.*, et al.*, Phylogeny and polyphasic taxonomy of *Caulobacter* species. Proposal of *Maricaulis* gen. nov. with *Maricaulis maris* (Poindexter) comb. nov. as the type species, and emended description of the genera *Brevundimonas* and *Caulobacter*. *International journal of systematic bacteriology* 1999, *49 Pt 3*, 1053-1073.

[2] Hanahan, D., Studies on transformation of *Escherichia coli* with plasmids. *J Mol Biol* 1983, *166*, 557-580.

[3] van der Rest, M. E., Lange, C., Molenaar, D., A heat shock following electroporation induces highly efficient transformation of *Corynebacterium glutamicum* with xenogeneic plasmid DNA. *Applied Microbiology and Biotechnology* 1999, *52*, 541-545.

[4] Abe, S., Takayama, K. I., Kinoshit.S, Taxonomical studies on glutamic acid producing bacteria. *Journal of General and Applied Microbiology* 1967, *13*, 279-301.

[5] Hoffelder, M., Raasch, K., van Ooyen, J., Eggeling, L., The E2 domain of OdhA of *Corynebacterium glutamicum* has succinyltransferase activity dependent on lipoyl residues of the acetyltransferase AceF. *J Bacteriol* 2010, *192*, 5203-5211.

[6] Meiswinkel, T. M., Gopinath, V., Lindner, S. N., Nampoothiri, K. M., Wendisch, V. F., Accelerated pentose utilization by *Corynebacterium glutamicum* for accelerated production of lysine, glutamate, ornithine and putrescine. *Microb Biotechnol* 2013, *6*, 131-140.

3.2.4 Main achievements of this manuscript

• Functional implementation of the Weimberg pathway from *C. crescentus* in *C. glutamicum* ATCC13032.

• A tri-phasic growth behavior on a mixture of D-glucose (μ_{max} = 0.28 h^{-1}) and D-xylose (μ_{max} = 0.08 h^{-1}) was found.

• Long lag phases were observed on pure D-xylose medium, especially at higher substrate concentrations (>60 g l^{-1}) with up to 50 hours.

• D-xylonate and xylitol were found as major by-products by GC-ToF-MS analysis. While D-xylonate was partly re-consumed by the cells, xylitol could be responsible for the observed very low growth rates on sole D-xylose (see chapter 3.3 for a detailed study).

3.3 Formation of xylitol and xylitol-5-phosphate and its impact on growth of D-xylose-utilizing *Corynebacterium glutamicum* strains

3.3.1 Short introduction to this manuscript

In the previous study xylitol was found as one major by-product of the newly engineered *C. glutamicum* strain harboring the $xylXABCD_{Cc}$ operon for the Weimberg pathway. Within the following manuscript the influence of xylitol and further xylitol-5-phosphate on growth of D-xylose utilizing strains is investigated in detail.

It is known that xylitol and more specifically its phosphorylated derivate xylitol-5-phoshate can inhibit the growth of some microorganisms. In particular, its effect on *Streptococcus mutans* as an oral microbe is well studied (Kakuta et al. 2003; Miyasawa et al. 2003). Here it was hypothesized that xylitol-5-phosphate or xylulose-5-phosphate can inhibit phosphofructokinase, lowering the overall glycolytic flux (Marsh et al. 2009). Xylitol-5-phosphate emerges through the uptake of xylitol via the PTSFru uptake system or by phosphorylation via the xylulose kinase (Marsh et al. 2009). Therefore, it was also assumed that the inhibition is related to this uptake system and xylitol enters an energy consuming "futile cycle" of import and export. PEP and NAD^+ are consumed by the importing phosphotransferase system and possibly ATP by the export (Hausman et al. 1984). An inhibition of several xylose isomerases through xylitol in *S. cerevisiae* is also described (Brat et al. 2009).

To get a closer look into the formation of xylitol and its impact on growth of *C. glutamicum*, additional mutant strains were constructed. Endogenous genes with high similarities to known xylose reductases from other prokaryotes and eukaryotes were deleted to identify putative enzyme candidates catalyzing the intracellular reduction of D-xylose to xylitol in *C. glutamicum*.

All mutant strains were screened with the BioLector system for growth phenotypes on media with different concentrations of extracellular xylitol as well as on different carbon sources. From the resulting data several conclusions on the strain specific effect of xylitol were drawn, which are presented in the following manuscript.

3.3.2 Manuscript III

Formation of xylitol and xylitol-5-phosphate and its impact on growth of D-xylose-utilizing *Corynebacterium glutamicum* strains

Published as:

Radek A, Müller M F, Gätgens J, Eggeling L, Krumbach K, Marienhagen J, Noack S, Formation of xylitol and xylitol-5-phosphate and its impact on growth of D-xylose-utilizing *Corynebacterium glutamicum* strains. *Journal of Biotechnology* 231 (2016) 160-166

Journal of Biotechnology 231 (2016) 160–166

Contents lists available at ScienceDirect

Journal of Biotechnology

journal homepage: www.elsevier.com/locate/jbiotec

Formation of xylitol and xylitol-5-phosphate and its impact on growth of D-xylose-utilizing *Corynebacterium glutamicum* strains

Andreas Radek, Moritz-Fabian Müller, Jochem Gätgens, Lothar Eggeling, Karin Krumbach, Jan Marienhagen, Stephan Noack*

Institute of Bio- and Geosciences, IBG-1: Biotechnology, Forschungszentrum Jülich GmbH, Jülich D-52425, Germany

ARTICLE INFO

Article history:
Received 24 March 2016
Received in revised form 6 June 2016
Accepted 9 June 2016
Available online 11 June 2016

Keywords:
Corynebacterium glutamicum
Xylitol
Xylitol-5-phosphate
D-xylose
Isomerase pathway
Weimberg pathway

ABSTRACT

Wild-type *Corynebacterium glutamicum* has no endogenous metabolic activity for utilizing the lignocellulosic pentose D-xylose for cell growth. Therefore, two different engineering approaches have been pursued resulting in platform strains harbouring a functional version of either the Isomerase (ISO) or the Weimberg (WMB) pathway for D-xylose assimilation. In a previous study we found for *C. glutamicum* WMB by-product formation of xylitol during growth on D-xylose and speculated that the observed lower growth rates are due to the growth inhibiting effect of this compound. Based on a detailed phenotyping of the ISO, WMB and the wild-type strain of *C. glutamicum*, we here show that this organism has a natural capability to synthesize xylitol from D-xylose under aerobic cultivation conditions. We furthermore observed the intracellular accumulation of xylitol-5-phosphate as a result of the intracellular phosphorylation of xylitol, which was particularly pronounced in the *C. glutamicum* ISO strain. Interestingly, low amounts of supplemented xylitol strongly inhibit growth of this strain on D-xylose, D-glucose and D-arabitol. These findings demonstrate that xylitol is a suitable substrate of the endogenous xylulokinase (XK, encoded by *xylB*) and its overexpression in the ISO strain leads to a significant phosphorylation of xylitol in *C. glutamicum*. Therefore, in order to circumvent cytotoxicity by xylitol-5-phosphate, the WMB pathway represents an interesting alternative route for engineering *C. glutamicum* towards efficient D-xylose utilization.

1. Introduction

It is a well-known fact that xylitol and, more specifically, its phosphorylated derivative xylitol-5-phosphate inhibits the growth of bacteria (London and Hausman, 1982; Trahan, 1995). Xylitol-5-phosphate is considered as a non-metabolizable sugar phosphate inhibiting the glycolytic enzymes phosphoglucose isomerase and phosphofructokinase. In addition, it was postulated that xylitol inhibits glucose uptake through competitive binding to the histidine-containing phosphocarrier protein HPr-P of the phosphoenolpyruvate phosphotransferase system (PEP-PTS) (Miyasawa-Hori et al., 2006).

Recently, it was suggested that the xylulokinase (XK, encoded by *xylB*) catalyses xylitol phosphorylation during growth of *Escherichia coli* in D-xylose containing media (Akinterinwa and Cirino, 2009). In another study, Sasaki et al. reported decreasing growth rates of *Corynebacterium glutamicum* R when cultivated on D-glucose with increasing concentrations of added xylitol (Sasaki et al., 2010). The authors argued that xylitol could be phosphorylated by a xylulokinase (cg0147), i.e. comparable to *E. coli*, or by the PTS-system PTS^{Fru} with the D-fructose specific component PtsF (encoded by *ptsF*, cg2120) (Fig. 1). Indeed, the deletion of *xylB* and *ptsF* in a recombinant *C. glutamicum* R strain expressing xylose reductase from *Candida tenuis* greatly increased xylitol formation from D-xylose under oxygen deprivation. This result could be attributed to a reduced intracellular accumulation of cytotoxic xylitol-5-phosphate, however, until now no xylitol-5-phosphate formation was shown by any *C. glutamicum* strain. Moreover, it remained unclear, which reaction is then mainly responsible for xylitol phosphorylation.

Interestingly, Sasaki et al. also showed that *Corynebacterium glutamicum* R accumulated small amounts of xylitol under oxygen deprivation when utilizing D-xylose as sole carbon source – but no xylitol formation was detected under aerobic conditions (Sasaki et al., 2010). By contrast, we could recently show that the D-xylose-converting strain *C. glutamicum* pEKEx3-$xylXABCD_{Cc}$, which

* Corresponding author.
E-mail address: s.noack@fz-juelich.de (S. Noack).

http://dx.doi.org/10.1016/j.jbiotec.2016.06.009
0168-1656/

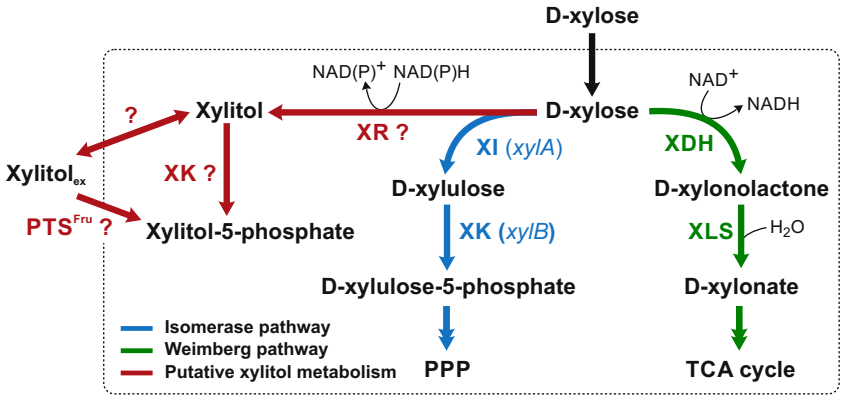

Fig. 1. Established pathways of D-xylose assimilation and putative xylitol metabolism in *Corynebacterium glutamicum*. Abbreviations: XI, D-xylose isomerase; XK, xylulokinase; XDH, D-xylose dehydrogenase; XLS, xylolactonase; XR, D-xylose reductase; PTS^{Fru}, fructose specific phosphotransferase component; PPP, Pentose phosphate pathway; TCA, Tricarboxylic acid cycle.

is based on *C. glutamicum* ATCC 13032 and employs the Weimberg (WMB) pathway from *Caulobacter crescentus* for D-xylose utilisation (cf. Fig. 1), accumulates small amounts of xylitol as by-product when grown aerobically on D-xylose/D-glucose mixtures (Radek et al., 2014). Moreover, this mutant exhibited slower growth on D-glucose when D-xylose was present in the media, which might be related to intracellular xylitol-5-phosphate formation. In case of *C. glutamicum* strains with heterologous expression of a D-xylose isomerase (*xylA*) as part of the Isomerase (ISO) pathway for D-xylose assimilation (cf. Fig. 1) as well as for wild-type *C. glutamicum* ATCC 13032, no xylitol formation has been reported so far.

In this work, we set out to investigate the xylitol metabolism in engineered *Corynebacterium glutamicum* WMB and ISO strains in more detail applying a series of phenotyping experiments including untargeted metabolomics and proteomics as well as xylitol inhibition studies.

2. Materials and methods

2.1. Construction of strains and plasmids

Routine methods like PCR, DNA restriction or DNA ligation were carried out according to standard protocols (Sambrook and Russell, 2001). Bacterial strains and plasmids used or constructed in the course of this work are listed in Table 1. The oligonucleotides used for cloning, colony-PCRs and DNA sequencing were obtained from EurofinsMWGOperon (Ebersberg, Germany) and are listed in the Supplementary Table S1. All experimental details regarding strain and plasmid construction can be found in the Supplementary Information.

2.2. Cultivations

The defined medium CGXII (Keilhauer et al., 1993) supplemented with indicated sugar concentrations was used for all cultivations. The pH of the medium was adjusted with 4 M NaOH to 7.0. Supplements such as biotin, protocatechuate, trace elements as well as 1 mM IPTG, 100 μg ml^{-1} spectinomycin and sugars were added after autoclaving.

Microtiterplate cultivations were carried out in 48-well FlowerPlates™ (m2p-labs GmbH, Baesweiler, Germany) incubated in a BioLector® (m2p-labs GmbH) embedded in a liquid handling station (JANUS™ working station, Perkin Elmer, Waltham MA, USA) for automated sampling and sample processing. The cultivation settings were always kept at 1400 rpm, 95% humidity and 30 °C. Depending on the experiment the online signals for biomass (backscatter; gain 20), dissolved oxygen (pO_2; gain 35) and pH (gain 35) were measured in intervals of 9 (unsampled process) or 22 min (triggered sampling process), respectively. The FlowerPlates were covered with a gas permeable sealing foil (m2p-labs GmbH) to prevent contaminations and to allow for an uniform gas exchange. Medium preparation and inoculation were performed manually under a sterile bench. For fast phenotyping of the WMB, ISO and WT_P strain, respectively, three wells of each culture series were harvested at four defined time-points (6, 12, 24 and 48 h) for subsequent at-line substrate and product analytics of cell-free supernatants. The residual unsampled wells ($n = 4$) were used for growth phenotyping and extracellular analysis at the end of the cultivation. For intracellular metabolite analyses cultivations were carried out in baffled shake flasks at 30 °C and 250 rpm. All cultures were inoculated to an initial OD about 0.8 either from cryo-stocks or fresh seed culture.

2.3. Substrate, intermediate and by-product analytics

For substrate analytics two enzymatic assays were transferred into an automated 384-well microtiter plate format using the JANUS™ working station and an integrated plate reader (EnSpire™ Multimode Plate Reader, Perkin Elmer, Waltham MA, USA). In both cases the NADH increase at 340 nm was monitored (Unthan et al., 2015b).

Untargeted metabolome analysis in culture supernatants was performed via an Agilent 6890 N gas chromatograph coupled to a Waters Micromass GCT Premier high resolution time of flight mass spectrometer. For details regarding sample preparation, MS operation and peak identification the reader is referred to (Paczia et al., 2012).

By product formation of D-xylonate and xylitol was quantified by HPLC with a 300 × 8 mm organic acid column (CS-Chromatographie Service GmbH, Langerwehe, Germany) at 80 °C using isocratic elution with 0.1 M H_2SO_4 at a flow rate of 0.6 ml min^{-1}. Xylitol was detected via refraction index and D-xylonate via DAD (Agilent, Santa Clara, CA, USA). Extracellular concentrations were determined by calibration with external standards.

2.4. Proteome analysis

Samples for proteome analysis were prepared according to (Voges and Noack, 2012). Peptide mixtures were separated by reversed phase HPLC prior to ESI–MS/MS measurements (Voges and Noack, 2012). Untargeted label-free LC-ESI-QTOFMS measurements (TripleTOF 6600, Sciex, Darmstadt, Germany) were conducted in SWATH mode with the following settings: A DuoSpray

Table 1
Strains and plasmids used in this study.

Strain or plasmid	Relevant characteristics or genotype	Source or reference
C. glutamicum strains		
ATCC 13032	Biotin-auxotrophic wild-type strain	Abe et al. (1967)
WT_P	ATCC 13032 pEKEx3	Radek et al. (2014)
ISO	*C. glutamicum* pEKEx3-$xylA_{Xc}$-$xylB_{Cg}$	Radek et al. (2014)
WMB	*C. glutamicum* pEKEx3-$xylXABCD_{Cc}$	(Radek et al. (2014)
Δ*ptsF*	*C. glutamicum* Δ*ptsF* pEKEx3	this study
Δ*xylB*	*C. glutamicum* Δ*xylB* pEKEx3	this study
Δ*ptsF*- Δ*xylB*	*C. glutamicum* Δ*ptsF* Δ*xylB* pEKEx3	this study
Δcg0612	In-frame deletion of cg0612	this study
Δcg1192	In-frame deletion of cg1192	this study
Δcg1423	In-frame deletion of cg1423	this study
Δ*dkgA*	In-frame deletion of *dkgA*	this study
Δ*oxiC*	In-frame deletion of *oxiC*	this study
GRS12	In-frame deletion of cg0116-cg0147	Unthan et al. (2015a)
GRS51	in-frame deletion of cg*rrnC*-cg3298	Unthan et al. (2015a)
GRS54	In-frame deletion of cg3365-cg3413	Unthan et al. (2015a)
E. coli strains		
DH5α	F^- ϕ80dlacΔ(*lacZ*)M15 Δ (*lacZYA-argF*) U169 *endA*1 *recA*1 *hsdR*17 (r_K^-, m_K^+) *deoR thi*-1 *phoA supE*44 λ^- *gyrA*96 *relA*1	Invitrogen (Karlsruhe, Germany)
Plasmids		
pEKEx3	$Spec^R$; *C. glutamicum*/*E. coli* shuttle vector for regulated gene expression; (P_{tac}, $lacI^Q$, pBL1 $oriV_{Cg}$, pUC18 $oriV_{Ec}$)	Hoffelder et al. (2010)
pVWEx3-$xylA_{Xc}$-$xylB_{Cg}$	$Spec^R$; pEKEx3 derivative for the regulated expression of $xylA_{Xc}$ of *X. campestris* and $xylB_{Cg}$ of *C. glutamicum*	Meiswinkel et al. (2013)
pVWEx3-$xylXABCD_{Cc}$	$Spec^R$; pEKEx3 derivative for the regulated expression of $xylXABCD_{Cc}$ of *C. crescentus*	Radek et al. (2014)
pK19*mobsacB*	Kan^r; vector for allelic exchange in *C. glutamicum* (pK18 $oriV_{Ec}$ *sacB lacZα*)	Schäfer et al. (1994)
pK19*mobsacB*Δ*ptsF*	Kan^r, pK19*mobsacB* derivative for in-frame deletion of *ptsF*	this study
pK19*mobsacB*Δ*xylB*	Kan^r, pK19*mobsacB* derivative for in-frame deletion of *xylB*	Laslo et al. (2012)
pK19*mobsacB*Δcg0612	Kan^r, pK19*mobsacB* derivative for in-frame deletion of cg0612	this study
pK19*mobsacB*Δcg1192	Kan^r, pK19*mobsacB* derivative for in-frame deletion of cg1192	this study
pK19*mobsacB*Δcg1423	Kan^r, pK19*mobsacB* derivative for in-frame deletion of cg1423	this study
pK19*mobsacB*Δ*dkgA*	Kan^r, pK19*mobsacB* derivative for in-frame deletion of *dkgA*	this study
pK19*mobsacB*Δ*oxiC*	Kan^r, pK19*mobsacB* derivative for in-frame deletion of *oxiC*	this study
$Spec^R$; spectinomycin resistance		
Kan^r; kanamycin resistance		

ion source was used with N_2 as curtain (35 psi) and source gas (30 psi). The ionisation potential (ISVF) was set to +5500 V at 300 °C. The interface heater was off and the declustering potential (DP) was set to 120 V. SWATH window width was calculated with SWATH Variable Window Calculator V1.0 (Sciex). Data acquisition and peak annotation were performed using manufacturer software (Peakview 2.1, Sciex).

3. Results and discussion

3.1. *C. glutamicum* accumulates extracellular xylitol during aerobic growth on D-xylose containing substrates

We investigated the potential of xylitol formation under aerobic conditions in the strain *C. glutamicum* pEKEx3-$xylXABCD_{Cc}$ (WMB) in comparison to *C. glutamicum* pEKEx3-$xylA_{Xc}$-$xylB_{Cg}$ (ISO) and wild-type *C. glutamicum* ATCC13032 with the empty plasmid pEKEx3 (WT_P). For fast phenotypic characterization, we applied our Mini Pilot Plant as introduced recently (Unthan et al., 2015b) and here one FlowerPlate was inoculated with 16 wells of each strain in CGXII medium containing 30 g l^{-1} D-xylose and 10 g l^{-1} D-glucose as carbon and energy sources (Fig. 2).

As expected, the WMB strain showed three separate growth phases with assimilation of D-glucose, D-xylose and D-xylonate in a subsequent manner (Radek et al., 2014). By contrast, growth of the ISO strain was bi-phasic, which is supported by the following observations: *i*) no significant by-product formation during assimilation of D-glucose (first growth phase) and D-xylose (second growth phase); *ii*) pronounced steady-state phase after D-xylose limitation with no further oxygen consumption and *iii*) continued backscatter increase is most likely caused by changes of the cell's morphology (a frequently observed effect after nutrient limitation).

All tested *C. glutamicum* strains excreted small amounts of xylitol under aerobic cultivation conditions (Fig. 2B). Most surprisingly, *C. glutamicum* WT_P consumed 34 mM D-xylose in parallel to D-glucose and showed the highest xylitol titer of 3.52 mM. This result is comparable to the experimental data obtained with *C. glutamicum* R, which produced 3.94 mM xylitol from D-xylose under oxygen deprivation (Sasaki et al., 2010).

Formation of xylitol in *C. glutamicum* WT_P and ISO started at the time-point when D-glucose was exhausted and growth stopped or continued on D-xylose, respectively. For *C. glutamicum* WMB an accumulation of xylitol (0.69 mM) in the culture supernatants could already be observed between 6 and 12 h of cultivation. In all cases, the amount of extracellularly accumulated xylitol remained nearly stable until the end of the cultivation.

3.2. Intracellular xylitol is partly converted to xylitol-5-phosphate by xylulokinase

Subsequently, we focused on the intracellular metabolism associated with D-xylose assimilation and xylitol formation in the three strains. Metabolic fingerprinting was carried out by cultivating *C. glutamicum* WMB, ISO and WT_P in shake flasks in the D-xylose/D-glucose mixture, followed by GC-ToF-MS analyses of cell extract samples taken after 12, 24 and 48 h of cultivation (Fig. 3).

Intracellular accumulation of xylitol could be observed for all strains, however, only in case of the WMB strain, xylitol could also

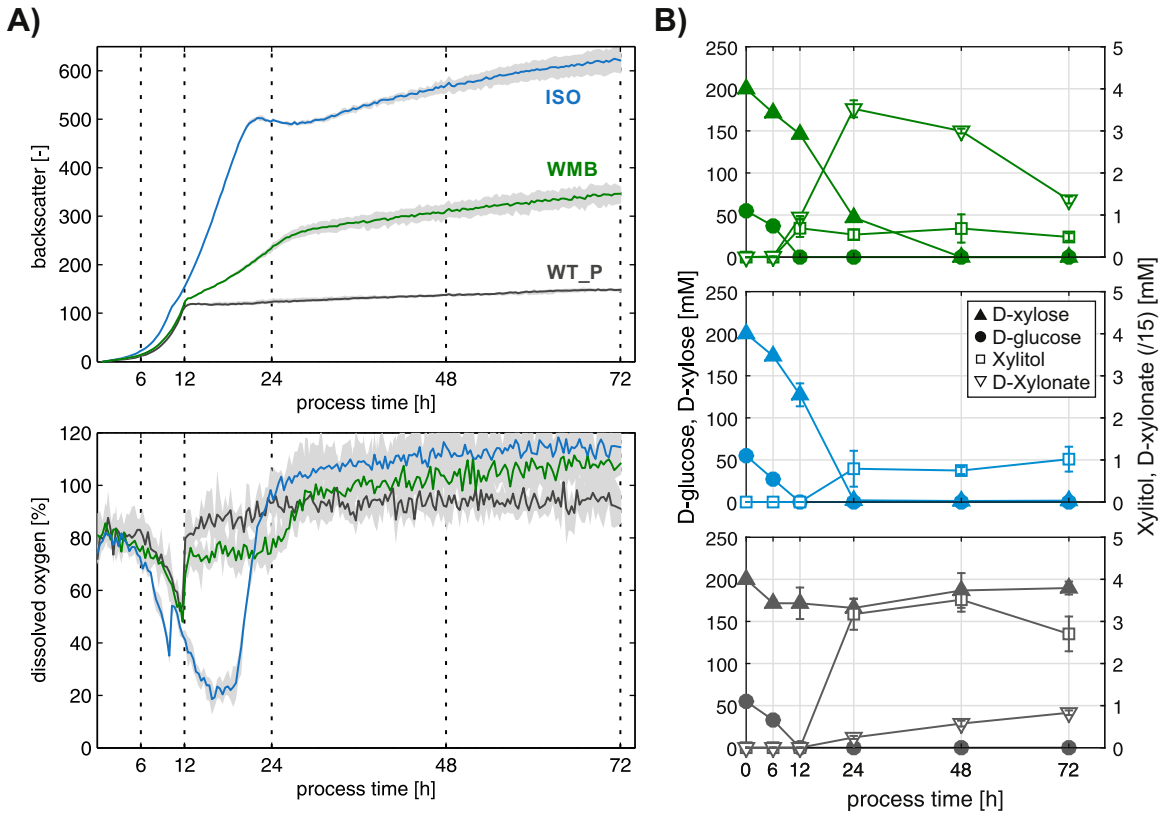

Fig. 2. Formation of xylitol in D-xylose converting *C. glutamicum* strains. A) Cultivation profiles of WMB, ISO and WT_P strains in one FlowerPlate ($n = 16$) on CGXII medium with 30 g l^{-1} D-xylose and 10 g l^{-1} D-glucose as carbon and energy sources. Dashed lines indicate the time-points of triggered harvesting. The dissolved oxygen profiles clearly indicate aerobic conditions throughout all cultivations. Mean values and confidence intervals (shaded in grey) were estimated from unsampled wells ($n = 4$). B) Concentration profiles of D-xylose, D-glucose, xylitol and D-xylonate in culture supernatants. Mean values and standard deviations were estimated from three biological and two analytical replicates, respectively.

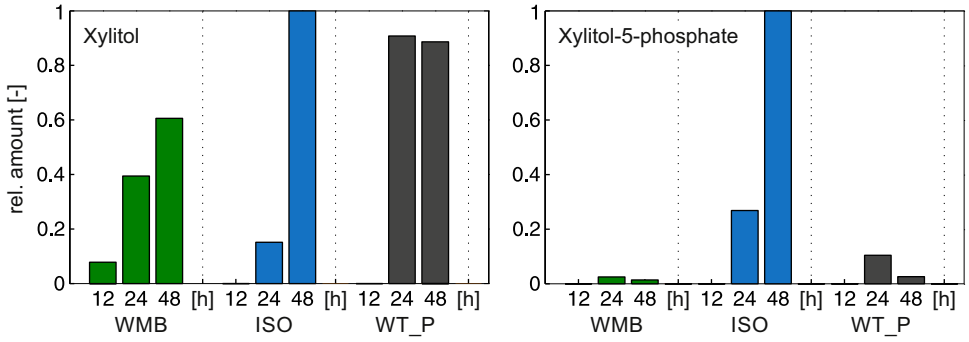

Fig. 3. Relative intracellular amounts of xylitol and xylitol-5-phosphate in D-xylose converting *C. glutamicum* strains. The strains *C. glutamicum* WMB, ISO and WT_P were cultivated in shake flasks ($n = 3$) on CGXII medium with 30 g l^{-1} D-xylose and 10 g l^{-1} D-glucose as carbon and energy source. After 12, 24 and 48 h samples were taken for GC-ToF-MS analysis and cell extracts were prepared by hot methanol extraction. Relative quantification was performed for all samples at the same split ratio. First, all peak areas were divided by the specific sample dry mass at the indicated time points and, secondly, related to the highest amount of the specific metabolite for all strains.

be detected during the first growth phase on D-glucose (cmp. Fig. 2). By contrast, a significant intracellular accumulation of the dead-end metabolite xylitol-5-phosphate was exclusively found for the *C. glutamicum* ISO strain. This finding is consistent with the fact that the ISO strain carries a plasmid-born overexpression of *xylB* and the resulting xylulokinase shows side activity in phosphorylating xylitol to xylitol-5-phosphate (Sasaki et al., 2010). Small amounts of xylitol-5-phosphate in the WMB and WT_P strain indicate that xylulokinase activity is comparably low in these strains, which might be due to the already described repression of *xylB* by D-glucose and absence of a suitable inducer such as D-arabitol (Laslo et al., 2012).

3.3. Xylitol is possibly formed through one or several unspecific reactions

Filamentous fungi, yeast and some bacteria are able to synthesise xylitol through the reduction of D-xylose, catalysed by an NADH- or NADPH-dependent D-xylose reductase (cf. Fig. 1). In the genome of *C. glutamicum* no gene encoding for an enzyme with such an activity is currently annotated and therefore we set out to identify putative xylulokinase genes for a gene deletion study.

Firstly, we analysed the genome of *C. glutamicum* ATCC13032 for open reading frames with similarities to known D-xylose reductase sequences from different prokaryotes and eukaryotes and

A)

Gene		Protein		Source
Locus	Name	ID	Function	
cg2591	*dkgA*	YP_226604.1	2,5-diketo-D-gluconic acid reductase	Homology analysis (this study)
cg1192	-	YP_225338.1	aldo/keto reductase	
cg1423	-	YP_225550.1	putative oxidoreductase	
cg0612	-	YP_224819.1	2,5-diketo-D-gluconic acid reductase	
cg3389	*oxiC*	YP_227308.1	myo-inositol dehydrogenase	Proteomics (this study)
cg3391	*oxiD*	YP_227310.1	myo-inositol dehydrogenase	
cg3392	*oxiE*	YP_227311.1	myo-inositol dehydrogenase	
cg0143	*mltD*	YP_224406.1	D-mannitol dehydrogenase	Transcriptomics (Buschke et al., 2013)
cg3290	-	YP_227216.1	putative oxidoreductase	

B)

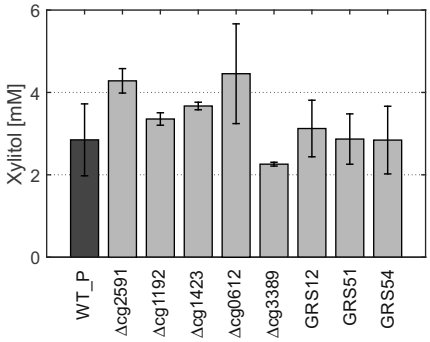

Fig. 4. Putative D-xylose reductase activities in *C. glutamicum*. A) Identified gene candidates for D-xylose reductases in the genome of *C. glutamicum* ATCC13032. B) Corresponding single and multiple deletion strains were grown aerobically on CGXII medium with 30 g l^{-1} D-xylose and 10 g l^{-1} D-glucose as carbon and energy sources ($n \geq 3$). After 48 h cell-free supernatants were analysed for xylitol accumulation and no significant changes compared to the *C. glutamicum* wild type were found by one-way ANOVA ($p < 0.01$).

found four promising gene candidates (Fig. 4A). Secondly, we performed an untargeted proteomics experiment to identify further targets from the altered gene expression pattern when switching the primary carbon source from D-glucose to D-xylose (Supplementary Table S2). Here the *myo*-inositol dehydrogenase (encoded by *oxiC*, cg3389) was found to be up-regulated in *C. glutamicum* WT_P during the stationary growth phase on the D-xylose/D-glucose mixture when only D-xylose is still available in the medium. This enzyme is part of the *myo*-inositol metabolism in *C. glutamicum* and the underlying gene cluster comprises another set of alternative oxidoreductases (*oxiD*, cg3391 and *oxiE*, cg3392) with potential D-xylose reductase activity (Krings et al., 2006). Thirdly, genes with less sequence homologies, namely *mtlD* (cg0143, encoding for a D-mannitol dehydrogenase) and cg3290 (encoding for a putative oxidoreductase), were reported to be up-regulated in an engineered *C. glutamicum* strain for cadaverine production, which was cultivated on D-xylose (Buschke et al., 2013).

All nine potential gene candidates for D-xylose-reductase activity were either deleted individually in the *C. glutamicum* WT_P background (this study) or deleted as part of a larger gene cluster in the *C. glutamicum* strains GRS12 (Δcg0116–cg0147), GRS51 (ΔcgrrnC–cg3298) and GRS54 (Δcg3365–cg3413) (Unthan et al., 2015a). When cultivating these strains under the same conditions as above, no significant changes in the phenotype (data not shown) and the xylitol titer compared to the *C. glutamicum* wild-type strain were found (Fig. 4B).

Consequently, the deleted genes can be excluded to specifically encode for the quested D-xylose reductase activity. From these results we cannot completely rule out that *C. glutamicum* carries an enzyme that solely catalyses the reduction of D-xylose to xylitol. However, since deletion of none of the nine tested genes (partly in combination) significantly reduced xylitol formation, it is more likely that D-xylose is converted by an unspecific side-reaction of one or several (unknown) enzymes with reductase activity.

3.4. D-xylose assimilation in *C. glutamicum* is impaired by extracellular xylitol

To study the impact of xylitol on the growth of *C. glutamicum* WMB and ISO, cultivation experiments were carried out on CGXII medium with 30 g l^{-1} D-xylose and 10 g l^{-1} D-glucose, and additional supplements of 10 mM and 100 mM xylitol, respectively (Fig. 5).

In the mixture with 10 mM xylitol the growth rate of the WMB strain was slightly reduced in the first (assimilation of D-glucose) and second (assimilation of D-xylose) growth phase (Fig. 5A). With 100 mM xylitol supplementation growth on D-glucose and D-xylose was significantly impaired. By contrast, the ISO strain also showed a strong growth inhibition at low xylitol concentrations (Fig. 5B). Apart from the bi-phasic growth behaviour the overall phenotype resembles the one of the culture on sole D-xylose. With higher xylitol supplementation the first growth phase on D-glucose was greatly reduced and no further growth was observed on D-xylose. In this case, overexpression of the xylulokinase gene *xylB* could directly lead to a high accumulation of the growth inhibiting compound xylitol-5-phosphate (cmp. Fig. 3) and provided that extracellular xylitol can enter the cell without any previous phosphorylation (cf. Fig. 1).

On the other hand, in the WMB strain without *xylB* expression, the resulting xylitol-5-phosphate concentration should be lower as it can only be formed when xylitol is actively taken up by PTS^{Fru}. Moreover, xylitol-5-phosphate might also have a lower impact on the growth of the WMB strain when cultivated on D-xylose because assimilation of this carbon source proceeds via the Weimberg pathway, reductive TCA-cycle, cataplerosis, gluconeogenesis and reductive pentose phosphate pathway. Thus, lower phosphoglucose isomerase activity and no phosphofructokinase activity (both targets of xylitol-5-phosphate inhibition) are required.

3.5. Low xylitol concentrations inhibit the growth of *C. glutamicum* on D-glucose and D-arabitol, but not on D-fructose

In the genome of *C. glutamicum* ATCC13032, the *xylB* gene is located in a gene cluster involved in ribitol, mannitol and arabitol metabolism and recently it was shown that D-arabitol activates the transcriptional regulator AtlR of the D-arabitol operon leading to the expression of several genes (including *xylB*) that are essential for growth on D-arabitol (Laslo et al., 2012). To further study the growth inhibiting effect of xylitol, mediated through the expression of *xylB* and/or *ptsF*, cultivation experiments with *C. glutamicum* WT_P, WMB and ISO were carried out on CGXII medium with either D-glucose, D-arabitol or D-fructose as carbon source, and additional supplements of 10 mM and 100 mM xylitol, respectively (Table 2).

When cultivated on D-glucose as carbon source, all strains grew with maximum specific growth rates that are comparable to previous data (Grünberger et al., 2013). With increasing xylitol supplementation all strains showed an increasing growth inhibition. For the ISO strain the inhibitory effect of xylitol was strongest, resulting in a growth rate reduction of 61 % when supplemented with 100 mM xylitol. These results further support the hypotheses that xylitol is a potential substrate of both xylulokinase (ISO strain)

A. Radek et al. / Journal of Biotechnology 231 (2016) 160–166 165

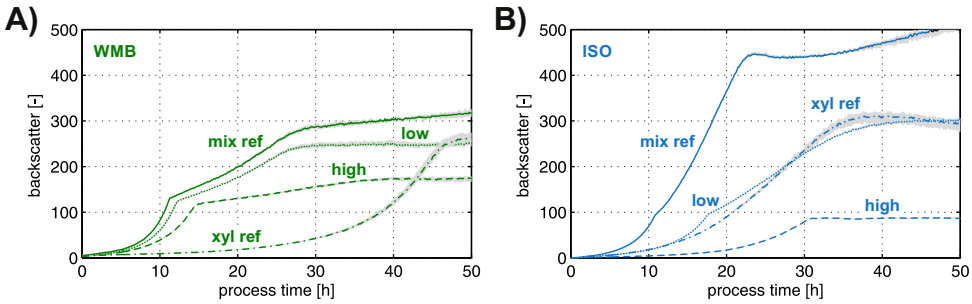

Fig. 5. Effect of extracellular xylitol on the growth of *C. glutamicum* WMB (A) and ISO (B) on D-xylose containing substrate. Cultivations were carried in CGXII medium with 30 g l^{-1} D-xylose and 10 g l^{-1} D-glucose as carbon and energy source. Additionally, each medium contained either no (mix ref), 10 mM (low) or 100 mM (high) xylitol as indicated. For comparison purposes the growth curves of *C. glutamicum* ISO and WMB on sole 40 g l^{-1} D-xylose (xyl ref) are plotted in all figures. Mean values and confidence intervals (shaded in grey) were calculated from three biological replicates.

Table 2
Effect of extracellular xylitol on the growth of different *C. glutamicum* strains on different carbon sources. Cultivations were carried out in CGXII medium with 10 g l^{-1} of either D-glucose, D-arabitol or D-fructose and varying supplementation of xylitol as indicated. Maximum specific growth rates are provided from the experiments without any xylitol supplementation as reference values. Mean values and standard deviations were estimated from three biological replicates. Coloured values represent the percentage change of a strains growth rate as compared to the reference state on D-glucose (yellow) and changes below 5 % were considered as not significant.

		Growth rate [h^{-1}]	Percentage change [%]		
Strain	**C-source**	**0 mM xylitol**	**0 mM xylitol**	**10 mM xylitol**	**100 mM xylitol**
WT_P	D-glucose	0.44 ± 0.02	0	-15	-32
WMB	D-glucose	0.46 ± 0.01	0	-14	-30
ISO	D-glucose	0.44 ± 0.01	0	-37	-61
WT_P	D-arabitol	0.40 ± 0.00	-10	-28	-58
WMB	D-arabitol	0.36 ± 0.02	-23	-34	-51
ISO	D-arabitol	0.21 ± 0.03	-52	-52	-66
WT_P	D-fructose	0.49 ± 0.02	11	8	8
WMB	D-fructose	0.56 ± 0.01	21	22	22
ISO	D-fructose	0.53 ± 0.02	20	23	-29
WT_P Δ*xylB*	D-glucose	0.46 ± 0.00	3	-7	-26
WT_P Δ*ptsF*	D-glucose	0.44 ± 0.00	-1	-3	-10
WT_P Δ*xylB* Δ*ptsF*	D-glucose	0.42 ± 0.01	-6	-7	-11

and PTS^{Fru} (all strains) and the resulting xylitol-5-phosphate is a strong growth-inhibiting compound.

On D-arabitol, all strains grew significantly slower as compared to the growth on D-glucose, and the additional supplementation of xylitol led to a further reduction of the respective growth rates (cf. Table 2). Interestingly, the growth rate of the ISO strain on sole D-arabitol was reduced by 52% as compared to D-glucose conditions. This could point to a competition between xylulokinase and D-xylose isomerase (assuming reaction reversibility) for the common substrate D-xylulose which comes from the reduction of D-arabitol (cf. Fig. 1). Furthermore, it was postulated that xylulokinase can also catalyse a phosphorylation of D-arabitol into arabitol-5-phosphate, which, under induced conditions of the p$XylA_{Xc}$-$XylB_{Cg}$ plasmid, could additionally inhibit the growth of the ISO strain (Laslo et al., 2012).

When cultivated on D-fructose as carbon source all strains showed higher growth rates as compared to the respective D-glucose conditions (cf. Table 2). Moreover, the growth of these strains was not impaired by increasing amounts of extracellular xylitol, except for the ISO strain at high xylitol supplementation. These results again underline the capability of PTS^{Fru} for transport and phosphorylation of external xylitol, however, under the applied test condition the preferred substrate of PTS^{Fru} is D-fructose and no xylitol can enter the cell in its phosphorylated state. The high reduction in the growth rate (−29 %) of the ISO strain when grown on D-fructose and 100 mM xylitol again indicates that another transport mechanism for xylitol exists and that the resulting intracellular xylitol can only be effectively converted to cytotoxic xylitol-5-phosphate in the ISO strain background in which *xylB* is overexpressed.

Finally, the deletion of *xylB* and/or *ptsF* in the wild-type strain nearly restored growth of the respective mutants on D-glucose and low extracellular xylitol concentration (10 mM) to the wild-type level. When supplementing 100 mM xylitol, deletion of *ptsF* is essential for reducing the inhibitory effect of xylitol. This shows the major relevance of PTS^{Fru} for xylitol transport and direct formation of cytotoxic xylitol-5-phosphate in wild-type *C. glutamicum*. Interestingly, the double deletion mutant *C. glutamicum* Δ*xylB* Δ*ptsF*

still showed a significant growth rate reduction at 100 mM xylitol supplementation, pointing to other inhibitory effects of high extracellular xylitol concentrations on cell growth.

4. Conclusions

Corynebacterium glutamicum ATCC13032, which cannot naturally utilize D-xylose, accumulates xylitol intracellularly and extracellularly during aerobic growth on D-xylose containing substrates. Analysis of *C. glutamicum* strains with selected single and multiple deletions of putative D-xylose reductase encoding genes did not reveal a specific enzyme that is responsible for the conversion of D-xylose into xylitol. This result rather points to an unspecific side-reaction of, at the least, one other reductase in *C. glutamicum* that has an affinity to D-xylose and is expressed under the applied culture conditions. Future optimisation of D-xylose assimilation in the *C. glutamicum* ISO strain background may require complete elimination of xylitol synthesis for preventing formation of cytotoxic xylitol-5-phosphate from xylitol. On the other hand, deletion of *ptsF* and *xylB* in the WMB background could eliminate xylitol-5-phosphate formation, thereby potentially increasing the growth rate on D-xylose containing substrates.

Acknowledgements

This work was partly funded by the German Federal Ministry of Education and Research (BMBF, Grant. No. 031L0015) as part of the project "XyloCut – Shortcut to the carbon efficient microbial production of chemical building blocks from lignocellulose-derived D-xylose", which is embedded in the ERASysAPP framework.

We would like to thank Bernhard Eikmanns for providing the plasmid pK19*mobsacB*Δ*xylB* for in-frame deletion of *xylB* in *C. glutamicum* ATCC 13032.

Appendix A. Supplementary data

Supplementary data associated with this article can be found, in the online version, at http://dx.doi.org/10.1016/j.jbiotec.2016.06.009.

References

Abe, S., Takayama, K., Kinoshita, S., 1967. Taxonomical studies on glutamic acid producing bacteria. J. Gen. Appl. Microbiol. 13, 279–301.

Akinterinwa, O., Cirino, P.C., 2009. Heterologous expression of D-xylulokinase from Pichia stipitis enables high levels of xylitol production by engineered *Escherichia coli* growing on xylose. Metab. Eng. 11, 48–55.

Buschke, N., Becker, J., Schafer, R., Kiefer, P., Biedendieck, R., Wittmann, C., 2013. Systems metabolic engineering of xylose-utilizing *Corynebacterium glutamicum* for production of 1,5-diaminopentane. Biotechnol. J. 8, 557–570.

Grünberger, A., van Ooyen, J., Paczia, N., Rohe, P., Schendzielorz, G., Eggeling, L., Wiechert, W., Kohlheyer, D., Noack, S., 2013. Beyond growth rate 0.6: *Corynebacterium glutamicum* cultivated in highly diluted environments. Biotechnol. Bioeng. 110, 220–228.

Hoffelder, M., Raasch, K., van Ooyen, J., Eggeling, L., 2010. The E2 domain of OdhA of *Corynebacterium glutamicum* has succinyltransferase activity dependent on lipoyl residues of the acetyltransferase AceF. J. Bacteriol. 192, 5203–5211.

Keilhauer, C., Eggeling, L., Sahm, H., 1993. Isoleucine synthesis in *Corynebacterium glutamicum*: molecular analysis of the *ilvB-ilvN-ilvC* operon. J. Bacteriol. 175, 5595–5603.

Krings, E., Krumbach, K., Bathe, B., Kelle, R., Wendisch, V.F., Sahm, H., Eggeling, L., 2006. Characterization of myo-inositol utilization by *Corynebacterium glutamicum*: the stimulon, identification of transporters, and influence on L-lysine formation. J. Bacteriol. 188, 8054–8061.

Laslo, T., von Zaluskowski, P., Gabris, C., Lodd, E., Ruckert, C., Dangel, P., Kalinowski, J., Auchter, M., Seibold, G., Eikmanns, B.J., 2012. Arabitol metabolism of *Corynebacterium glutamicum* and its regulation by AtlR. J. Bacteriol. 194, 941–955.

London, J., Hausman, S., 1982. Xylitol-mediated transient inhibition of ribitol utilization by *Lactobacillus casei*. J. Bacteriol. 150, 657–661.

Meiswinkel, T.M., Gopinath, V., Lindner, S.N., Nampoothiri, K.M., Wendisch, V.F., 2013. Accelerated pentose utilization by *Corynebacterium glutamicum* for accelerated production of lysine, glutamate, ornithine and putrescine. Microbiol. Biotechnol. 6, 131–140.

Miyasawa-Hori, H., Aizawa, S., Takahashi, N., 2006. Difference in the xylitol sensitivity of acid production among *Streptococcus* mutans strains and the biochemical mechanism. Oral Microbiol. Immunol. 21, 201–205.

Paczia, N., Nielgen, A., Lehmann, T., Gätgens, J., Wiechert, W., Noack, S., 2012. Extensive exometabolome analysis reveals extended overflow metabolism in various microorganisms. Microb. Cell Fact. 11.

Radek, A., Krumbach, K., Gatgens, J., Wendisch, V.F., Wiechert, W., Bott, M., Noack, S., Marienhagen, J., 2014. Engineering of *Corynebacterium glutamicum* for minimized carbon loss during utilization of D-xylose containing substrates. J. Biotechnol. 192 (Pt A), 156–160.

Sambrook, J., Russell, D., 2001. Molecular Cloning. A Laboratory Manual, 3rd ed. Cold Spring Harbor Laboratory Press, Cold Spring Harbor, NY.

Sasaki, M., Jojima, T., Inui, M., Yukawa, H., 2010. Xylitol production by recombinant *Corynebacterium glutamicum* under oxygen deprivation. Appl. Microbiol. Biotechnol. 86, 1057–1066.

Schäfer, A., Tauch, A., Jager, W., Kalinowski, J., Thierbach, G., Puhler, A., 1994. Small mobilizable multipurpose cloning vectors derived from the *Escherichia-coli* plasmids pk18 and pk19 – selection of defined deletions in the chromosome of *Corynebacterium-glutamicum*. Gene 145, 69–73.

Trahan, L., 1995. Xylitol: a review of its action on mutans streptococci and dental plaque–its clinical significance. Int. Dent. J. 45, 77–92.

Unthan, S., Radek, A., Wiechert, W., Oldiges, M., Noack, S., 2015a. Bioprocess automation on a mini pilot plant enables fast quantitative microbial phenotyping. Microb. Cell Fact. 14, 32.

Unthan, S., Radek, A., Wiechert, W., Oldiges, M., Noack, S., 2015b. Bioprocess automation on a mini pilot plant enables fast quantitative microbial phenotyping. Microb. Cell Fact., 14.

Voges, R., Noack, S., 2012. Quantification of proteome dynamics in *Corynebacterium glutamicum* by ^{15}N-labeling and selected reaction monitoring. J. Proteomics 75, 2660–2669.

3.3.3 Supplementary material

Used oligonucleotides & plasmid construction & untargeted proteome of *C. glutamicum* wild-type grown on D-xylose

TABLE 3.3: Oligonucleotides used in manuscript III

Oligonucleotides used in manuscript III.

Name	DNA Sequence (5´- 3´)[a]	Restriction site
Construction of pK19*mobsacB*Δ*ptsF*		
pptsF_No	CGCCCCGGGGCTGTCGATACCTCAGACAAG	*Sma*I
pptsF_Ni	GGGTAGGTGATTTGAATTTGTATTATTTACGCTATTCATGCTGATTCT	
pptsF_Co	GCGCCCGGGAGCTTCTAACGAGCTTTTAACAAGC	*Sma*I
pptsF_Ci	ACAAATTCAAATCACCTACCCGCGAAGCAAGAAGCACAACAAG	
Construction of pK19mobsacBΔcg0612		
pcg0612_No	CGCCCCGGGAACAGCCGAATCAAGCACGCGAAG	*Sma*I
pcg0612_Ni	GGGTAGGTGATTTGAATTTGTACCAATTGGAGGAAGGGAAAGAGTC	
pcg0612_Co	GCGCCCGGGTTTGCGCTATTCCGTGATCAACTGCC	*Sma*I
pcg0612_Ci	ACAAATTCAAATCACCTACCCAAAGATCAAGATCCAGCCGTCTATG	
Construction of pK19*mobsacB*Δcg1192		
pcg1192_No	CGCCCCGGGGTGTTTGCTGGTCTGGAGGAG	*Sma*I
pcg1192_Ni	GGGTAGGTGATTTGAATTTGTCTGAGAGGTTGCCACCATGCGT	
pcg1192_Co	GCGCCCGGGATATTGACGGCATCCTCGATTCC	*Sma*I
pcg1192_Ci	ACAAATTCAAATCACCTACCCGGCGAGCACAGCGGTTTTCCTGT	
Construction of pK19*mobsacB*Δcg1423		
pcg1423_No	CGCCCCGGGTCTCGCAGGCAAGACCGTTATCGATATC	*Sma*I
pcg1423_Ni	GGGTAGGTGATTTGAATTTGTTGCTGGTTGATATGCCATGACAG	
pcg1423_Co	GCGCCCGGGTGCTCGATATTATGCGCTGGGG	*Sma*I
pCg1423_Ci	ACAAATTCAAATCACCTACCCTGGGCGAAGGCCACCGATTCCAAAAC	

Table 3.3. Continued.

Construction of pK19*mobsacB*Δ*dkgA*		
pcg2591_No	CGCCCCGGGCTTCAGGCGCATGACTTCCAC	*Sma*I
pcg2591_Ni	GGGTAGGTGATTTGAATTTGTGGTACCCACAACAGACATATTTTC	
pcg2591_Co	GCGCCCGGGCCATTCGCCAACGTCACGGAAC	*Sma*I
pcg2591_Ci	ACAAATTCAAATCACCTACCCAATGATCGTGGTGGTTCACACCC	
Construction of pK19*mobsacB*Δ*oxiC*		
pcg3389_No	AAAAGTACTAACTTAGGATTCGAGGGCCATAACTG	*Sma*I
pcg3389_Ni	GGGTAGGTGATTTGAATTTGTGCCAACAACAATTTTTTGATCAC	
pcg3389_Co	AAAAGTACTGCGTCGTAGATGGTCTTCAGGTGAG	*Sma*I
pcg3389_Ci	ACAAATTCAAATCACCTACCCGAATCCGACAACAACCAGGGC	
Control oligonucleotides in-frame deletion of *ptsF*		
pptsF_proof_f	CACCGCGTTGATCCATTCAGC	
pptsF_proof_c	ACATCCAAATCGGATGCGGCAC	
Control oligonucleotides in-frame deletion of *xylB*		
pxylB_proof_f	GGTTGAGAAGTTGCCGCAGCG	
pxylB_proof_c	CTGCTTGAAGAGGCAGGTGTG	
Control oligonucleotides in-frame deletion of cg0612		
pCg0612_proof_f	GTTCGGGGCAACAAGTTTAACC	
pCg0612_proof_c	GACCAAATACCGAGAACATCTT	
Control oligonucleotides in-frame deletion of cg1192		
pcg1192_proof_f	GCCTCAAGGACAAGGAAGTG	
pcg1192_proof_c	ATGGACCTGCCCAAGGAAAG	
Control oligonucleotides in-frame deletion of cg1423		
pCg1423_proof_f	CAGTAGAGTCCATCATTGCAAGC	
pCg1423_proof_c	CCTTGGGCGTTGATCTTTTGTC	
Control oligonucleotides in-frame deletion of *dkgA*		
pcg2591_proof_f	CTGCAGCAAGTGTGACTCGAAG	
pcg2591_proof_c	CCTTTGGAAACCGCATGGGAATC	
Control oligonucleotides in-frame deletion of *oxiC*		
pcg3389_proof_f	GGCGATCGTGTGAATAGTGAGTTC	
pcg3389_proof_c	GGTGTGCAGATATCAACCATGAG	

[a] Recognition sites for restriction endonucleases are underlined.

TABLE 3.4: Differential expression of proteins in C. glutamicum WT P during growth on D-xylose containing media.

Cells were grown on defined CGXII medium with 10 g l^{-1} D-glucose (G) or a mixture of 30 g l^{-1} D-xylose and 10 g l^{-1} D-glucose (M) as carbon and energy sources. Samples were taken during exponential growth phase (t1) and at stationary phase (t2) and analysed by label-free LC-ESI-QTOFMS measurements. For each protein the depicted number of peptides and fragments thereof (given in brackets) were measured. Protein ratio were determined from the summed peak areas over all fragments and peptides of a protein and given as log2 values. Only proteins regulated more than 2.5-fold (p-value ≤ 0.05) under either condition are indicated.

Protein					Gene	
ID	**Function**	**Peptides**	**M(t1)/ G(t1)**	**M(t2)/ G(t1)**	**Locus**	**Name**
YP_226247.1	putative secreted or membrane protein	1(7)	-	3.74	cg2196	
YP_226474.1	hypothetical protein	4 (≥ 10)	-	3.56	cg2451	
YP_226442.1	nicotinate-nucleotide--dimethylbenzimidazole phosphoribosyltransferase	1 (12)	2.51	3.45	cg2414	*cobT*
YP_227089.1	UDP-glucose 6-dehydrogenase	1 (9)	3.43	2.60	cg3154	*udgA2*
YP_226953.1	porin	2 (12)	1.69	3.29	cg3008	*porA*
YP_225152.1	phosphoribosylglycinamide formyltransferase	1 (9)	2.36	2.31	cg0983	*purN*
YP_226173.1	DeoR-type transcriptional regulator of ptsG, ptsS and cg2118-fruK-ptsF	2 (≥ 9)	-	2.09	cg2115	*sugR*
YP_226947.1	putative ferredoxin reductase	9 (≥ 11)	-	2.03	cg2999	
YP_226368.1	DNA polymerase III subunit alpha	1 (12)	-	2.01	cg2338	*dnaE1*
YP_225165.1	putative two component response regulator	3 (≥ 11)	1.55	1.99	cg0996	*cgtR2*
YP_227116.1	trehalose corynomycolyl transferase	3 (≥ 6)	-	1.95	cg3182	*cop1*
YP_224529.1	hypothetical protein	10 (≥ 10)	-	1.94	cg0282	*csbD*
YP_224634.1	dTDP-glucose 4,6-dehydratase	1 (10)	1.94	-	cg0403	*rmlB1*
YP_225206.1	thiol-disulfide isomerase and thioredoxins	3 (12)	2.00	1.88	cg1043	
YP_225312.1	exodeoxyribonuclease VII small subunit	1 (12)	1.88	1.68	cg1162	*xseB*
YP_226728.1	nicotinamidase/ pyrazinamidase	2 (≥ 11)	-	1.86	cg2734	*pncA*
YP_226522.1	bacterial regulatory proteins, ArsR family	2 (≥ 8)	-	1.81	cg2500	*znr*
YP_226225.1	exopolyphosphatase-related protein	1 (10)	1.77	-	cg2174	
YP_226483.1	protein-tyrosine-phosphatase	5 (≥ 9)	-	1.74	cg2459	*ptpA*
YP_225783.1	putative aminopeptidase 2	4 (≥ 7)	-	1.73	cg1693	*pepC*
YP_226432.1	rieske iron-sulfur protein	1 (12)	1.72	1.64	cg2404	*qcrA*
YP_226758.1	uncharacterized protein with SCP/PR1 domain	1 (12)	-	1.70	cg2773	
YP_225892.1	putative integration host factor cIHF	10 (≥ 7)	1.57	1.66	cg1811	*ihf*
YP_227094.1	universal stress protein UspA or related nucleotide-binding proteins	4 (12)	-	1.65	cg3159	
YP_225900.1	hypothetical protein	2 (12)	1.59	1.65	cg1821	
YP_227118.1	trehalose corynomycolyl transferase	8 (≥ 7)	-	1.63	cg3186	*cmt2*
YP_224805.1	50S ribosomal protein L23	8 (≥ 8)	1.62	-	cg0597	*rplW*
YP_226490.1	pyruvate dehydrogenase subunit E1	10 (≥ 9)	-	1.62	cg2466	*aceE*
YP_227183.1	universal stress protein family	10 (≥ 7)	-	1.61	cg3255	*uspA3*
YP_224643.1	trehalose corynomycolyl transferase	9 (≥ 9)	-	1.61	cg0413	*cmt1*
YP_226289.1	tRNA (guanine-N(1)-)-methyltransferase	1 (11)	1.61	-	cg2249	*trmD*
YP_224880.1	ATPase or kinase	1(12)	1.57	-	cg0682	
YP_225764.1	polyprenol-phosphate-mannose synthase domain 1	3 (≥ 10)	-	1.56	cg1672	*ppmC*
YP_226702.1	ABC-type sugar transport system, permease component	1 (8)	-	1.55	cg2704	
YP_224443.1	hypothetical protein	2 (12)	1.52	-	cg0184	
YP_226686.1	short chain dehydrogenase	4 (≥ 8)	-	1.51	cg2685	
YP_225136.1	thymidylate synthase	2 (≥ 8)	1.50	-	cg0966	*thyA*
YP_225048.1	ribosome-associated protein Y (PSrp-1)	10 (≥ 8)	-	1.50	cg0867	

Table 3.4. Continued.

YP_224978.1	putative N-acyl-L-amino acid amidohydrolase	1 (7)	-	1.49	cg0789	*amiA*
YP_227181.1	TetR-type transcriptional regulator of sulfur metabolism	5 (≥ 9)	-	1.48	cg3253	*mcbR*
YP_224584.1	MarR fam	1 (11)	-	1.48	cg0343	*phdR*
YP_224323.1	putative secreted protein	2 (12)	-	1.47	cg0040	
YP_227308.1	myo-Inositol dehydrogenase	4 (≥ 10)	-	1.46	cg3389	*oxiC*
YP_225172.1	5-formyltetrahydrofolate cyclo-ligase	1 (12)	-	1.45	cg1003	
YP_226249.1	methionine aminopeptidase	2 (≥ 9)	1.43	1.34	cg2198	*map2*
YP_225209.1	polyphosphate kinase	7 (≥ 9)	-	1.42	cg1046	*ppk2A*
YP_224416.1	haloacid dehalogenase-like hydrolase	7 (≥ 10)	-	1.40	cg0154	
YP_226702.1	ABC-type sugar transport system, permease component	1 (8)	1.37	-	cg2704	
YP_225143.1	glucose-6-phosphate isomerase	9 (12)	-	1.37	cg0973	*pgi*
YP_224805.1	50S ribosomal protein L23	8 (≥ 8)	-	1.36	cg0597	*rplW*

3.3.4 Main achievements of this manuscript

• *C. glutamicum* wild-type accumulates extracellular xylitol during aerobic growth on D-xylose containing substrates.

• Extracellular xylitol inhibits growth of D-xylose utilizing strains as well as wild-type *C. glutamicum* when cultivated on different carbon sources.

• Intracellular xylitol is partly converted to cytotoxic xylitol-5-phosphate, especially in *C. glutamicum* pEKEx3-xylA$_{Xc}$-xylB$_{Cg}$ (ISO strain).

• The Weimberg route, operating independently from xylulokinase activity, could be an effective substitute towards a more efficient D-xylose utilization in *C. glutamicum*.

3.4 Miniaturized and automated adaptive laboratory evolution: Evolving *Corynebacterium glutamicum* towards an improved D-xylose utilization

3.4.1 Short introduction to this manuscript

The classical way of engineering *C. glutamicum* was discussed in the two previous manuscripts. Two synthetic pathways were introduced into *C. glutamicum* and the resulting growth phenotypes were investigated and compared. Most importantly, the functional integration of the Weimberg pathway from *C. crescentus* resulted in the highly promising new strain *C. glutamicum* WMB, which can grow on D-xylose as sole carbon and energy source. However, the obtained specific growth rates were comparably low, compared to established strains harboring the isomerase pathway.

After the first successful integration of the Weimberg pathway from *C. crescentus*, the inserted genes could be codon optimized for *C. glutamicum* for a better performing WMB strain. Thus, this was initially aimed within the following manuscript.

Additional strain improvement should be reached, by the alternative approach of adaptive laboratory evolution (ALE). Initially, the ALE process was transferred into microliter scale and should run completely automated on the MPP. To achieve this, a repetitive batch cultivation process had to be developed as a new process on the MPP. These repetitive batch cultivations can be obtained by pipetting fresh cultivation media, sterile stored on the robotic deck of the MPP, into the running BioLector. Afterwards a pre-defined volume is transferred from the previous batch into the next cultivation well. To establish and fine-tune this process, first experiments were conducted with the wild-type strain on standard growth medium.

Subsequently, the codon optimized Weimberg strain (WMB2) was applied in different ALE experiments with D-xylose as sole carbon source. Finally, new mutant strains with significantly improved growth properties were obtained and these were further studied by whole genome sequencing.

3.4.2 Manuscript IV

Miniaturized and automated adaptive laboratory evolution: Evolving *Corynebacterium glutamicum* towards an improved D-xylose utilization

Published as:

Radek A*, Tenhaef N*, Müller M F, Brüsseler C, Wiechert W, Marienhagen J, Polen T, Noack S, Miniaturized and automated adaptive laboratory evolution: Evolving *Corynebacterium glutamicum* towards an improved D-xylose utilization. *Bioresource technology* (2017) *equal contribution

Bioresource Technology 245 (2017) 1377–1385

Contents lists available at ScienceDirect

Bioresource Technology

journal homepage: www.elsevier.com/locate/biortech

Miniaturized and automated adaptive laboratory evolution: Evolving *Corynebacterium glutamicum* towards an improved D-xylose utilization

Andreas Radek [1], Niklas Tenhaef [1], Moritz Fabian Müller, Christian Brüsseler, Wolfgang Wiechert, Jan Marienhagen, Tino Polen, Stephan Noack *

Institute of Bio- and Geosciences, IBG-1: Biotechnology, Forschungszentrum Jülich GmbH, Jülich D-52425, Germany

HIGHLIGHTS

- Automated procedures for Adaptive Laboratory Evolution of microbial strains were developed.
- Growth rate of engineered *C. glutamicum* strain was increased by 260% on sole D-xylose.
- Results from small-scale ALE experiments were successfully transferred to lab-scale operation.
- Genome sequencing revealed up to 15 potential key mutations for improved D-xylose assimilation.

ARTICLE INFO

Article history:
Received 31 March 2017
Received in revised form 8 May 2017
Accepted 10 May 2017
Available online 12 May 2017

Keywords:
Adaptive Laboratory Evolution
Untargeted strain optimization
Lab automation
Corynebacterium glutamicum
Xylose utilization

ABSTRACT

Adaptive Laboratory Evolution (ALE) is increasingly being used as a technique for untargeted strain optimization. This work aimed at developing an automated and miniaturized ALE approach based on repetitive batch cultivations in microtiter plates. The new method is applied to the recently published strain *Corynebacterium glutamicum* pEKEx3-*xylXABCD*$_{Cc}$, which is capable of utilizing D-xylose via the Weimberg (WMB) pathway. As a result, the significantly improved strain WMB2$_{evo}$ was obtained, showing a specific growth rate of 0.26 h^{-1} on D-xylose as sole carbon and energy source. WMB2$_{evo}$ grows stable during lab-scale bioreactor operation, demonstrating the high potential of this strain for future biorefinery applications. Genome sequencing of cell samples from two different ALE processes revealed potential key mutations, e.g. in the gene cg0196 (encoding for the transcriptional regulator IolR of the *myo*-inositol metabolism). These findings open up new perspectives for the rational engineering of *C. glutamicum* towards improved D-xylose utilization.

1. Introduction

The ability to adapt quickly to different environmental conditions is vital for any microorganism. Adaptive Laboratory Evolution (ALE) exploits this characteristic and is increasingly being used as a technique for untargeted strain optimization (Portnoy et al., 2011). ALE was successfully applied to adapt biotechnologically relevant organisms to lignocellulosic material (Qin et al., 2016; Wang et al., 2014), to improve biodegradation capabilities (Lasik et al., 2010; Wang et al., 2016a) or to enhance growth performance (Cheng et al., 2014; Li et al., 2015; Wang et al., 2016b). Furthermore, strategies were developed to increase productivity, i.e. by using stress conditions (Reyes et al., 2014; Yu et al., 2013), by selection using a biosensor and FACS (Mahr et al., 2015) or by enhancing tolerance against the target product (Mundhada et al., 2017).

Key principle of ALE is the application of a selection criterion to the culture. In most cases, this criterion is increased growth rate, since cells with a higher growth rate inherently prevail during cultivation. ALE experiments are routinely performed in shaking flasks or laboratory bioreactors either in continuous cultivation or repetitive batch mode (Dragosits and Mattanovich, 2013; Portnoy et al., 2011). Due to long experimentation times and many manual handling steps these approaches are laborious and prone to errors. Therefore recent developments aim for a miniaturization and automation of ALE approaches, and first microfluidic systems have already been developed (Sjostrom et al., 2014). However, no system is currently available that enables to run ALE experiments under process conditions similar to lab-scale bioreactors and in a fully automated manner without any user intervention.

* Corresponding author.
E-mail address: s.noack@fz-juelich.de (S. Noack).
[1] These authors contributed equally to this work.

http://dx.doi.org/10.1016/j.biortech.2017.05.055
0960-8524/

Table 1
Strains and plasmids used in this study.

Strain or plasmid	Relevant characteristics[a]	Source or reference
C. glutamicum		
ATCC 13032 (WT)	Biotin auxotroph wild-type strain	(Abe et al., 1967)
WMB2	*C. glutamicum* pEKEx3-*xylXABCD*$_{Cc}$-opt	This work
E. coli		
DH5α	F$^-$ Φ80*lac*ZΔM15 Δ(*lac*ZYA-*arg*F)U169 *rec*A1 *end*A1 *hsd*R17 (r_K^-, m_K^+) *pho*A *sup*E44 λ– *thi*-1 *gyr*A96 *rel*A1	Invitrogen (Karlsruhe, Germany)
Plasmids		
pEKEx3	Spec^R; *C. glutamicum*/ *E. coli* shuttle vector for regulated gene expression; (P_{tac}, lacI^Q, pBL1 *ori*V*Cg*, pUC18 *ori*V*Ec*)	(Hoffelder et al., 2010)
pEKEx3-*xylXABCD*$_{Cc}$-opt	Spec^R; pEKEx3 derivative for the regulated expression of *xylXABCD* of *C. crescentus*. All five genes were codon optimized for a heterologous expression in *C. glutamicum*	This work

[a] Spec^r; spectinomycin resistance.

Currently established large-scale microbial production processes rely on feedstock containing primarily D-glucose, D-fructose or sucrose as carbon sources. However, when taking costs and competition with food production for arable land into account (Ekman et al., 2013; Viikari et al., 2012), so called 2nd generation feedstocks based on lignocellulosic biomass represent promising alternatives (Straathof, 2014). Lignocellulosic biomass is composed of up to 40% hemicellulose, whose key building block is the pentose D-xylose. Unfortunately, D-xylose cannot be directly utilized by important microbial platform organisms such as *Saccharomyces cerevisiae* (Bettiga et al., 2009) and *Corynebacterium glutamicum* (Meiswinkel et al., 2013), since both are missing assimilation pathways for this carbon source.

In this study, the development of an automated ALE approach is presented, which is based on repetitive batch cultivations in milliliter-scale using the recently introduced Mini Pilot Plant (MPP) technology (Unthan et al., 2015b). Essentially, the MPP combines a liquid handling robot with a BioLector® cultivation device. The latter enables to online monitor pH, dissolved oxygen and backscatter-biomass in all 48-wells of a FlowerPlate® and, thus, provides an instantaneous recording of metabolic adaptation events during ALE experimentation. Sophisticated workflows, employing automated liquid handling operations for sample transfer and processing, were developed that offer detailed characterization of growth and production performances of evolved strains.

In a proof of concept study, the novel ALE technique is applied to a recently constructed *C. glutamicum* strain harboring the Weimberg pathway from *Caulobacter crescentus* for D-xylose assimilation (Radek et al., 2014). As a starting point, this strain showed a comparable low specific growth rate of 0.07 ± 0.01 h^{-1} on defined medium with D-xylose as sole carbon and energy source.

Firstly, codon optimization increased the growth rate by 43%. Secondly, untargeted strain optimization in two different ALE approaches further increased the growth rate by 260%, which was also verified in subsequent lab-scale bioreactors cultivations. Transient sampling during the ALE process followed by genome sequencing led to the identification of several mutations, which are potentially responsible for the improved growth phenotype and build the basis for future rational strain development.

2. Materials and methods

2.1. Construction of strains and plasmids

All used bacterial strains and plasmids are listed in Table 1. *Escherichia coli* DH5α was used for cloning purposes and was grown aerobically on a rotary shaker (170 rpm) at 37 °C in 5 mL Lysis Broth (LB) medium (Bertani, 1951) or on LB agar plates (LB medium with 1.8% [wt vol^{-1}] agar). *C. glutamicum* strains are derived from *C. glutamicum* ATCC 13032 (Abe et al., 1967) and were routinely cultivated aerobically in 500 mL baffled shake flasks with 50 mL medium on a rotary shaker (130 rpm) at 30 °C. All used enzymes for performing cloning methods were purchased from Thermo Scientific (Schwerte, Germany). Synthetic genes were obtained in codon-optimized version for expression in *C. glutamicum* from LifeTechnologies (Darmstadt, Germany). Standard protocols for molecular cloning, such as PCR, DNA restriction, and ligation were carried out for recombinant DNA work (Sambrook and Russell, 2001). *C. glutamicum* strains were transformed by electroporation as described previously (Eggeling and Bott, 2005) and constructed plasmids were finally verified by DNA sequencing at Eurofins MWG Operon (Ebersberg, Germany).

2.2. Cultivation media and conditions

Cultivations in complex media were performed on Brain-heart infusion (BHI) supplied by Sigma-Aldrich (Steinheim, Germany). CGXII medium (Eggeling and Bott, 2005) was used for cultivations in defined medium. It contained per liter of deionized water: 1 g K_2HPO_4, 1 g KH_2PO_4, 5 g urea, 13.25 mg $CaCl_2 \cdot 2\,H_2O$, 0.25 g $MgSO_4 \cdot 7\,H_2O$, 10 mg $FeSO_4 \cdot 7\,H_2O$, 10 mg $MnSO_4 \cdot H_2O$, 0.02 mg $NiCl_2 \cdot 6\,H_2O$, 0.313 mg $CuSO_4 \cdot 5\,H_2O$, 1 mg $ZnSO_4 \cdot 7\,H_2O$, 0.2 mg biotin, 30 mg protocatechuate and 42 g MOPS. D-glucose and D-xylose were added in varying amounts. Certain components were added sterile after autoclaving (D-xylose, D-glucose, protocatechuate, trace elements). All chemicals were purchased from Sigma-Aldrich (Steinheim, Germany) or Carl Roth GmbH (Karlsruhe, Germany). Strain storage was done via cryo-conservation as described elsewhere (Unthan et al., 2015a).

Microtiter plate cultivations were performed in specialized, disposable FlowerPlates® (m2plabs GmbH, Baesweiler, Germany), which provide increased mass transfer and enable online measurement of pH and dissolved oxygen via optodes. The following conditions were applied: Shaking frequency 1200 rpm, temperature 30 °C, humidity > 80%, backscatter gain 15, filling volume 1000 or 800 μL. Cultures were started at OD_{600} = 0.2 by inoculation from a cryo-culture.

Bioreactor cultivations were done in a parallel cultivation platform (Eppendorf/DASGIP, Jülich, Germany). A pH of 7 was held constant during the cultivation by feeding 5 M H_3PO_4 and 5 M NH_4OH on demand. Temperature and air flow was set to 30 °C and 0.5 vvm, respectively. Aerobic process conditions were maintained by controlling the stirrer speed (400–1.200 rpm) to achieve a dissolved oxygen concentration (DO) of at least 30%. Online measurements were taken for pH (405-DPAS-SC-K80/225, Mettler Toledo), DO (Visiferm DO 225, Hamilton) and exhaust gas compo-

sition (GA4, DASGIP AG). The vessels were inoculated from an exponential growing pre-culture to a final OD_{600} of 1. Pre-cultures were inoculated from cryo-cultures.

2.3. Automated repetitive batch procedures

Automated repetitive batch procedures were carried out using the "Mini Pilot Plant" (MPP) described in detail by (Unthan et al., 2015b) or in a similar setup using a Freedom Evo 200 (Tecan, Switzerland) robotic platform. Both robotic workstations employ a liquid handling arm using eight steel needles and a gripper arm for transport of plates. Additionally, BioLector cultivation devices are embedded in both workstations.

The BioLector uses 48-well FlowerPlates® for high-throughput cultivations. During the cultivation, each well was monitored using the RoboLector agent software to perform automated inoculation and media filling. The RoboLector software checks if predefined triggers are fulfilled. An exemplary trigger condition was "backscatter signal greater than 250". If the condition was satisfied, the robotic workstation transferred 250 μL or 50 μL of culture liquid to the next empty well on the same Flowerplate. Subsequently, this well was filled with fresh CGXII media stored at 4 °C on the robotic platform.

Some wells were harvested after the first trigger or at the end of cultivation depending on the experimental layout. Harvesting was done by transferring the cultivation liquid into a deep well plate. The deep well plate was then centrifuged at 4000 rpm for 10 min to gain culture supernatants. The supernatant was pipetted into a sealed multititer plate and stored at 4 °C. The whole process was carried out fully automated by the robotic workstation.

2.4. Substrate and by-product analytics

Samples were prepared by passing the supernatants through a cellulose acetate syringe filter (0.2 μm, DIA-Nielsen, Düren, Germany).

By-product formation and carbohydrate content (except for D-xylose) was analyzed by high performance liquid chromatography (Agilent 1100 Infinity, Agilent Technologies, Santa Clara, CA) using isocratic ion exchange on an Organic Acid Resin HPLC Column 300 x 8 mm (CS Chromatography, Düren, Germany) as stationary phase and 0.1 M H_2SO_4 as mobile phase with a flow rate of 0.6 mL/min. The column temperature was 80 °C and the injection volume 10 μL. Carbohydrates were detected using a Refractive Index Detector. Organic acids were detected using UV light absorption at 230 nm with a Diode Array Detector. For external calibration, standards of organic acids or carbohydrates (D-xylonate supplied by Santa Cruz Biotechnology, Dallas, USA; other organic acids and carbohydrates suplied by Sigma-Aldrich, Steinheim, Germany) were applied in the dynamic linear range. Estimation of measurement errors was done by Gaussian error propagation.

D-xylose concentration was quantified by an enzymatic assay (D-xylose Assay Kit, Megazyme, Wicklow, Ireland). The protocol used was modified: One well of a 96-well plate contained 290 μL master mix and 10 μL sample or standard. Seven standard concentrations were measured to cover the linear range of 0.1–1 g/L. Master mix for one MTP consisted of 32 mL TRIS-maleate buffer (pH

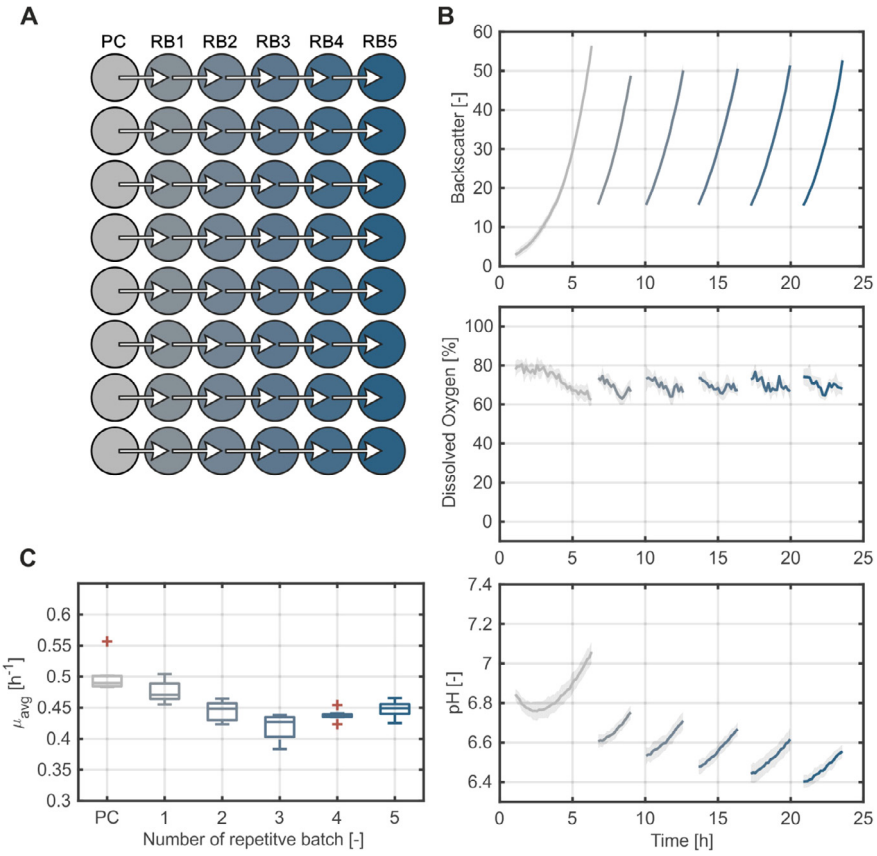

Fig. 1. Simple repetitive batch setup with prefilled defined media containing 10 g/L D-glucose and whole plate incubation at 30 °C. (A) Experimental layout in a 48-well FlowerPlate. (B) Time course of online backscatter, DO and pH signals. Mean values (thick lines) and standard deviations (grey areas) were estimated from eight independent replicate cultures, respectively. (C) Average specific growth rates, estimated from eight independent replicate cultures (see Supplementary Material for more details). Red crosses mark outliers. (For interpretation of the references to colour in this figure legend, the reader is referred to the web version of this article.)

6.8), 1 mL 100 mM $MgCl_2$ solution, 0.5 mL 50 g/L NAD solution and 0.1 mL XDH/XMR solution (from kit). After incubation for 30 min, absorption at 340 nm was measured using an Infinite 200 (Tecan, Switzerland) microplate reader. External standards were used for linear regression within the linear range. Estimation of measurement errors was done by Gaussian error propagation.

2.5. Genome sequencing

Sequencing libraries of genomic DNA from relevant cell samples were prepared using the TruSeq DNA PCR-free sample preparation kit (Illumina). To obtain an average DNA fragment size of 550 bp, genomic DNA (4 μg) was fragmented using the ultrasonic device Bioruptor® Pico (Diagenode). Then, 2 μg of fragmented DNA was end-repaired and size-selected using magnetic beads, followed by the ligation of a single A nucleotide to the 3′ end. Illumina PE index adapters were ligated to the fragments and the indexed libraries were quantified *via* qPCR using the KAPA library quantification kit (Peqlab). Normalized libraries (2 nM) were pooled, diluted to an average final concentration of 10 pM and paired-end sequenced on a MiSeq desktop sequencer (Illumina) with a read length of 2 × 150 nt. An automated workflow for read data analysis and variant detection was designed using tools of the CLC Genomics Workbench (Qiagen Aarhus A/S). The read data were preprocessed for removing adapter sequences and quality trimming to filter out reads or sequence ends having a Phred quality value < 30. Using default parameters, reads were mapped to the *C. glutamicum* ATCC 13032 reference genome BX927147. SNVs (single nucleotide variants), MNVs (multiple nucleotide variants), InDels and structural variants were detected using quality-based variant detection tools of the CLC Genomics Workbench. The individual variant lists of the samples were combined in Excel (Microsoft) and further analyzed to check the occurrence, frequencies and overlap of variants in all samples.

3. Results and discussion

3.1. Miniaturization and automation of ALE

For establishing an automated adaptive laboratory evolution (ALE) approach, the existing Mini Pilot Plant (MPP) was extended by implementing a repetitive batch process in microtiter plate (MTP) format.

As a starting point, a simple experimental setup was defined in which one FlowerPlate was prefilled with freshly prepared CGXII media containing 10 g/L D-glucose as sole carbon and energy source. The wells of the first column (pre-culture, PC) of the MTP was then inoculated with *C. glutamicum* wild type to an OD of 0.2 (Fig. 1A). By monitoring each well, the automated inoculation of the next batch was triggered when the backscatter (BS) signal reached a threshold of BS = 70, ensuring that the culture was in the middle of the exponential growth phase. 250 μL of each culture was then transferred to the wells of the next column (repetitive batch 1, RB1) of the MTP. In total, this setup allowed for five repetitive batches in eight replicates. By taking the online backscatter data, both average (μ_{avg}) and maximum (μ_{max}) specific growth

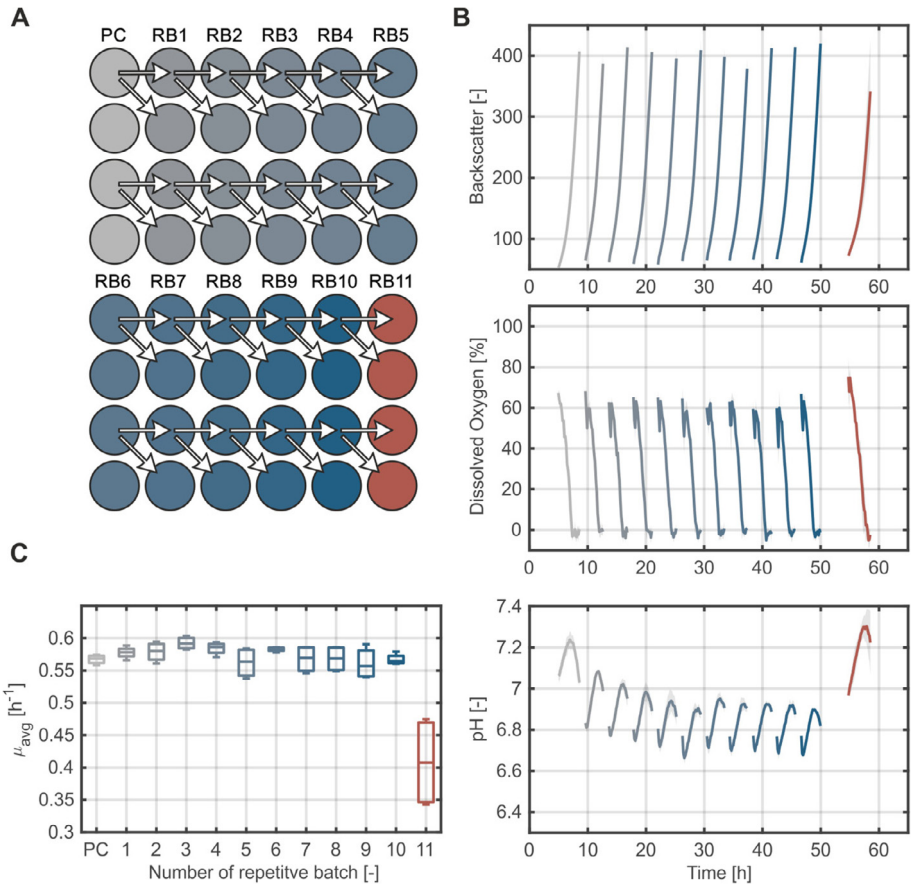

Fig. 2. Advanced repetitive batch setup with medium dosing at trigger time-point and untouched cultivations. Fresh defined medium containing 40 g/L D-glucose was stored at room temperature in the robotic workstation. (A) Experimental layout in a 48-well FlowerPlate. (B) Time course of online backscatter, DO and pH signals. Mean values (thick lines) and standard deviations (grey areas) were estimated from four independent replicate cultures, respectively. (C) Average specific growth rates, estimated from four independent replicate cultures.

rates were calculated for each batch culture. These calculations posed some challenges due to the noise inherited in the optical signal of freshly inoculated cultures and the amount of data to be analyzed. Hence, a new algorithm for the automated calculation of μ_{avg} and μ_{max} from online backscatter data was developed (see Supplementary Information for more details).

The first experiment demonstrated the feasibility of this approach to realize automated repetitive batch cultivations in microtiter plates. However, the pH significantly decreased over the course of the experiment (Fig. 1B), and this effect was accompanied by a decrease in specific growth rates (Fig. 1C). The decrease in pH is probably due to the prefilling and storage of the MTP at 30 °C long before the cultivation experiments starts. Thus, a more sophisticated inoculation sequence using external media storage at lower temperature is needed, in order to ensure stable growth conditions. For the determination of specific growth rates another challenge was revealed by this experiment: The removal of 25% of the cultivation broth alters the backscatter signal and renders it unsuitable for growth rate estimation beyond the trigger threshold.

Both challenges were addressed in the next setup with two major changes: Firstly, the medium to be used in the repetitive batch cultivations was stored separately at room temperature on the robotic platform. The filling of a next well with fresh medium and its inoculation is now both triggered when the predefined backscatter threshold of a running batch is reached. Secondly, two wells are inoculated from each previous well (Fig. 2A). One well is used for continuation of the repetitive batch series, the other one is left undisturbed for monitoring growth and increasing the number of measurements for growth rate estimation. Moreover, a higher concentration of D-glucose (40 g/L) was used in order to elongate the exponential phase of each culture. The last repetitive batch was carried out with CGXII medium lacking protocatechuate to investigate the effect of this component on the culture when the media is stored over several hours.

In total, two independent series of eleven repetitive batch cultivations were performed on one MTP (Fig. 2B and C). The highly reproducible growth rate over the course of ten batches demonstrates the feasibility of this setup to maintain stable conditions during the experiment. There is still a slight pH shift observable, but with negligible influence on growth. For the last batch cultivation on CGXII medium without protocatechuate a negative effect on growth was observed. This is in agreement with previous results where protocatechuate was found to serve as co-substrate for *C. glutamicum* wild type, enhancing the maximum specific growth up to $\mu_{avg} = 0.61 \pm 0.02\ h^{-1}$ (Unthan et al., 2014). It is likely that protocatechuate availability during the repetitive batches is higher due to the external storage of fresh medium at room temperature. This would explain the consistent average growth rate of $\mu_{avg} = 0.57 \pm 0.02\ h^{-1}$, which is significantly higher than the growth rate ($\mu_{avg} = 0.46 \pm 0.02\ h^{-1}$) of the second exponential phase when protocatechuate is depleted (Unthan et al., 2014).

In the following, the novel automated repetitive batch procedures were applied to evolve *C. glutamicum* towards an improved D-xylose utilization.

3.2. ALE of C. glutamicum WMB

Recently, the strain *C. glutamicum* pEKEx3-*xylXABCD*$_{Cc}$ which employs the Weimberg (WMB) pathway from *Caulobacter crescentus* was introduced (Radek et al., 2014). This pathway opens a metabolic route for the conversion of D-xylose into α-ketoglutarate without carbon loss and, thus, is particularly interesting for the production of TCA-cycle derived organic acids. The strain (here denoted as *C. glutamicum* WMB) showed a maximum specific growth rate of $\mu_{max} = 0.07 \pm 0.01\ h^{-1}$ on defined medium using D-xylose as sole carbon and energy source. Following codon optimization of all WMB genes increased the maximum growth rate only slightly to $\mu_{max} = 0.10 \pm 0.02\ h^{-1}$ (data not shown, strain henceforth denoted *as C. glutamicum* WMB2). By contrast, a strain harboring the alternative isomerase pathway was shown to grow with $\mu_{max} = 0.20\ h^{-1}$ (Meiswinkel et al., 2013). Therefore, it was assumed that there is still room for improvement of D-xylose assimilation in *C. glutamicum* WMB2.

With the aim to enhance the growth performance of *C. glutamicum* WMB2 on D-xylose, ALE experiments were initiated in two different ways as will be described in the following. In the first approach, six independent clones of *C. glutamicum* WMB2 were used, and these clones were individually picked from a BHI agar plate, to inoculate a FlowerPlate similar to the simple repetitive batch setup, but with medium dosing at trigger time-point (Fig. 3A) and fresh media stored separately at 4 °C. From a preculture (PC) using BHI medium, 50 µL of each culture was transferred to the first repetitive batch well (RB1). Clones A to C were cultivated in RB1 on CGXII medium containing 20 g/L D-xylose. For clones D to F, 2 g/L D-glucose was additionally added to aid expression of Weimberg proteins in the initial growth phase. For all following RBs, 20 g/L D-xylose was used as sole carbon and energy source. The backscatter threshold for all inoculation events was set to BS = 250 realizing biomass transfer in the late exponential phase of the cultivation. Together with the smaller transfer vol-

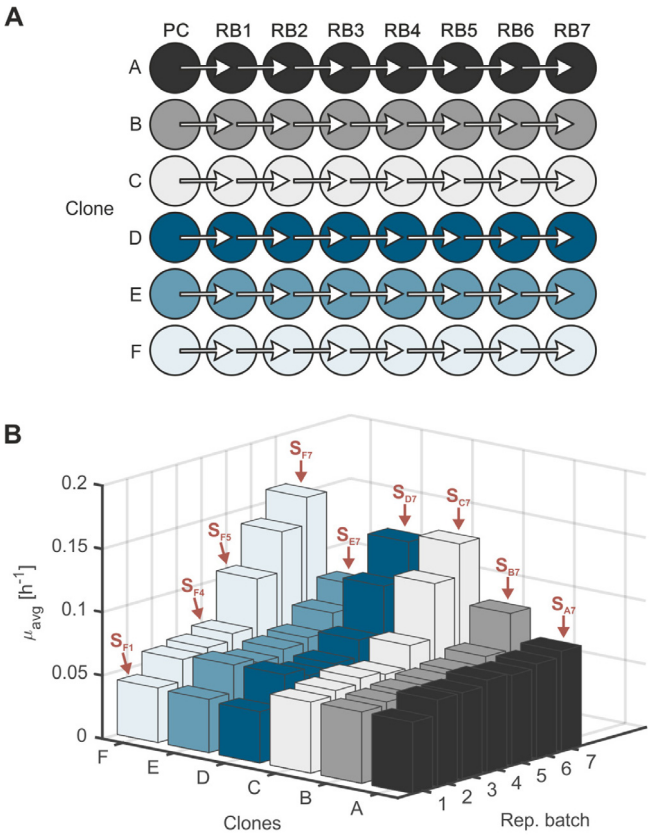

Fig. 3. ALE of *C. glutamicum* WMB2 starting from 6 independent clones and following automated repetitive batch cultivations in microtiter plates. Fresh defined medium containing 2 g/L D-glucose and 20 g/L D-xylose (for first batches of A, B and C) or 20 g/L D-xylose (for all other batches) was stored at 4 °C in the robotic workstation prior use. (A) Experimental layout. (B) Average specific growth rates, estimated from single cultures. Red arrows mark cultivations which were chosen for genome sequencing. (For interpretation of the references to colour in this figure legend, the reader is referred to the web version of this article.)

ume of 50 µL this enhanced the number of generations per RB. In total, the experiment ran for 13 days and provided 35 generations of growth-selection. This is notably shorter both in time and generations than in previously described *E. coli* ALE processes, which use e.g. 2000 generations in 261 days (Jantama et al., 2008) or 360 generations over 90 days (Qin et al., 2016).

As a result, five of the six clones showed an increasing average specific growth rate over the course of the experiment (Fig. 3B). The fastest-growing clone F showed a threefold increase in growth rate (up to $\mu_{avg} = 0.16 \pm 0.02\ h^{-1}$ and $\mu_{max} = 0.18\ h^{-1}$) along the ALE experiment. Notably, the time-point and extent of the growth rate increase varied from clone to clone, suggesting that individual mutation events occurred. For genome sequencing cell samples from relevant cultivations were used as indicated (Fig. 3B).

In the second approach, the ALE experiment was started from a cryo-culture of *C. glutamicum* WMB2. The cryo-culture was prepared from a shaking flask culture of *C. glutamicum* WMB2 grown on defined CGXII medium with D-xylose. Following the hypothesis that this step already had induced genetic heterogeneity in the culture, the subsequent repetitive batch process should enable an enrichment of cells with beneficial mutations for D-xylose assimilation.

The experimental design for this ALE experiment is shown in Fig. 4A. Similar to the advanced setup (cf. Fig. 2A), in every trigger event two cultures were inoculated from the previous batch and a total of two independent repetitive batch series were performed. In one of the series, the second inoculated well was harvested at the end of the cultivation in stationary phase (endpoint harvest, EH). In the other series, the second inoculated well was harvested when the first well reached the backscatter threshold (trigger harvest, TH). The supernatant resulting from these wells was used for by-product analysis. For all cultures defined media containing 40 g/L D-xylose was used.

As a result, the specific growth rate of *C. glutamicum* WMB2 showed a steady increase over the course of the ALE experiment and, eventually, reached a maximum at $\mu_{max} = 0.26 \pm 0.02\ h^{-1}$

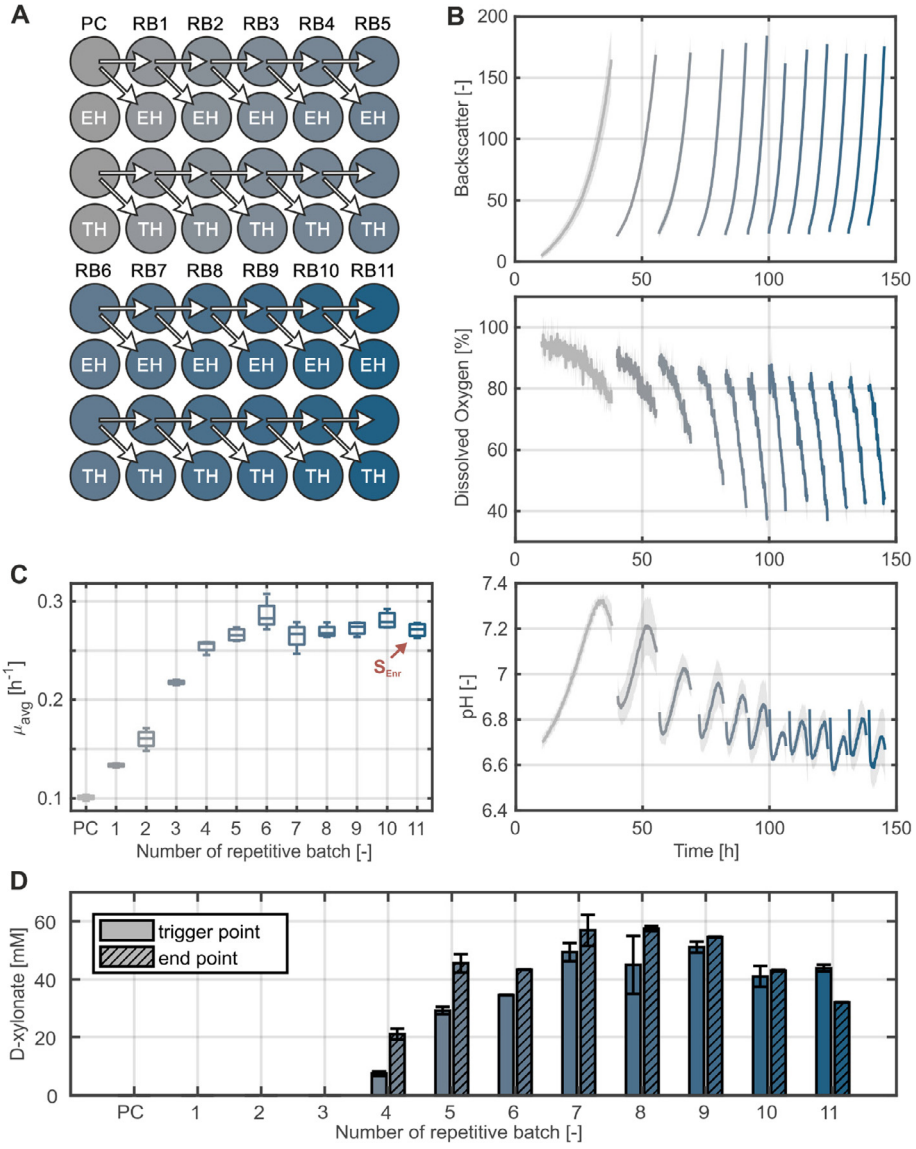

Fig. 4. ALE of *C. glutamicum* WMB2 starting from a common cryo-culture and following automated repetitive batch cultivations in microtiter plates. Fresh defined medium containing 40 g/L D-xylose was stored at room temperature in the robotic workstation. (A) Experimental layout. (B) Mean values (thick lines) and standard deviations (grey areas) of online backscatter, DO and pH signals were estimated from four independent replicate cultures, respectively. (C) Average specific growth rates, estimated from four independent replicate cultures. (D) D-xylonate concentrations in culture supernatant at trigger points and endpoints. Mean values and standard deviations were estimated from two analytical replicates, respectively.

(Fig. 4B and C). Most interestingly, the analysis of the supernatant samples gathered at the trigger points and endpoints, respectively, revealed significant by-product formation of D-xylonate (Fig. 4D). Accumulation of this Weimberg pathway intermediate was also found in a previous study (Radek et al., 2014), pointing to a still non-optimal carbon flow along this pathway into the TCA-cycle. Analogous to the prior experiment using single clones, here cells from RB11 were used for genome sequencing and the resulting strain is henceforth denoted WMB2$_{evo}$.

3.3. Verification of improved D-xylose utilization of WMB2$_{evo}$

To be used as a platform strain for industrially relevant bioprocesses, an evolved strain must be phenotypically stable, even under changing media conditions. In the following, a modified version of the presented ALE setup was used to test the stability of WMB2$_{evo}$ by following consecutive cultivations on CGXII medium containing 20 g/L of either D-glucose or D-xylose, respectively (Fig. 5A). The experiment was started by inoculating the first repetitive batch on D-glucose from an exponentially growing pre-culture on D-xylose. After the backscatter trigger in mid-exponential phase was reached, the next repetitive batch using D-glucose and a parallel batch using D-xylose were inoculated. From the latter, an average growth rate over all eight cultivations (each in three independent replicates) was estimated as $\mu_{avg} = 0.27 \pm 0.01\ h^{-1}$ (Fig. 5B), clearly demonstrating the stability of the evolved strain WMB2$_{evo}$ on D-xylose medium.

Moreover, in order to verify the results from the MTP-based ALE experiments under process relevant conditions, WMB2$_{evo}$ was cultivated in 1 L lab-scale bioreactors using defined media containing 20 g/L D-xylose as sole carbon and energy source (Fig. 5B). During cultivation, samples were withdrawn for analyzing specific substrate uptake, biomass growth and by-product formation. As a result, WMB2$_{evo}$ showed an specific average growth rate of $\mu_{avg} = 0.26 \pm 0.01\ h^{-1}$, verifying the improvement of D-xylose utilization under lab-scale conditions. The specific D-xylose uptake rate was estimated as $upt_{Xyl} = 5.7 \pm 0.1$ mmol/g/h. Additionally, formation of D-xylonate up to a concentration of 40 mM was observed, resulting in a carbon loss of 30%.

To the best of our knowledge, the evolved strain *C. glutamicum* WMB2$_{evo}$ is currently the fastest growing strain on pure D-xylose media gained from untargeted strain optimization experiments.

3.4. Genome sequencing during ALE

The underlying mutations in the cell cultures exhibiting increasingly improved growth rates with D-xylose in the course of the two ALE experiments (cf. Fig. 3B and Fig. 4C) were determined by sequencing of genomic DNA from relevant samples using the Illumina technology. Within the sequencing results and detected variants, a number of highly meaningful variants with various frequencies were found, suggesting some heterogeneity in the cultures (Table 2). In samples from both the first ALE approach using six independent clones of *C. glutamicum* WMB2 and the second one starting from a cryo-culture, two transcriptional regulators were found to be affected.

On one hand, a deletion and structural variants within cg0196 was found. This gene encodes the repressor IolR of the *iol* gene cluster for proteins involved in *myo*-inositol uptake and degradation (Klaffl et al., 2013). These variants in cg0196 most likely result in functional inactivation of IolR.

On the other hand, cg3388 was affected, which encodes a hitherto putative transcriptional regulator. The detected variants are partial gene deletions as well as point mutations resulting in amino acid exchanges or premature stop of translation. The partial deletions and the premature stop codon likely inactivate the encoded

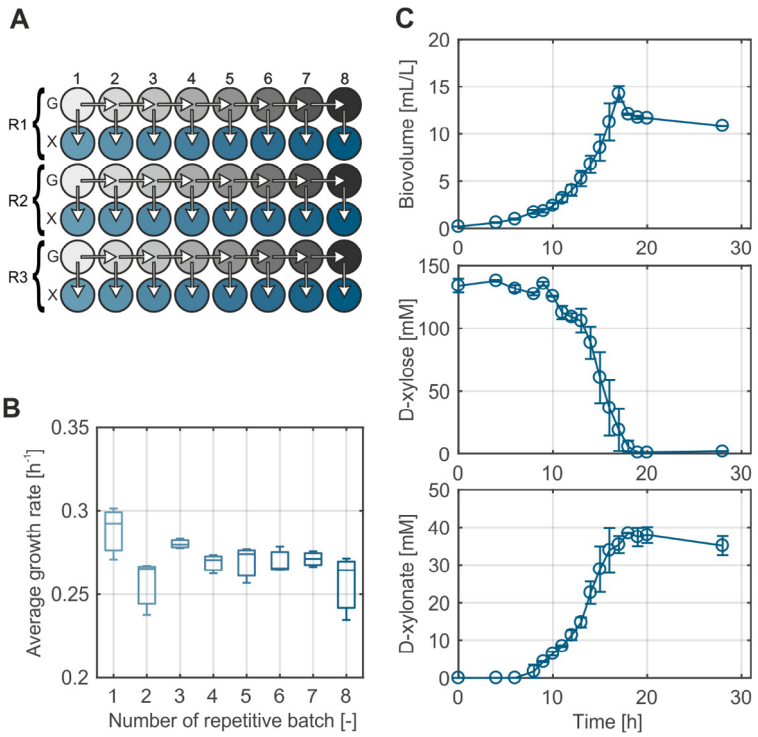

Fig. 5. Verification of improved D-xylose utilization of WMB2$_{evo}$. (A) Experimental layout for testing the phenotypic stability on changing carbon sources. Eight repetitive batches (each in three independent replicates R1 to R3) were performed using defined CGXII media with 20 g/L D-glucose (Rows "G"). Each finished batch cultivation with D-glucose was used to subsequently inoculate a batch cultivation on defined CGXII medium containing 20 g/L D-xylose (Rows "X"). (B) Average specific growth rates of cultivations using D-xylose, estimated from three independent replicate cultures. (C) Lab-scale bioreactor cultivation of strain WMB2$_{evo}$ on defined CGXII medium containing 20 g/L D-xylose. Mean values and standard deviations were estimated from two independent replicate cultures, respectively.

Table 2
Meaningful variants revealed by genome sequencing of samples from single-clone and cryo-culture ALE experiments. Variants are listed according to the sample annotation of Figs. 3B and 4C. The observed frequency of occurrence of a particular variant is given in brackets. # refers to the BX927147 accession.

Sample	Batch	μ_{avg} [h^{-1}]	Variant type	Comment
S_{F1}	1	0.04 ± 0.02	–	–
S_{F4}	4	0.07 ± 0.02	–	–
S_{F5}	5	0.10 ± 0.03	Deletion (23%) nt 3,234,237…3,234,336	In cg3388, putative transcriptional regulator
S_{F7}	7	0.16 ± 0.02	Deletion (29%) nt 3,234,237…3,234,336	In cg3388, putative transcriptional regulator
S_{E7}	7	0.10 ± 0.03	SNV G to A (17%) nt 3,234,893	Exchange A360T in cg3388, putative transcriptional regulator
S_{D7}	7	0.14 ± 0.02	SNV A to G (13%) nt 526,417	Exchange I15V in cg0587, tuf, elongation factor Tu
			SNV G to A (19%) nt 527,353	Exchange D327N in cg0587, tuf, elongation factor Tu
			SNV G to A (15%) nt 527,392	Exchange V340I in cg0587, tuf, elongation factor Tu
			SNV G to A (14%) nt 527,452	Exchange D360N in cg0587, tuf, elongation factor Tu
			SNV C to G (14%) nt 527,454	Exchange D360E in cg0587, tuf, elongation factor Tu
S_{C7}	7	0.15 ± 0.02	SNV G to A (12%) nt 527,353	Exchange D327N in cg0587, tuf, elongation factor Tu
			SNV G to A (12%) nt 527,392	Exchange V340I in cg0587, tuf, elongation factor Tu
S_{B7}	7	0.10 ± 0.02	Multiple breakpoints (45%) nt 168,365… > 168,464;	In cg0196, *iolR*, repressor of *myo*-inositol utilization genes
			SNV A to G (16%) nt 526,417	Exchange I15V in cg0587, tuf, elongation factor Tu
			SNV G to A (16%) nt 527,353	Exchange D327N in cg0587, tuf, elongation factor Tu
			SNV G to A (15%) nt 527,392	Exchange V340I in cg0587, tuf, elongation factor Tu
			SNV C to T (29%) nt 3,234,618	Exchange T268I in cg3388, putative transcriptional regulator
S_{A7}	7	0.08 ± 0.02	MNV GG to AA (98%) nt 192,844…192,845	Upstream of cg0223, *iolT1*, *myo*-inositol transporter 1
			MNV GGG to ATC (98%) nt 192,850…192,852	Upstream of cg0223, *iolT1*, *myo*-inositol transporter 1
			SNV A to G (98%) nt 192,857	Upstream of cg0223, *iolT1*, *myo*-inositol transporter 1
			SNV G to A (19%) nt 3,234,734	Exchange A307T in cg3388, putative transcriptional regulator
S_{Enr1}		0.27 ± 0.01	SNV G to A (100%) nt 3,234,078	Stop W88* in cg3388(+), putative transcriptional regulator, IclR-family
S_{Enr2}		0.27 ± 0.01	Deletion (41%) nt 168,324…168,423	In cg0196, *iolR*, repressor of *myo*-inositol utilization genes

regulator. The three amino acid exchanges T268I, A307T and A360T are located within conserved helix-turn-helix and IclR superfamily domains and probably also inactivate or modulate the DNA-binding activity of Cg3388.

In one sample also single and multiple nucleotide polymorphisms (SNV/MNV) upstream of *iolT1* (cg0223) encoding the *myo*-inositol transporter 1 were found. However, the positional distances of these SNPs/MNVs (−668 to −681 bp) to the transcriptional starts of *iolT1* (−85 bp and −113 bp) are large and it is currently unknown whether the repression of *iolT1* by IolR could be affected (Klaffl et al., 2013).

Besides genes shown or annotated to be involved in *myo*-inositol metabolism, *tuf* (cg0587) encoding the elongation factor Tu (EF-Tu) was affected in three series of the ALE experiment initiated from the six individual WMB2 clones. The prokaryotic EF-Tu is responsible for catalyzing the binding of an aminoacyl-tRNA to the ribosome and recently was also found to be involved in a first step of proofreading for maintaining a high accuracy of translation (Ieong et al., 2016). Here, point mutations in *tuf* resulting in the amino acid exchanges D327 N and V340I were found in all three series, suggesting some higher relevance, while exchange I15V was found in two of the three and D360 N as well as D360E in only one of the three series where *tuf* was affected. It should be mentioned that also numerous mutations in the 23S rRNA with various frequencies were found (data not shown).

4. Conclusions

In this study, a miniaturized and automated Adaptive Laboratory Evolution (ALE) approach for untargeted strain optimization was developed. The approach is highly flexible and provides access to detailed system levels studies on potential adaption strategies of microbes under different selection pressures. ALE was used to optimize D-xylose utilization in a recently developed *C. glutamicum* strain expressing the Weimberg pathway. The resulting strain $WMB2_{evo}$ currently shows the best growth performance of a *C. glutamicum* strain on defined D-xylose medium.

Acknowledgements

This work was partly funded by the German Federal Ministry of Education and Research (BMBF, Grant. No. 031L0015) as part of the project "XyloCut – Shortcut to the carbon efficient microbial pro-

duction of chemical building blocks from lignocellulose-derived D-xylose", which is embedded in the ERASysAPP framework. Further funding was received from the Innovation Lab initiative of the German Helmholtz Association to support the "Microbial Bioprocess Lab – A Helmholtz Innovation Lab."

Appendix A. Supplementary data

Supplementary data associated with this article can be found, in the online version, at http://dx.doi.org/10.1016/j.biortech.2017.05.055.

References

Abe, S., Takayama, K., Kinoshita, S., 1967. Taxonomical studies on glutamic acid producing bacteria. J. Gen. Appl. Microbiol. 13, 279–301.

Bertani, G., 1951. Studies on Lysogenesis I.: the mode of phage liberation by lysogenic *Escherichia coli*. J. Bacteriol. 62 (3), 293–300.

Bettiga, M., Bengtsson, O., Hahn-Hagerdal, B., Gorwa-Grauslund, M.F., 2009. Arabinose and xylose fermentation by recombinant *Saccharomyces cerevisiae* expressing a fungal pentose utilization pathway. Microb. Cell Fact. 8, 40.

Cheng, K.K., Lee, B.S., Masuda, T., Ito, T., Ikeda, K., Hirayama, A., Deng, L., Dong, J., Shimizu, K., Soga, T., Tomita, M., Palsson, B.O., Robert, M., 2014. Global metabolic network reorganization by adaptive mutations allows fast growth of *Escherichia coli* on glycerol. Nat. Commun. 5, 3233.

Dragosits, M., Mattanovich, D., 2013. Adaptive laboratory evolution – principles and applications for biotechnology. Microb. Cell Fact. 12 (1), 64.

Eggeling, L., Bott, M., 2005. Handbook of *Corynebacterium glutamicum*. CRC Press.

Ekman, A., Wallberg, O., Joelsson, E., Börjesson, P., 2013. Possibilities for sustainable biorefineries based on agricultural residues – a case study of potential straw-based ethanol production in Sweden. Appl. Energy 102, 299–308.

Hoffelder, M., Raasch, K., van Ooyen, J., Eggeling, L., 2010. The E2 domain of OdhA of *Corynebacterium glutamicum* has succinyltransferase activity dependent on lipoyl residues of the acetyltransferase AceF. J. Bacteriol. 192 (19), 5203–5211.

Ieong, K.W., Uzun, U., Selmer, M., Ehrenberg, M., 2016. Two proofreading steps amplify the accuracy of genetic code translation. Proc. Natl. Acad. Sci. U.S.A. 113 (48), 13744–13749.

Jantama, K., Haupt, M.J., Svoronos, S.A., Zhang, X., Moore, J.C., Shanmugam, K.T., Ingram, L.O., 2008. Combining metabolic engineering and metabolic evolution to develop nonrecombinant strains of *Escherichia coli* C that produce succinate and malate. Biotechnol. Bioeng. 99 (5), 1140–1153.

Klaffl, S., Brocker, M., Kalinowski, J., Eikmanns, B.J., Bott, M., 2013. Complex regulation of the phosphoenolpyruvate carboxykinase gene *pck* and characterization of its GntR-type regulator IolR as a repressor of *myo*-inositol utilization genes in *Corynebacterium glutamicum*. J. Bacteriol. 195 (18), 4283–4296.

Lasik, M., Nowak, J., Krzywonos, M., Cibis, E., 2010. Impact of batch, repeated-batch (with cell recycle and medium replacement) and continuous processes on the course and efficiency of aerobic thermophilic biodegradation of potato processing wastewater. Bioresour. Technol. 101 (10), 3444–3451.

Li, D., Wang, L., Zhao, Q., Wei, W., Sun, Y., 2015. Improving high carbon dioxide tolerance and carbon dioxide fixation capability of *Chlorella sp.* by adaptive laboratory evolution. Bioresour. Technol. 185, 269–275.

Mahr, R., Gätgens, C., Gätgens, J., Polen, T., Kalinowski, J., Frunzke, J., 2015. Biosensor-driven adaptive laboratory evolution of L-valine production in *Corynebacterium glutamicum*. Metab. Eng. 32, 184–194.

Meiswinkel, T.M., Gopinath, V., Lindner, S.N., Nampoothiri, K.M., Wendisch, V.F., 2013. Accelerated pentose utilization by *Corynebacterium glutamicum* for accelerated production of lysine, glutamate, ornithine and putrescine. Microb. Biotechnol. 6.

Mundhada, H., Seoane, J.M., Schneider, K., Koza, A., Christensen, H.B., Klein, T., Phaneuf, P.V., Herrgard, M., Feist, A.M., Nielsen, A.T., 2017. Increased production of L-serine in *Escherichia coli* through Adaptive Laboratory Evolution. Metab. Eng. 39, 141–150.

Portnoy, V.A., Bezdan, D., Zengler, K., 2011. Adaptive laboratory evolution–harnessing the power of biology for metabolic engineering. Curr. Opin. Biotechnol. 22 (4), 590–594.

Qin, D., Hu, Y., Cheng, J., Wang, N., Li, S., Wang, D., 2016. An auto-inducible *Escherichia coli* strain obtained by adaptive laboratory evolution for fatty acid synthesis from ionic liquid-treated bamboo hydrolysate. Bioresour. Technol. 221, 375–384.

Radek, A., Krumbach, K., Gatgens, J., Wendisch, V.F., Wiechert, W., Bott, M., Noack, S., Marienhagen, J., 2014. Engineering of *Corynebacterium glutamicum* for minimized carbon loss during utilization of D-xylose containing substrates. J. Biotechnol. 192 (Pt. A), 156–160.

Reyes, L.H., Gomez, J.M., Kao, K.C., 2014. Improving carotenoids production in yeast via adaptive laboratory evolution. Metab. Eng. 21, 26–33.

Sambrook, J., Russell, D., 2001. Molecular Cloning: a Laboratory Manual. Cold Spring Harbor Laboratory Press, Cold Spring Harbor.

Sjostrom, S.L., Huang, M., Nielsen, J., Joensson, H.N., Svahn, H.A. 2014. Micro-droplet based directed evolution outperforms conventional laboratory evolution. In: International Conference on Miniaterized Systems for Chemistry and Life Sciences (proceedings), 169–171.

Straathof, A.J.J., 2014. Transformation of biomass into commodity chemicals using enzymes or cells. Chem. Rev. 114 (3), 1871–1908.

Unthan, S., Baumgart, M., Radek, A., Herbst, M., Siebert, D., Bruhl, N., 2015a. Chassis organism from *Corynebacterium glutamicum* - a top-down approach to identify and delete irrelevant gene clusters. Biotechnol. J. 10.

Unthan, S., Grunberger, A., van Ooyen, J., Gatgens, J., Heinrich, J., Paczia, N., Wiechert, W., Kohlheyer, D., Noack, S., 2014. Beyond growth rate 0.6: what drives *Corynebacterium glutamicum* to higher growth rates in defined medium. Biotechnol. Bioeng. 111 (2), 359–371.

Unthan, S., Radek, A., Wiechert, W., Oldiges, M., Noack, S., 2015. Bioprocess automation on a Mini Pilot Plant enables fast quantitative microbial phenotyping. Microb. Cell Fact. 14 (1), 32.

Viikari, L., Vehmaanperä, J., Koivula, A., 2012. Lignocellulosic ethanol: from science to industry. Biomass Bioenergy 46, 13–24.

Wang, D., Ju, X., Zhou, D., Wei, G., 2014. Efficient production of pullulan using rice hull hydrolysate by adaptive laboratory evolution of *Aureobasidium pullulans*. Bioresour. Technol. 164, 12–19.

Wang, L., Xue, C., Wang, L., Zhao, Q., Wei, W., Sun, Y., 2016. Strain improvement of *Chlorella sp.* for phenol biodegradation by adaptive laboratory evolution. Bioresour. Technol. 205, 264–268.

Wang, Z., Wu, J., Zhu, L., Zhan, X., 2016. Activation of glycerol metabolism in *Xanthomonas campestris* by adaptive evolution to produce a high-transparency and low-viscosity xanthan gum from glycerol. Bioresour. Technol. 211, 390–397.

Yu, S., Zhao, Q., Miao, X., Shi, J., 2013. Enhancement of lipid production in low-starch mutants *Chlamydomonas reinhardtii* by adaptive laboratory evolution. Bioresour. Technol. 147, 499–507.

3.4.3 Supplementary material

Automated estimation of specific growth rates from online backscatter data

FIGURE 3.8: Automated estimation of specific growth rates from online backscatter data

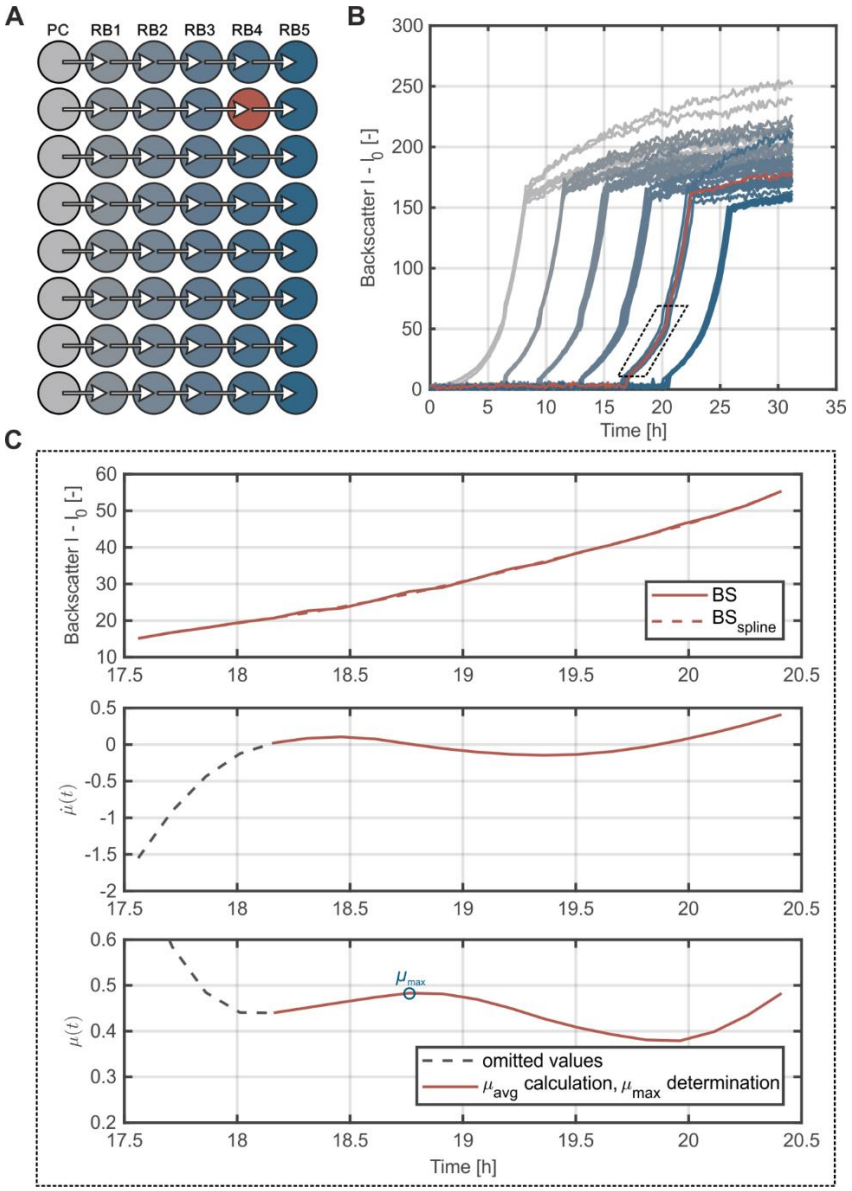

(A) Layout of the simple repetitive batch process of Figure 1. All calculations described above were done for each well separately. One representative cultivation was chosen to demonstrate the data processing (red well). **(B)** Backscatter values of all six repetitive batch cultivations with wild-type *C. glutamicum*. **(C)** Spline approximation of the example backscatter signal with measurements taken between cultivation start and trigger point. From the 1st order derivative of the spline function the specific growth rate over time ($\mu(t)$) was estimated. The 2nd order derivative ($\dot{\mu}(t)$) is used to omit those noisy backscatter values from growth rate estimation which do not hold the criterion $\dot{\mu}(t) > 0$ during the first growth phase. Finally, from the remaining data the average and maximum specific growth rate was calculated as μ_{avg} and μ_{max}, respectively.

Source Code

Requirements:

- MATLAB
- Statistics and Machine Learning Toolbox
- SPLINEFIT and PPDIFF by Jonas Lundgren, splinefit@gmail.com, https://mathworks.com/matlabcentral/fileexchange/13812-splinefit

```
% Definition of parameters
% splineKnots: How many spline knots will be used
% minPoints: Minimum number of data points to be used for calculation of
% mue avg and mue_max
splineKnots = 4;
minPoints = 10;

% Data input
x = time;
y = blankedBackscatterData;

% Spline approximation of data and derivation
spline = splinefit(x,y,splineKnots,'r');
splinefirstder = ppdiff(spline,1);

% Evaluation of approximations at given time points
splineeval = ppval(spline,x);
splinefirstdereval = ppval(splinefirstder,x);

% Calculation of specific growth rate
splinemue = splinefirstdereval ./ splineeval;

% Spline approximation of calculated mue curve and derviation
splinemueapprox = splinefit(x,splinemue,splineKnots,'r');
splinemueapproxder = ppdiff(splinemueapprox,1);

% Evaluation of derivation
splinemueapproxdereval = ppval(splinemueapproxder,x);

% Search for first data point > 0 in first derviation of mue curve
checkSplinemueapproxdereval = find(splinemueapproxdereval > 0);
if ~isempty(checkSplinemueapproxdereval)
      dataPointsForMueEst = [checkSplinemueapproxdereval(1):length(y)];
else
      dataPointsForMueEst= [];
end

% Create vector for restriction of mue data based on prior calculation
or minimum number of points
if isempty(dataPointsForMueEst) || length(dataPointsForMueEst) <
minPoints
      dataPointsForMueEst = length(y)-minPoints:length(y);
end

% Generation of final mue curve and descriptive statistics
splinemueCriterionApplied = splinemue(dataPointsForMueEst);
mue.mean = mean(splinemueCriterionApplied);
mue.std = std(splinemueCriterionApplied);
mue.max = max(splinemueCriterionApplied);
```

3.4.4 Main achievements of this manuscript

• Automated procedures for execution of adaptive laboratory evolution (ALE) experiments at microtiter plate scale were developed.

• Application of the novel ALE approach with engineered *C. glutamicum* led to an increase of the growth rate by 260 % on sole D-xylose (μ_{max} = 0.26 h^{-1}).

• Results from small-scale ALE experiments were successfully transferred to lab-scale operations.

• Genome sequencing revealed up to 15 potential key mutations for improved D-xylose assimilation.

Chapter 4

Conclusions and Outlook

The final D-xylose utilizing strain

The $WMB2_{evo}$ strain finishes this work's aim to establish an efficient alternative pathway for D-xylose utilization in *C. glutamicum*. This strain grows very stable and even faster than the reference strain, which expresses the isomerase pathway (Meiswinkel et al. 2013). Especially the stable growth in laboratory scale bioreactors shows the high potential of this strain for follow up projects.

The initial successful integration of the Weimberg pathway from *C. crescentus* into *C. glutamicum* in this work, and the weak growth behavior of the first strain construct (c.f. chapter 3.2) gave the motivation for further strain optimization and process development. The first WMB strain had many growth limitations (e.g. long lag-phase) coupled with a very low growth rate on D-xylose as substrate. Especially the triphasic growth in medium with D-glucose and D-xylose was predominant. But it showed clearly, that the Weimberg pathway is working in general and finally enables *C. glutamicum* to utilize D-xylose via this new alternative pathway. The codon optimized strain (WMB2) showed an slightly increased maximum specific growth rate of μ= 0.10 h^{-1} instead of μ = 0.07 h^{-1} of the initial Weimberg strain on solely D-xylose as substrate.

However, this slightly improved growth rate was then significantly enhanced by the developed automated and miniaturized ALE process by 260 % up to $\mu = 0.26$ h^{-1}.

The obtained results from the genome sequencing of this adapted strain can be used for further directed strain engineering, which could result in an additional improved strain. Nevertheless, it could be interesting to integrate the pathway genes directly into the genome of *C. glutamicum* for an even better expression thereof. Furthermore, it would be interesting to characterize the found key mutations of the adapted strain in detail. There might be mutations which influence either the better conversion of D-xylose via the Weimberg pathway or for example the uptake of the non-natural substrate D-xylose for *Corynebacterium glutamicum*.

The *myo*-inositol regulator IolR and its relevance for D-xylonate production

One key mutation for improved D-xylose utilization might be found in the *myo*-inositol pathway. The gene cg0196 expresses the repressor for the *myo*-inositol pathway IolR, and a mutation in that gene could express the *myo*-inositol genes partly or completely. Therefore, the relevance of *IolR* deletion in *C. glutamicum* was also investigated in this thesis.

It was found that the deletion of this regulator already enabled a slightly faster growth on D-xylose in strains expressing either the isomerase or the Weimberg pathway (data not shown). But more interestingly is the deletion of the IolR gene in the wild-type background, which lead to the conversion of D-xylose to D-xylonate in high amounts (Radek A, et al., 2016 *Verfahren zur Herstellung von D-Xylonat und coryneformes Bakterium* PT1.2754). D-xylonate is a high-valuable product itself (Toivari et al. 2012) and the wild-type with a deletion of the IolR gene produces 20.76 g l^{-1} D-xylonate from 30 g l^{-1} D-xylose in mixture with 10 g l^{-1} D-glucose in a standard batch cultivation. Clearly, the productivity could be further enhanced by process development, e.g., fed-batch cultivation, which will be carried out in following projects.

The role of the other *myo*-inositol pathway genes for D-xylose utilization in *C. glutamicum* is still under investigation. For example, it is possible that the import of D-xylose can be further improved by the overexpression of the genes *iolT1* and *iolT2*, which encode for *myo*-inositol transporters (Klaffl et al. 2013; Krings et al. 2006).

The two by-products D-xylonate and xylitol of the final $WMB2_{evo}$ strain have to be kept in mind. For example, it would be interesting to investigate if the $WMB2_{evo}$ strain shows better resistance against xylitol than the other tested strains (cf. chapter 3.3). Further on, D-xylonate is still accumulating during growth of the $WMB2_{evo}$ strain on D-xylose containing media (cf. chapter 3.4), thus additional improvement is required for a complete conversion of D-xylose.

By-products and the influence of xylitol on growth

Within the first investigation of the newly constructed WMB strains the two by-products D-xylonate and xylitol were found by GC-ToF-MS analyses and the partly re- consumption of D-xylonate could be confirmed therewith (cf. chapter 3.2).

Before the xylitol inhibition studies started, it was astonishing that *C. glutamicum* ATCC13032 wild-type produces xylitol under aerobic conditions, and not only under oxygen deprivation as reported recently for *Corynebacterium glutamicum* R (Sasaki et al. 2009). For the first time it was shown that *C. glutamicum* strains accumulate

the cytotoxic xylitol-5-phosphate intracellular, especially the ISO strain. That finding underlines the high impact on growth of xylitol on the ISO strain. Whereas the WMB and the wild-type strain showed comparable inhibition of extracellular xylitol (cf. chapter 3.3). Moreover, it was found, that the uptake system from fructose is partly responsible for the phosphorylation of external xylitol as well as the partly responsibility of the xylolukinase (encoded by the gene *xylB*) for the internal phosphorylation of xylitol. For future strain optimizations of the $WMB2_{Evo}$ strain it could be worthwhile to delete the *ptsF* and *xylB* genes additionally, if still small amounts of xylitol-5-phosphate accumulate intracellular.

Further, it is still unknown why *C. glutamicum* produces xylitol during growth in D-xylose containing media. Within this study selected deletions of putative D-xylose reductase encoding genes did not reveal a specific enzyme that is responsible for this conversion. Thus, there is remaining potential for strain improvement for obtaining a more efficient D-xylose utilizing strain without loss of carbon in form of xylitol.

Potential of lab automation and automated workflows on the Mini Pilot Plant

The extended Mini Pilot Plant is used as standard screening and cultivation platform in diverse projects and the developed assays are used as additional laboratory analytic methods. The developed Ninhydrin assay (chapter 3.1), for example, was used to evaluate a newly developed L-lysine biosensor at-line to the cultivation in the BioLector (Steffen et al. 2016). Further, additional assays were recently modified to conduct them automatically on the MPP, like a cutinase assay (Hemmerich et al. 2016) or a Nile red staining assay (Morschett et al. 2016).

Nevertheless, there is more potential for lab automation for this and further robotic platforms for microbial phenotyping and industrial biotechnology in general. For more throughput and more expressiveness of one cultivation run, it would be better to schedule the separate processes more and to conduct the at-line analytics directly during the process and not after the cultivation. This would generate semi-online data, which could be used directly to adjust the running process automatically. A transfer and automated analysis of the at-line obtained results has to be provided by software solutions during the cultivation run.

Furthermore, it could be worthwhile to connect a second robotic platform to the cultivation platform, for example, to couple two cultivation runs or to separate an analytic platform from the cultivation platform completely or partly. A transfer station between the two robotic stations would than be necessary to link both systems.

Application of the ALE process

In contrast to conventional adaptive laboratory evolution approaches where the cells are transferred, e.g., every two days into fresh medium (Lee and Palsson 2010), the new developed ALE process on the MPP allows, for example, the transfer exactly when the cells are in the exponential growth phase. The significant scale reduction and the automation of the process are further tremendous advantages against conventional manual approaches in lab-scale devices.

The presented growth improvement of the Weimberg strain impressively showed the potential of the developed ALE process for future strain optimizations. Additionally, the underlying developed method for repetitive batch cultivations can be used for diverse other investigations, e.g., long term strain stability investigations (Baumgart et al. 2017).

Especially, when performing ALE processes, it is majorly important after running the process and getting an adapted mutant strain, to connect in depth investigation of the finally obtained strain. Of main interest are normally the genetic changes of the adapted strain, whereas genome sequencing becomes necessary. But also metabolomic, proteomic or transcriptomic changes could be interesting and worthwhile to investigate as well.

Although, within this study only with the codon optimized WMB2 strain an automated ALE process was performed, also strains harboring the isomerase pathway might be improved by this method as well. But in recent studies, neither by other ALE processes (Lee et al. 2016) nor by introduction or overexpression of additional heterologous genes (e.g. from the PPP or the PHK-pathway) (Jo et al. 2017), the specific maximum growth rate of the $WMB2_{evo}$ is reached yet.

Biobased economy and lignocellulose as feedstock in place of defined media

Comparable to petroleum refineries, which produce several different products from petroleum (mostly fuels, but also chemicals), biorefineries convert biomass to biofuels, power, heat and high value-added chemicals. Hence, biorefineries combine chemical, physical and biotechnological processes and depend therefore on the type of used biomass. The biotechnological process has to be flexible with respect to the carbon source mixture generated. In future this dependence has to be the basis for metabolic engineering strategies to allow the optimal conversion of multiple carbon sources simultaneously and efficiently. This development requires time until it reaches the efficiency of petroleum refineries (Wendisch et al. 2016). Therefore, it is and it will be the aim of biorefineries to yield a multitude of biofuels and biochemicals without non-utilized residues.

This general aim for biorefineries summarizes also the major part of this work to broaden the substrate spectrum of *C. glutamicum* by efficient utilization of D-xylose. The $WMB2_{evo}$ strain could be used as basis strain for further utilization of substrates which could be necessary for biorefineries. These substrates are, e.g., glycerol, as a by product of the biodiesel process (Khanna et al. 2012) or C1 compounds as methanol (Olah 2013) or CO_2 (Litsanov et al. 2013).

To finally use lignocellulosic biomass as source for industrial biotechnological approaches, instead of defined media, it will be necessary to develop processes for the degradation thereof as well. The mixture of different sugars and polymers of phenylpropanoid units (cf. Figure 1.2) remains a hurdle for one pot reactions (Maurya et al. 2015), where the conversion and production process is directly connected to the degradation of the biomass. Research has to be performed in the field of hydrolysis of biomass, to make the biomass degradation more efficient and to find enzymes or methods, which can be performed at lower temperature optima of microorganisms, e.g., at 30°C for *C. glutamicum* (Lee et al. 2016).

But for now the basis has been set, also with this thesis, to integrate industrial biotechnology into the biobased economy as well. The usage of renewable resources, in this case the pentose sugar D-xylose derived from lignocellulose, was shown by the successful introduction of an alternative efficient pathway into the industrial relevant microorganism *Corynebacterium glutamicum*.

Bibliography

Abe, S., K. I. Takayama, and S. Kinoshita (1967). "Taxonomical studies on glutamic acid-producing bacteria". *Journal of General and Applied Microbiology* 13.3, pp. 279–301.

Acatech (2012). "Biotechnologische Energieumwandlung in Deutschland. Stand, Kontext, Perspektiven, (acatech POSITION)." *Springer Verlag*.

Almeida, João R. M., Tobias Modig, Anneli Petersson, Bärbel Hähn-Hägerdal, Gunnar Lidén, and Marie F. Gorwa-Grauslund (2007). "Increased tolerance and conversion of inhibitors in lignocellulosic hydrolysates by Saccharomyces cerevisiae". *Journal of Chemical Technology and Biotechnology* 82.4, pp. 340–349.

Alvira, P., E. Tomas-Pejo, M. Ballesteros, and M. J. Negro (2010). "Pretreatment technologies for an efficient bioethanol production process based on enzymatic hydrolysis: A review". *Bioresource Technology* 101.13, pp. 4851–4861.

Aristidou, Aristos and Merja Penttilä (2000). "Metabolic engineering applications to renewable resource utilization". *Current Opinion in Biotechnology* 11, 187–198.

Atsumi, S., T. Y. Wu, I. M. Machado, W. C. Huang, P. Y. Chen, M. Pellegrini, and J. C. Liao (2010). "Evolution, genomic analysis, and reconstruction of isobutanol tolerance in Escherichia coli". *Molecular Systems Biology* 6.449, pp. 1–11.

Barrett, E., C. Stanton, O. Zelder, G. Fitzgerald, and R. P. Ross (2004). "Heterologous expression of lactose- and galactose-utilizing pathways from lactic acid bacteria in Corynebacterium glutamicum for üroduction of lysine in whey". *Applied and Environmental Microbiology* 70.5, pp. 2861–2866.

Baumgart, M. et al. (2017). "Corynebacterium glutamicum chassis C1*: Building and testing a nvel platform host for synthetic biology and industrial biotechnology". *ACS Synthetic Biology*.

Brat, D., E. Boles, and B. Wiedemann (2009). "Functional expression of a bacterial xylose isomerase in Saccharomyces cerevisiae". *Applied and Environmental Microbiology* 75.8, pp. 2304–2311.

Cheng, K. K. et al. (2014). "Global metabolic network reorganization by adaptive mutations allows fast growth of Escherichia coli on glycerol". *Nature Communications* 5.3233, pp. 1–9.

Choi, J. W., S. S. Yim, and K. J. Jeong (2017). "Development of a high-copy-number plasmid via adaptive laboratory evolution of Corynebacterium glutamicum". *Applied Microbiology and Biotechnology*.

Cleto, S., J. V. Jensen, V. F. Wendisch, and T. K. Lu (2016). "Corynebacterium glutamicum Metabolic Engineering with CRISPR Interference (CRISPRi)". *ACS Synthetic Biology* 5.5, pp. 375–385.

Dragosits, Martin and Diethard Mattanovich (2013). "Adaptive laboratory evolution – principles and applications for biotechnology". *Microbial Cell Factories* 12.64, pp. 1–17.

Eggeling, Lothar and Michael Bott (2005). *Handbook of Corynebacterium glutamicum*. CRC press.

Fischer, C. R., H. C. Tseng, M. Tai, K. L. Prather, and G. Stephanopoulos (2010). "Assessment of heterologous butyrate and butanol pathway activity by measurement of intracellular pathway intermediates in recombinant Escherichia coli". *Applied Microbiology and Biotechnology* 88.1, pp. 265–275.

Fong, S. S., A. P. Burgard, C. D. Herring, E. M. Knight, F. R. Blattner, C. D. Maranas, and B. O. Palsson (2005). "In silico design and adaptive evolution of Escherichia coli for production of lactic acid". *Biotechnology and Bioengineering* 91.5, pp. 643–648.

Funke, M., S. Diederichs, F. Kensy, C. Muller, and J. Büchs (2009). "The baffled microtiter plate: increased oxygen transfer and improved online monitoring in small scale fermentations". *Biotechnology and Bioengineering* 103.6, pp. 1118–1128.

Galbe, Mats and Guido Zacchi (2012). "Pretreatment: The key to efficient utilization of lignocellulosic materials". *Biomass and Bioenergy* 46, pp. 70–78.

Hausman, S. Z., J. O. H. N Thompson, and J. A. C. K. London (1984). "Futile xylitol cycle in Lactobacillus casei". *Journal of bacteriology* 160.1, pp. 211–215.

Hemmerich, J. and F. Kensy (2013). "Automation of microbioreactors operating 48 parallel fed-batch fermentations at microscale". *BioProcess International* 11.8, pp. 68–76.

Hemmerich, J., P. Rohe, B. Kleine, S. Jurischka, W. Wiechert, R. Freudl, and M. Oldiges (2016). "Use of a Sec signal peptide library from Bacillus subtilis for the optimization of cutinase secretion in Corynebacterium glutamicum". *Microbial Cell Factories* 15.1, p. 208.

Hermann, R., M. Lehmann, and J. Büchs (2003). "Characterization of gas-liquid mass transfer phenomena in microtiter plates". *Biotechnology and Bioengineering* 81.2, pp. 178–186.

Huber, R., D. Ritter, T. Hering, A. K. Hillmer, F. Kensy, C. Muller, L. Wang, and J. Büchs (2009). "Robo-Lector - a novel platform for automated high-throughput cultivations in microtiter plates with high information content". *Microbial Cell Factories* 8.42, pp. 1–15.

Jo, S., J. Yoon, S. M. Lee, Y. Um, S. O. Han, and H. M. Woo (2017). "Modular pathway engineering of Corynebacterium glutamicum to improve xylose utilization and succinate production". *Journal of Biotechnology*.

John, G. T., I. Klimant, C. Wittmann, and E. Heinzle (2003). "Integrated optical sensing of dissolved oxygen in microtiter plates: a novel tool for microbial cultivation". *Biotechnology and Bioengineering* 81.7, pp. 829–836.

Johnsen, U., M. Dambeck, H. Zaiss, T. Fuhrer, J. Soppa, U. Sauer, and P. Schonheit (2009). "D-xylose degradation pathway in the halophilic archaeon Haloferax volcanii". *The Journal of Biological Chemistry* 284.40, pp. 27290–303.

Kakuta, Hatsue, Yoshimichi Iwami, Hideaki Mayanagi, and Nobuhiro Takahashi (2003). "Xylitol inhibition of acid production and growth of mutans streptococci in the presence of various dietary sugars under strictly anaerobic conditions". *Caries Research* 37.6, pp. 404–409.

Kalinowski, Jörn et al. (2003). "The complete Corynebacterium glutamicum ATCC 13032 genome sequence and its impact on the production of l-aspartate-derived amino acids and vitamins". *Journal of Biotechnology* 104.1-3, pp. 5–25.

Kawaguchi, H., A. A. Vertes, S. Okino, M. Inui, and H. Yukawa (2006). "Engineering of a xylose metabolic pathway in Corynebacterium glutamicum". *Applied Environmental Microbiology* 72.5, pp. 3418–3428.

Kensy, F., E. Zang, C. Faulhammer, R. K. Tan, and J. Büchs (2009). "Validation of a high-throughput fermentation system based on online monitoring of biomass and fluorescence in continuously shaken microtiter plates". *Microbial Cell Factories* 8.31, pp. 1–17.

Khanna, S., A. Goyal, and V. S. Moholkar (2012). "Bioconversion of biodiesel derived crude glycerol by immobilized Clostridium pasteurianum: Effect of temperature". *International Journal of Chemical Engineering* 6.4, pp. 289–292.

Kind, S. and C. Wittmann (2011). "Bio-based production of the platform chemical 1,5-diaminopentane". *Applied Microbiology Biotechnology* 91.5, pp. 1287–1296.

Kinoshita, S., K. Nakayama, and S. Akita (1957). "Taxonomical atudy of glutamic acid accumulating bacteria, Micrococcus glutamicus". *Bulletin of the Agricultural Chemical Society of Japan* 22.3, pp. 176–185.

Klaffl, S., M. Brocker, J. Kalinowski, B. J. Eikmanns, and M. Bott (2013). "Complex regulation of the phosphoenolpyruvate carboxykinase gene pck and characterization of its GntR-type regulator IolR as a repressor of myo-inositol utilization genes in Corynebacterium glutamicum". *Journal of Bacteriology* 195.18, pp. 4283–96.

Knepper, A., M. Heiser, F. Glauche, and P. Neubauer (2014). "Robotic platform for parallelized cultivation and monitoring of microbial growth parameters in microwell plates". *Journal of Lab Automation* 19.6, pp. 593–601.

Kotrba, P., M. Inui, and H. Yukawa (2003). "A single V317A or V317M substitution in Enzyme II of a newly identified beta-glucoside phosphotransferase and utilization system of Corynebacterium glutamicum R extends its specificity towards cellobiose". *Microbiology* 149.Pt 6, pp. 1569–1580.

Krings, E., K. Krumbach, B. Bathe, R. Kelle, V. F. Wendisch, H. Sahm, and L. Eggeling (2006). "Characterization of myo-inositol utilization by Corynebacterium glutamicum: the stimulon, identification of transporters, and influence on L-lysine formation". *Journal of Bacteriology* 188.23, pp. 8054–61.

Langeveld, J. W. A., J. Dixon, and J. F. Jaworski (2010). "Development perspectives of the biobased economy: A review". *Crop Science* 50, pp. 142 –151.

Lasik, M., J. Nowak, M. Krzywonos, and E. Cibis (2010). "Impact of batch, repeated-batch (with cell recycle and medium replacement) and continuous processes on the course and efficiency of aerobic thermophilic biodegradation of potato processing wastewater". *Bioresource Technology* 101.10, pp. 3444–3451.

Lee, D. H. and B. O. Palsson (2010). "Adaptive evolution of Escherichia coli K-12 MG1655 during growth on a Nonnative carbon source, L-1,2-propanediol". *Applied and Environmental Microbiology* 76.13, pp. 4158–4168.

Lee, J., J. N. Saddler, Y. Um, and H. M. Woo (2016). "Adaptive evolution and metabolic engineering of a cellobiose- and xylose- negative Corynebacterium glutamicum that co-utilizes cellobiose and xylose". *Microbial Cell Factories* 15, p. 20.

Li, D., L. Wang, Q. Zhao, W. Wei, and Y. Sun (2015). "Improving high carbon dioxide tolerance and carbon dioxide fixation capability of Chlorella sp. by adaptive laboratory evolution". *Bioresource Technology* 185, pp. 269–275.

Litsanov, B., M. Brocker, and M. Bott (2013). "Glycerol as a substrate for aerobic succinate production in minimal medium with Corynebacterium glutamicum". *Microbial Biotechnology* 6.2, pp. 189–95.

Liu, L., Y. Li, S. Li, N. Hu, Y. He, R. Pong, D. Lin, L. Lu, and M. Law (2012). "Comparison of next-generation sequencing systems". *Journal of Biomedicine and Biotechnology* 2012, p. 251364.

Maaheimo H, Fiaux J, Cakar ZP, Bailey JE, Sauer U, and Szyperski T (2001). "Central carbon metabolism of Saccharomyces cerevisiae explored by biosynthetic fractional (13)C labeling of common amino acids." *European Journal of Biochemistry* 268, pp. 2464–2479.

Mahr, R., C. Gatgens, J. Gatgens, T. Polen, J. Kalinowski, and J. Frunzke (2015). "Biosensor-driven adaptive laboratory evolution of l-valine production in Corynebacterium glutamicum". *Metabolic Engineering* 32, pp. 184–194.

Marsh, P. D., M. V. Martin, M. A. Lewis, and D. Williams (2009). "Oral Microbiology". *E-Book: Elsevier health sciences.*

Maurya, D. P., A. Singla, and S. Negi (2015). "An overview of key pretreatment processes for biological conversion of lignocellulosic biomass to bioethanol". *3 Biotechnology* 5.5, pp. 597–609.

McLaren, J. S. (2005). "Crop biotechnology provides an opportunity to develop a sustainable future". *Trends in Biotechnology* 23.7, pp. 339–342.

Meiswinkel, T. M., V. Gopinath, S. N. Lindner, K. M. Nampoothiri, and V. F. Wendisch (2013). "Accelerated pentose utilization by Corynebacterium glutamicum for accelerated production of lysine, glutamate, ornithine and putrescine". *Microbial Biotechnology* 6.2, pp. 131–140.

Miyasawa, H., Y. Iwami, Mayanagi H., and N. Takahashi (2003). "Xylitol inhibition of anaerobic acid production by Streptococcus mutans at various pH levels." *Molecular Oral Microbiology* 18.4, pp. 215–219.

Morschett, H., W. Wiechert, and M. Oldiges (2016). "Automation of a Nile red staining assay enables high throughput quantification of microalgal lipid production". *Microbial Cell Factories* 15, p. 34.

Mundhada, H. et al. (2017). "Increased production of L-serine in Escherichia coli through Adaptive Laboratory Evolution". *Metabolic Engineering* 39, pp. 141–150.

Olah, G. A. (2013). "Towards oil independence through renewable methanol chemistry". *Angewandte Chemie International Edition* 52.1, pp. 104–7.

Olsson L., Jorgenson H. Krogh K. B.R. Roca C. (2004). "Bioethanol Production from Lignocellulosic Material". *Marcel Dekker* 2, pp. 957–993.

Peng, F., X. Wang, Y. Sun, G. Dong, Y. Yang, X. Liu, and Z. Bai (2017). "Efficient gene editing in Corynebacterium glutamicum using the CRISPR/Cas9 system". *Microbial Cell Factories* 16.1, p. 201.

Portnoy, V. A., D. Bezdan, and K. Zengler (2011). "Adaptive laboratory evolution-harnessing the power of biology for metabolic engineering". *Current Opinion in Biotechnology* 22.4, pp. 590–594.

Qin, D., Y. Hu, J. Cheng, N. Wang, S. Li, and D. Wang (2016). "An auto-inducible Escherichia coli strain obtained by adaptive laboratory evolution for fatty acid synthesis from ionic liquid-treated bamboo hydrolysate". *Bioresource Technology* 221, pp. 375–384.

Reyes, L. H., J. M. Gomez, and K. C. Kao (2014). "Improving carotenoids production in yeast via adaptive laboratory evolution". *Metabolic Engineering* 21, pp. 26–33.

Rohe, P., D. Venkanna, B. Kleine, R. Freudl, and M. Oldiges (2012). "An automated workflow for enhancing microbial bioprocess optimization on a novel microbioreactor platform". *Microbial Cell Factories* 11.144, pp. 1–13.

Rubin, E. M. (2008). "Genomics of cellulosic biofuels". *Nature* 454.7206, pp. 841–845.

Sahm, H., L. Eggeling, and A. A. de Graaf (2000). "Pathway analysis and metabolic engineering in Corynebacterium glutamicum". *Biological Chemistry* 381.9-10, pp. 899–910.

Samorski, M., G. Muller-Newen, and J. Büchs (2005). "Quasi-continuous combined scattered light and fluorescence measurements: a novel measurement technique for shaken microtiter plates". *Biotechnology and Bioengineering* 92.1, pp. 61–68.

Sanders, J., E. Scott, R. Weusthuis, and H. Mooibroek (2007). "Bio-refinery as the bio-inspired process to bulk chemicals". *Macromolecular Bioscience* 7.2, pp. 105–117.

Sasaki, M., T. Jojima, H. Kawaguchi, M. Inui, and H. Yukawa (2009). "Engineering of pentose transport in Corynebacterium glutamicum to improve simultaneous

utilization of mixed sugars". *Applied Microbiology and Biotechnology* 85.1, pp. 105–15.

Scheller, H. V. and P. Ulvskov (2010). "Hemicelluloses". *Annual Review of Plant Biology* 61, pp. 263–289.

Scott C., McLeod L. D. (2010). "The time has come for automation in bioprocessing". *BioProcess International*, pp. 17–25.

Seibold, G., M. Auchter, S. Berens, J. Kalinowski, and B. J. Eikmanns (2006). "Utilization of soluble starch by a recombinant Corynebacterium glutamicum strain: growth and lysine production". *Journal of Biotechnology* 124.2, pp. 381–391.

Sjostrom, Staffan L., Mingtao Huang, Jens Nielsen, Haakan N. Joensson, and Helene Andersson Svahn (2014). "Micro-droplet based directed evolution outperforms conventional laboratory evolution". *International Conference on Miniaterized Systems for Chemistry and Life Sciences (proceedings)*, 169–171.

Smith, A. (2002). "Screening for drug discovery: the leading question". *Nature* 418.6896, pp. 453–459.

Sonnleitner, B. (1997). "Bioprocess automation and bioprocess design". *Journal of Biotechnology* 52.3, pp. 175–179.

Steffen, V., J. Otten, S. Engelmann, A. Radek, M. Limberg, B. W. Koenig, S. Noack, W. Wiechert, and M. Pohl (2016). "A toolbox of genetically encoded FRET-based biosensors for rapid l-lysine analysis". *Sensors (Basel)* 16.10.

Stephens, C., B. Christen, T. Fuchs, V. Sundaram, K. Watanabe, and U. Jenal (2007). "Genetic analysis of a novel pathway for D-xylose metabolism in Caulobacter crescentus". *Journal of Bacteriology* 189.5, pp. 2181–5.

Unthan, S. et al. (2015). "Chassis organism from Corynebacterium glutamicum–a top-down approach to identify and delete irrelevant gene clusters". *Biotechnology Journal* 10.2, pp. 290–301.

Wang, D., X. Ju, D. Zhou, and G. Wei (2014). "Efficient production of pullulan using rice hull hydrolysate by adaptive laboratory evolution of Aureobasidium pullulans". *Bioresource Technology* 164, pp. 12–19.

Wang, X., I. Khushk, Y. Xiao, Q. Gao, and J. Bao (2017). "Tolerance improvement of Corynebacterium glutamicum on lignocellulose derived inhibitors by adaptive evolution". *Applied Microbiology and Biotechnology*.

Weimberg, R. (1961). "Pentose oxidation by Pseudomonas fragi". *The Journal of Biological Chemistry* 236, pp. 629–35.

Wendisch, V. F., L. F. Brito, M. Gil Lopez, G. Hennig, J. Pfeifenschneider, E. Sgobba, and K. H. Veldmann (2016). "The flexible feedstock concept in Industrial Biotechnology: Metabolic engineering of Escherichia coli, Corynebacterium glutamicum, Pseudomonas, Bacillus and yeast strains for access to alternative carbon sources". *Journal of Biotechnology* 234, pp. 139–57.

Wendisch, Volker F. (2007). "Amino acid biosynthesis - pathways, regulation and metabolic engineering". *Microbiology Monographs* 5.

Wiechert, W. and S. Noack (2011). "Mechanistic pathway modeling for industrial biotechnology: challenging but worthwhile". *Current Opinion in Biotechnology* 22.5, pp. 604–610.

Yu, S., Q. Zhao, X. Miao, and J. Shi (2013). "Enhancement of lipid production in low-starch mutants Chlamydomonas reinhardtii by adaptive laboratory evolution". *Bioresource Technology* 147, pp. 499–507.